

ABSTRACT

Title of Dissertation: JAK/STAT AND HIPPO SIGNALING PATHWAYS
INDEPENDENTLY REGULATE THE SAME TARGET
GENES TO CONTROL CELL PROLIFERATION

Lijuan Du, Doctor of Philosophy, 2014

Dissertation directed by: Professor Jian Wang
Department of Entomology
University of Maryland

Drosophila mushroom bodies, centers of olfactory learning and memory, are generated by four neuroblasts in each brain hemisphere. Through a forward genetic screen, I found that mutations in the Janus Kinase (JAK) / Signal Transducer and Activator of Transcription (STAT) pathway genes *domeless* (*dome*) and *hopscotch* (*hop*) cause precocious disappearance of mushroom body neuroblasts. Further evidence indicates that JAK/STAT signaling prevents neuroblast termination and promotes neuroblast division in *Drosophila* mushroom bodies.

Remarkably, ectopic expression of *yorkie* (*yki*), the downstream effector of the Hippo signaling pathway, efficiently rescues *dome* mutant phenotypes, and overexpression of Yki target-genes *CycE* or/and *Diap1* partially rescues the γ -only phenotype that results from lack of JAK/STAT signaling. Further studies indicate that loss of *yki* function causes a similar but less severe phenotype in mushroom bodies, and

this phenotype could be rescued by dominant activation of JAK/STAT. I conclude that both JAK/STAT and Yki activities are required for mushroom body neurogenesis, and higher levels of one can compensate for lack of the other.

I also found that Stat92E directly controls *CycE* expression in mushroom body neuroblasts via a consensus STAT-binding site. Furthermore, mushroom body neuroblast clones with no *CycE* expression or an excess of *CycE* expression phenocopy mushroom bodies with decreased or increased JAK/STAT signaling activities, respectively. Together these results suggest that *CycE* is transcriptionally regulated by STAT92E and is required for mediating cell proliferation. Moreover, I showed that Stat92E and Yki regulate the transcription of *CycE* by interacting with two independent enhancers.

It is known that the transcription factor *E2f1* is induced by Yki, and my transgenic analysis suggested that two STAT-binding sites are required for *E2f1* expression in *Drosophila* brain and wing disc. Therefore, *E2f1* is another shared target of Stat92E and Yki. Together with the findings of others that *Diap1* is a direct target of STAT92E and Yki, I propose that JAK/STAT and Hippo signaling pathways are integrated to control development of *Drosophila* by independently regulating the transcription of common target genes, such as *CycE* and *E2f1* to control cell proliferation, and *Diap1* to control cell survival.

JAK/STAT AND HIPPO SIGNALING PATHWAYS INDEPENDENTLY REGULATE
THE SAME TARGET GENES TO CONTROL CELL PROLIFERATION

by

Lijuan Du

Dissertation submitted to the Faculty of the Graduate School of the
University of Maryland, College Park in partial fulfillment
of the requirements for the degree of
Doctor of Philosophy
2014

Advisory Committee:

Professor Jian Wang, Chair
Professor Leslie Pick
Professor Caren Chang
Professor David O'Brochta
Professor Stephen Mount, Dean's Representative

©Copyright by

Lijuan Du

2014

Acknowledgement

First of all I would like to thank my PhD advisor, Dr. Jian Wang, for his big support throughout my PhD study. I also want to thank my committee members, Dr. Leslie Pick, Dr. Caren Chang, Dr. David O’Brochta and Dr. Stephen Mount, for their help during my PhD study.

I also would like to thank all previous and current members of the Wang lab and the Pick lab for all the help. Dr. Jianhua Huang, a former postdoctoral fellow in the Wang lab, taught me useful knowledge and skills about *Drosophila* at the beginning of my study in Wang lab, and kindly contributed some valuable reagents even after he left the lab. Dr. Siqian Feng, a former graduate student in the Wang lab, inspired me a lot new ideas and information in my dissertation research, and gave me a lot of help on both my study and my life here.

I would also like to thank many colleagues in the *Drosophila* research community for sharing with me their fly strains and other reagents. I thank Dr. Steven Hou, Dr. Erika Bach, Dr. Jianhua Huang, Dr. Duoia Pan, and Dr. Chris Doe for sending me *Drosophila* strains and/or reagents throughout my PhD study. Their help made my dissertation project possible.

I also want to acknowledge the core facilities at the University of Maryland for helping me with many image collections. I thank Dr. Amy Beaven for her help with confocal microscopy.

I would also like to acknowledge the Ann G. Wylie Dissertation Fellowship for supporting me, letting me focus on the writing. Finally and most importantly, I want to thank all my family members for their huge support in these years.

Table of Contents

Acknowledgement	ii
Table of Contents	iv
List of Tables	vii
List of Figures	viii
Chapter 1: Introduction	1
JAK/STAT signaling pathway: one of the major growth controlling pathways	2
JAK/STAT signaling pathway in mammals and in <i>Drosophila</i>	2
The JAK/STAT pathway activation and regulation.....	4
Non-canonical JAK/STAT pathway	8
JAK/STAT signaling and the control of cellular proliferation	10
JAK/STAT signaling and stem/germ cell maintenance or self-renewal.....	11
The Hippo signaling pathway: a key regulator for organ size control.....	15
Hippo signaling pathway in <i>Drosophila</i>	15
Hippo signaling pathway in mammals.....	17
Hippo signaling pathway and tissue regeneration, stem cell self-renewal and expansion	18
Cell cycle control	20
Cell cycle control system in eukaryotic cells.....	20
Regulation of cell cycles in <i>Drosophila</i>	23
Cell apoptosis pathway	26
<i>Drosophila</i> mushroom body: an excellent model to study genes essential for neuronal morphogenesis	28
The early history of mushroom body research	28
The function of the mushroom bodies in insect behavior	30
The cellular organization and the development of the <i>Drosophila</i> mushroom bodies	31
Mushroom body neuroblasts.....	33
MARCM technique facilitates mushroom body studies	34
Chapter 2: A MARCM-based genetic screen for genes necessary for <i>Drosophila</i> mushroom body neuronal morphogenesis	43
Abstract	44
A small-scale genetic screen for genes required for mushroom body development	45

Chapter 3: JAK/STAT signaling prevents neuroblast termination and promotes neuroblast division in <i>Drosophila</i> mushroom bodies	60
Abstract	61
Loss of <i>dome</i> function leads to defects in mushroom body neurogenesis	62
Lack of JAK/STAT signaling causes the γ -only phenotype in adult mushroom bodies	65
JAK/STAT pathway activity is not required for the survival and cell fate specification of mushroom body neurons	69
JAK/STAT signaling prevents premature neuroblast termination and promotes cell division of mushroom body neuroblasts	73
Chapter 4: Both JAK/STAT signaling activity and Hippo pathway effector Yki activity are required for mushroom body neurogenesis, and higher activation of one can compensate for lack of the other	79
Abstract	80
<i>yorkie</i> (<i>yki</i>) overexpression rescues the phenotype resulting from the loss of JAK/STAT signaling in mushroom bodies	81
Loss of <i>yki</i> expression also causes a phenotype similar to that caused by the loss of JAK/STAT signaling in mushroom bodies, and ectopic expression of <i>Stat92E</i> ^{<i>ΔNAC</i>} rescues this phenotype	89
Chapter 5: Stat92E directly activates <i>CycE</i> expression in mushroom body neuroblasts, and Stat92E and Yki regulate the <i>CycE</i> transcription by each interacting with an independent enhancer on <i>CycE</i>	94
Abstract	95
The Stat92E DNA-binding sequence at the <i>CycE</i> locus is required for full <i>CycE</i> transcriptional activity in wing imaginal discs	96
Stat92E regulates the expression of <i>CycE</i> in mushroom bodies	103

Clones of mushroom body neuroblasts either lacking <i>CycE</i> expression or with elevated <i>CycE</i> expression phenocopy clones with decreased or increased JAK/STAT signaling activities, respectively	108
Stat92E and Yki regulate the transcription of <i>CycE</i> by interacting with two independent enhancers in the <i>CycE cis</i> -regulatory region	113
Chapter 6: Stat92E directly regulates the expression of the cell-cycle regulatory gene <i>E2f1</i> , another common target gene of Stat92E and Yki.....	117
Abstract	118
Conserved STAT DNA-binding sites in the <i>E2f1</i> locus are required for <i>E2f1</i> transcriptional activity in <i>vivo</i>	119
Chapter 7: Conclusions and Scientific impacts	125
<i>CycE</i> as the direct target of the JAK/STAT signaling pathway and promotes cell-cycle progression	128
Novel function of JAK/STAT signaling pathway in neurogenesis	131
The new mechanism of the interaction between JAK/STAT and Hippo signaling pathways	131
Future directions and implications.....	133
Chapter 8: Materials and methods	139
Materials	140
Methods.....	142
References.....	148

List of Tables

Table 2-1. The 250 lines obtained from the Kyoto DGRC that were used for screening..	48
Table 2-2. A list of mutant lines causing abnormalities in mushroom body morphogenesis that were identified from the mosaic genetic screen.....	58
Table 4-1. List of genes tested as potential downstream mediators for the JAK/STAT signaling pathway in mushroom body neurogenesis.....	83

List of Figures

Figure 1-1. The <i>Drosophila</i> JAK/STAT signaling pathway.....	37
Figure 1-2. The <i>Drosophila</i> Hippo signaling pathway.....	39
Figure 1-3. Schematic illustration of the GAL80/GAL4/UAS expression system and the MARCM system.....	41
Figure 3-1. Loss of <i>dome</i> function causes γ -only phenotype in adult mushroom bodies..	63
Figure 3-2. Lack of JAK/STAT signaling causes the γ -only phenotype in adult mushroom bodies.....	67
Figure 3-3. Loss of <i>dome</i> does not affect differentiation and survival of the post-mitotic neurons.....	71
Figure 3-4. JAK/STAT signaling promotes division and prevents premature termination of mushroom body neuroblasts.....	76
Figure 4-1. Excess <i>CycD.Cdk4</i> or <i>myc</i> in the <i>dome</i> mutant mushroom body neuroblasts failed to rescue the γ -only phenotype.....	85
Figure 4-2. The cell proliferation defects of <i>dome</i> mushroom bodies are rescued by excess of <i>yki</i> , <i>CycE</i> , or <i>Diap1</i>	87
Figure 4-3. Loss of <i>yki</i> also causes the cell proliferation defects similar to that caused by loss of JAK/STAT signaling in mushroom bodies, and ectopic expression of <i>Stat92E</i> can rescue this phenotype.....	91
Figure 5-1. Stat92E directly regulate <i>CycE</i> transcription in the wing imaginal discs by binding to a consensus STAT DNA-binding site.....	99
Figure 5-2. JAK/STAT signaling directly regulates <i>CycE</i> expression in the mushroom body neuroblasts.....	105
Figure 5-3. <i>CycE</i> mushroom body neuroblast clone phenocopies loss of JAK/STAT pathway activity, and excess <i>CycE</i> leads to neuronal overgrowth to the same extent as excess <i>Stat92E</i> does.....	110
Figure 5-4. Stat92E and Yki regulate the transcription of <i>CycE</i> by interacting with two independent enhancers.....	115
Figure 6-1. Stat92E directly regulate <i>E2f1</i> transcription by binding to two STAT DNA-binding sequences.....	121
Figure 7-1. Working model for roles of JAK/STAT signaling in mushroom body development.....	135
Figure 7-2. Working model for the relationship between JAK/STAT and Hippo pathways in controlling cell proliferation and survival.....	137

Chapter 1: Introduction

JAK/STAT signaling pathway: one of the major growth controlling pathways

JAK/STAT signaling pathway in mammals and in *Drosophila*

The transduction of signals from outside a cell to produce a specific response is essential for development and homeostasis, and is usually mediated by a small number of signal transduction cascades (Arbouzova & Zeidler, 2006). The JAK (Janus Kinase)-STAT (Signal Transducer and Activator of Transcription) pathway is such a cascade that has been a focus of research in recent years. The JAK/STAT signaling pathway was originally identified in vertebrates (Fu et al., 1992; Schindler et al., 1992; Darnell et al., 1994). In mammals, this pathway can be activated by a great number of growth factors and cytokines (Decker, 1999; Levy, 1999; Mui, 1999; Yeh & Pellegrini, 1999; O'Shea et al., 2002). These signals are crucial to the proper growth and development of mammalian tissues by regulating various biological processes such as cell growth, proliferation, differentiation, migration, apoptosis, transformation, inflammation, and immune response. Increases or decreases in the activity of this signaling pathway lead to severe consequences. In particular, constitutive activation of JAKs or STATs is linked to many oncogenic transformations (Hou et al., 2002; Arbouzova & Zeidler, 2006). Moreover, in recent years, increasing amounts of evidence have suggested the neuronal specific functions of JAK/STAT pathway in the central nervous system (CNS) (Nicolas et al., 2012). For example, the JAK/STAT pathway is involved in the control of food intake (Tups, 2009). And it has also been linked to Alzheimer's disease and memory (Chiba et al., 2009). But the cellular and molecular mechanism by which the JAK/STAT pathway regulates neuronal function is largely unknown.

Early studies of transcriptional activation in response to interferon α (IFN- α) and interferon γ (IFN- γ) established the JAK/STAT pathway that connects events at the cell surface directly to gene activation (Darnell et al., 1994). STATs were initially identified as a class of interferon-stimulated transcription factors over 21 years ago (Fu et al., 1992; Schindler et al., 1992). Since then, extensive studies have led to the characterization of the core components of the JAK/STAT signaling pathway, including a variety of extracellular ligands and their transmembrane receptors, four JAKs and seven STATs (Kisseleva et al., 2002). The four mammalian JAKs are JAK1-3 and tyrosine kinase 2 (TYK2). JAKs belong to a family of non-receptor protein tyrosine kinases that were discovered while searching for protein kinases in the early 1990s (Pellegrini & Dusanter-Fourt, 1997; Yeh & Pellegrini, 1999). Subsequently, their ability to complement mutant phenotypes of cells otherwise insensitive to interferons and their activation by a variety of cytokines demonstrated their central signaling function as essential intracellular effectors (Darnell et al., 1994). There are seven STAT proteins (STAT-1-4, 5A, 5B and 6) presently identified in mammals (Levy, 1999; Mui, 1999).

In *Drosophila*, the JAK/STAT signaling pathway was first identified by its function in embryonic segmentation. The first JAK/STAT gene identified was *hopscotch* (*hop*), which encodes a nonreceptor-tyrosine-kinase of the Janus Kinase family. It was found that the maternal product of *hop* is involved in the control of pair-rule gene transcription in a stripe-specific pattern (Binari & Perrimon, 1994). Later, additional studies contributed to identify the genes encoding the core components of the JAK/STAT pathway in *Drosophila*, including three cytokine-like ligands (*unpaired/outstretched* (*upd*), *upd2* and *upd3*) (Harrison et al., 1998; Agaisse et al., 2003; Gilbert et al., 2005;

Hombria et al., 2005); one transmembrane receptor gene *domeless* (*dome*) (also called *master of marelle*), which is distantly related to the mammalian gp130 cytokine receptor gene (Brown et al., 2001; Chen et al., 2002); one JAK-like kinase gene known as *hopscotch* (*hop*), which is most similar to mammalian *Jak2* (Binari & Perrimon, 1994); and one gene encoding a transcription factor, *Stat92E*, homolog of the mammalian genes *Stat3* and *Stat5* (Hou et al., 1996; Yan et al., 1996). Recently, a second receptor *eye transformer* (*et*) also called *latran* (*lat*) (referred to as *et/lat*) was identified (Kallio et al., 2010; Makki et al., 2010). Et/Lat can form heterodimers with Dome and inhibit JAK/STAT signaling. So, in contrast with the high levels of redundancy of JAK/STAT homologs found in mammals, *Drosophila* contains a simpler pathway but sufficient to regulate many different processes (Hou et al., 2002). As a result, the reduced genetic redundancy of *Drosophila* JAK/STAT pathway components, together with the advanced genetic tools, and the ease of gain- and loss-of-function manipulations, make *Drosophila* an excellent model for studying the JAK/STAT pathway (Arbouzova & Zeidler, 2006). Figure 1-1 illustrates the *Drosophila* JAK/STAT pathway.

The JAK/STAT pathway activation and regulation

The mechanism by which the JAK/STAT pathway is activated is conserved among insects and mammals (Luo & Dearolf, 2001; Arbouzova & Zeidler, 2006). A model of JAK/STAT pathway activation was summarized and illustrated by Pellegrini and Dusanter-Fourt in 1997: Upon the binding of an extracellular ligand to its specific homodimeric or heterodimeric transmembrane receptors, the receptor-associated JAKs are activated. These tyrosine kinases then transphosphorylate each other and phosphorylate their associated receptors on tyrosine residues, generating docking sites for

the Src homology 2 (SH2) domains of STATs. STATs are normally present in the cytoplasm as inactive monomers before being recruited to the receptor/JAK complex. It has also been shown that STAT proteins shuttle between nuclear and cytoplasmic compartments (Vinkemeier, 2004). Once bound to the receptor/JAK complex, STATs are tyrosine phosphorylated. Phosphorylated STATs form homodimers or heterodimers by reciprocal interactions of the SH2 domain of one STAT with the phosphor-Tyr of the other. In the nucleus, activated STAT dimers bind to specific DNA sequences in the regulatory regions of target genes to activate transcription. After transient activation, the signaling process is downregulated through negative regulation: de-phosphorylation by phosphotyrosine phosphatases (PTPs), and direct inhibition by families of negative regulatory proteins such as SOCS (Suppressors of Cytokine Signaling) and PIAS (Protein Inhibitors of Activated STAT) (Starr & Hilton, 1999). PIAS proteins negatively regulate the JAK/STAT signaling by binding to STAT and inhibiting its activity (Shuai, 2000), while SOCS proteins negatively regulate the JAK/STAT signaling by binding to and inhibiting the activity of the receptor or JAK (Starr & Hilton, 1999; Stec et al., 2013).

In addition to the core pathway components, additional components and regulators that modulate JAK/STAT pathway signaling activity have been identified in *Drosophila*.

There are both positive regulators and negative regulators of JAK/STAT pathway.

Positive regulators include: pathway ligands; the *Drosophila* homologue of BRWD3, a bromo-domain-containing protein disrupted in leukaemia (Muller et al., 2005); and other signaling pathways such as the Notch signaling pathway, DPP/BMP pathway and the Hedgehog signaling pathway (Bach et al., 2003; Chao et al., 2004; Moberg et al., 2005; Mukherjee et al., 2006). The known negative regulators include: SOCS proteins (Krebs &

Hilton, 2003; Rawlings et al., 2004); ZIMP/PIAS proteins (Betz et al., 2001); an alternatively spliced form of *Stat92E* that encodes an N-terminal truncated dominant negative protein lacking an N-terminal protein:protein interaction domain, Δ NSTAT92E (Henriksen et al., 2002); protein tyrosine phosphatases PTP61F (Muller et al., 2005); the transcriptional repressors Ken & Barbie (KEN) (Arbouzova et al., 2006); and a short receptor Eye transformer also called Latran (usually referred to as Et/Lat (Kallio et al., 2010; Makki et al., 2010). Some of these regulators were identified based on sequence homology to their mammalian counterparts, such as the *Socs* genes (Rawlings et al., 2004) and *pias/zimp* (Betz et al., 2001), while others were identified in genome wide screens, such as *BRWD3* and *ptp61f* (Baeg et al., 2005; Muller et al., 2005).

Among JAK/STAT pathway regulators, SOCS proteins have been most widely studied. The mammals have eight SOCS proteins, SOCS1-7 and CIS. And each of them contains a centrally located SH2 domain and a SOCS box located in the C-terminus (Stec & Zeidler, 2011). The association of SH2 domains to phosphorylated tyrosine residues allows SOCS proteins to bind to phosphorylated JAKs or receptors to specifically inhibit JAK kinase activity, or physically block the recruitment of STATs to the receptor, thus negatively regulating the JAK/STAT activity. The SOCS form a negative feedback loop in the JAK/STAT pathway: activated STATs induce expression of the *Socs* genes and the resulting SOCS proteins inhibit phosphorylated JAKs or receptors to turn off the pathway activity (Rawlings et al., 2004). The *Drosophila* genome encodes three SOCS proteins, termed SOCS16D, SOCS36E, and SOCS44A based on their chromosomal location. Conserved SH2 and SOCS-box domains are revealed by sequence analysis (Stec & Zeidler, 2011). However, only SOCS36E and SOCS44A have been found to regulate

JAK/STAT pathway signaling. SOCS36E is a strong negative regulator and SOCS44A can suppress signaling to a weaker extent (Stec & Zeidler, 2011). The *Socs36E cis*-regulatory region contains 19 putative STAT92E consensus binding sites, and *Socs36E* has been suggested as a direct target gene of STAT92E. Therefore, the down-regulation of the pathway elicited by SOCS36E completes a negative feedback loop and is analogous to role of other SOCS-family proteins in vertebrates (Starr et al., 1997).

The consensus binding sites of STATs have been reported (Ivashkiv, 1995). STATs recognize a palindromic sequence, with 2- to 4- base spacing between dyad half sites 5'-TTC-3' (Seidel et al., 1995). STAT1 and STAT5 complexes favor a 3-bp spacing (TTCNNNGAA), STAT3 favors a 2- or 3-bp spacing (TTCNNGAA or TTCNNNGAA), STAT4 favors a 3-bp spacing (TTCNNNGAA), and STAT6 favors a 3- or 4-bp spacing (TTCNNNGAA or TTCNNNNGAA) (Yamamoto et al., 1997; Ehret et al., 2001). The *cis*-acting elements of many genes responsive to different STAT proteins have been analyzed. Among those target genes analyzed by Ehret et al., ~75% contain one STAT consensus binding site (Ehret et al., 2001). These include the human and mouse *Bcl-x* gene (Dumon et al., 1999), mouse *Toll-like receptor 2 (mTLR2)* (Musikacharoen et al., 2001), human *Mcl-1* (Isomoto et al., 2005), and human *IL-8* (Gharavi et al., 2007). Approximately 25% contain two STAT consensus binding sites (Ehret et al., 2001), examples include the *Mig* in mice (Wong et al., 1994), and the *HLA-E* in humans (Gustafson & Ginder, 1996).

The single *Drosophila* Stat prefers to bind to sites with 3n spacing (TTCNNNGAA) (Yan et al., 1996). In *Drosophila*, Stat92E binding of 3n-sites was confirmed for the *even*

skipped (eve) gene (Yan et al., 1996), *Drosophila raf* proto-oncogene (*D-raf*) (Kwon et al., 2000), *Suppressor of cytokine signaling at 36E* (*Socs36E*) (Baeg et al., 2005; Muller et al., 2005), and *Death-associated inhibitor of apoptosis 1* (*Diap1*) (Betz et al., 2008). A recent study indicated that *Drosophila* Stat92E was able to activate transcription using consensus sequences referred to as “4n sites” (TTCNNNNGAA) (Rivas et al., 2008). Stat92E activates *dome* using two conserved 4n-sites, and another direct target of Stat92E *crb* is also regulated through two 4n-sites (Rivas et al., 2008). The results of Rivas et al (2008) indicated that Stat92E has higher binding affinity to 3n-sites than to 4n-sites. They also showed that two adjacent sites were able to bind Stat92E better than a single binding site (Rivas et al., 2008). But two binding sites were not always required, as the case for STAT-responsive genes in mammals. For example, *D-raf* is activated by Stat92E through one consensus STAT-binding site (Kwon et al., 2000).

Non-canonical JAK/STAT pathway

Besides the canonical JAK/STAT signaling pathway activation involving Upd/Dome/Hop/STAT92E, JAK/STAT signaling can involve non-canonical activation that has been shown to affect cellular epigenetic status by globally modulating heterochromatin stability (Shi et al., 2006; Shi et al., 2008). Non-canonical JAK/STAT signaling involves non-phosphorylated-STATs localized in the nucleus on heterochromatin in association with heterochromatin protein 1 (HP1), the major component and a determinant of heterochromatin. The heterochromatin-associated unphosphorylated STATs are essential for maintaining HP1 localization and heterochromatin stability. Activation of STATs by phosphorylation reduces the amount of non-phosphorylated STATs localized on heterochromatin, and, in turn, leads to HP1

displacement and heterochromatin destabilization. Phosphorylated-STATs bind to consensus sites in euchromatin to induce transcription of target genes. Genes originally localized in heterochromatin are now accessible to STATs or other transcription factors (Li, 2008). It is not known yet whether activation of STATs always cause heterochromatin destabilization under physiological conditions and it may depend on the intensity of activation signals.

More recently, the same non-canonical mode of STAT activity was identified in mammals. Non-phosphorylated human STAT5A binds to HP1 α and stabilizes heterochromatin and functions as a tumor suppressor capable of repressing multiple oncogenes (Hu et al., 2013). Notably, the majority of genes found to be repressed by non-phosphorylated STAT5A and HP1 α have been implicated in cancer development (Hu et al., 2013). As a transcription factor, activated phosphorylated STAT is found in many cancers. On the other hand, non-phosphorylated STAT5A was now shown to have a tumor suppressor effect via epigenetic gene regulation (Hu et al., 2013). This finding will definitely shed new light into the therapeutic options for treating human cancers (Hu et al., 2013).

Given the high levels of conservation in JAK/STAT signaling pathway, the newly identified regulators and developmental roles discovered in *Drosophila* will improve our understanding of JAK/STAT pathway in mammals and its roles in human diseases. Many studies have identified conserved mechanisms and functions of the JAK/STAT pathway among mammals and *Drosophila*. In particular, JAK/STAT signaling is involved in regulating cell proliferation and stem/germ cell development.

JAK/STAT signaling and the control of cellular proliferation

Conserved roles for JAK/STAT signaling in the regulation of cell proliferation have been found in vertebrates and *Drosophila* (Hou et al., 2002; Arbouzova & Zeidler, 2006). The constitutive activation of the pathway has been observed in multiple human cancers, including blood malignancies and solid tumors (Calo et al., 2003). Similarly, gain-of-function mutations in *Drosophila* JAK/STAT pathway components, such as *hop*^{T42} and *Stat92E*^{ΔNΔC}, also induce tissue overproliferation (Luo et al., 1997; Ekas et al., 2010). Conversely, a reduction in JAK/STAT pathway activity results in a striking decrease in tissue size (Perrimon & Mahowald, 1986; Mukherjee et al., 2005).

The activation of JAK/STAT signaling regulates cell proliferation in multiple tissues, however, the molecular mechanism by which this pathway controls cell division is not yet clear (Arbouzova & Zeidler, 2006). Studies in vertebrates suggest that STAT proteins participate in tumorigenesis through up-regulating genes encoding apoptosis inhibitors such as Mcl-1 and Bcl-x, cell-cycle regulators such as Cyclin D1/D2 and c-Myc, and inducers of angiogenesis such as VEGF. These could contribute to the proliferative effect of JAK/STAT signaling in vertebrates by promoting cell cycle progression or preventing apoptosis (Bowman et al., 2000; Calo et al., 2003).

In *Drosophila*, fluorescence-activated cell sorting (FACS) analysis of cells from eye and wing imaginal discs that have sustained JAK/STAT signaling showed faster G1/S and G2/M cell cycle progression compared to control cells (Bach et al., 2003). These results suggest that JAK/STAT signaling may control the expression or activation of factors involved in cell cycle progression. In fact, Cyclin D-Cdk4 as well as Cyclin E-Cdk2 have

been reported to function downstream of the HOP tyrosine kinase, bind and stabilize STAT92E protein and promote its transcription-activating activity (Chen et al., 2003). Chen et al (2003) demonstrated a role for Cyclin D-Cdk4 in regulating expression of pair-rule genes and pattern formation, independent of effects on cell cycle. JAK/STAT has also been found to induce up-regulation of *CycD* in eye imaginal discs (Tsai & Sun, 2004). However, *Drosophila* CycD-Cdk4 does not act as a direct regulator of the G1/S transition, but instead promotes cellular growth (accumulation of mass) (Datar et al., 2000). Other results indicated that the cell cycle progression could occur in the absence of Cdk4 (Meyer et al., 2000). Furthermore, mutations in genes encoding core cell-cycle regulatory proteins, such as *CycD*, do not reduce the eye overgrowth phenotype induced by ectopic activation of JAK/STAT pathway (Mukherjee et al., 2006). In fact, two independent genetic screens and three independent whole-genome RNAi screens failed to identify a connection between JAK/STAT pathway and genes known to regulate cell proliferation (Bach et al., 2003; Baeg et al., 2005; Muller et al., 2005; Mukherjee et al., 2006). Taken together, although certain links have been suggested, the exact mechanisms how the *Drosophila* JAK/STAT pathway controls cell cycle remain to be elucidated.

JAK/STAT signaling and stem/germ cell maintenance or self-renewal

The identification and the potential use of pluripotent stem cells are of great significance to human health. A thorough understanding of the micro-environment where stem cells are maintained *in vivo* (the so-called stem cell niche) is important for understanding stem cell biology. Several signaling pathways, such as the Wnt and BMP pathways, are found to be required for defining stem cell niches in mammals and *Drosophila* (Li & Xie,

2005). The JAK/STAT pathway is also one of the conserved pathways that regulate stem cell self-renewal in multiple tissues.

It has been reported that the self-renewal of pluripotent embryonic mouse stem cells was mediated by the activation of STAT3 (Niwa et al., 1998). Similarly, the *Drosophila* JAK/STAT pathway is also found to be essential for stem/germ cell maintenance. At early stages of embryogenesis, JAK/STAT signaling is required at multiple stages: in the early blastoderm, STAT92E activity is required for pole cell proliferation (Li et al., 2003); at 6-7 hours after egg laying, STAT92E activity is required for the migration of pole cells towards the embryonic gonads (Li et al., 2003); after 12 hours, the localized expression of JAK/STAT pathway ligands provides guidance for pole cells, which forms the embryonic gonads (Li et al., 2003).

In addition, a role for JAK/STAT signaling in embryonic male gonads has been reported. It has been shown that *upd* ligand expressed in somatic cells of the embryonic testis can induce the activation of STAT92E specifically in the male germ cells (Wawersik et al., 2005). JAK/STAT signaling also plays critical roles in the maintenance and proliferation of the stem cells within adult male and female gonads. In adult *Drosophila* male testis, a small group of somatic cells at the apical tip of testis called the hub expresses *upd* ligand, and self-renewing germline stem cells (GSCs) are arranged around the hub (Tulina & Matunis, 2001). The expression of *upd* in hub cells suggests the requirement of JAK/STAT signaling for maintaining the stem cell state in GSCs. In addition, the ovarian niche also requires JAK/STAT signaling (Decotto & Spradling, 2005). In female *Drosophila* ovary, JAK/STAT signaling is required for the maintenance of the escort

stem cells (ESCs), border cell migration and the development of the polar/stalk cells (Ghiglione et al., 2002; Decotto & Spradling, 2005; Montell et al., 2012).

Recently, JAK/STAT has been shown to control self-renewal of several other stem cell lineages in *Drosophila*, such as intestinal stem cells (ISCs) and renal and nephric stem cells (RNSCs) that are multipotent stem cells identified in Malpighian tubules. The paracrine Unpaired signal from the muscular niche can activate JAK/STAT signaling in *Drosophila* ISCs, thus to regulate ISC self-renewal (Lin et al., 2010). An autocrine JAK/STAT signaling has been reported to regulate self-renewal of RNSCs in *Drosophila* Malpighian tubules (Singh et al., 2007). Besides that, a recent study has shown that JAK/STAT activity is required for optic lobe neuroepithelial maintenance and proliferation (Wang et al., 2011).

Taken together, JAK/STAT signaling regulates self-renewal and maintenance of embryonic stem cells in mammals (Matsuda et al., 1999). This pathway also has intrinsic function to maintain stem cells in *Drosophila*, including GSCs and CySCs (cyst stem cells, also called somatic stem cells [SSCs]) in the testis, escort stem cells in the ovary, neuro-epithelial cells in the optic lobe of the brain, intestinal stem cells in the midgut, and renal and nephric stem cells in Malpighian tubules (Tulina & Matunis, 2001; Decotto & Spradling, 2005; Singh et al., 2007; Lin et al., 2010; Wang et al., 2011). Based on those facts, we may say that JAK/STAT signaling is a general stem cell signaling, which might also regulate stem cell self-renewal in other systems. However, in these stem cells whose maintenance depends on JAK/STAT signaling, the effector genes activated by Stat92E that regulate self-renewal are largely unknown, except *zfh1* and *chinmo*, which were

found to be two Stat92E-regulated genes required for CySC self-renewal (Leatherman & Dinardo, 2008; Flaherty et al., 2010). Therefore, identifying more JAK/STAT downstream effector genes that mediate stem cell self-renewal is important for stem cell research.

The Hippo signaling pathway: a key regulator for organ size control

Hippo signaling pathway in *Drosophila*

First discovered in *Drosophila*, the Hippo signaling pathway has been identified as a conserved regulatory pathway essential for the proper control of organ growth in *Drosophila* and vertebrates. The pathway is shown to promote cell death and suppress cell proliferation (Halder & Johnson, 2011). The first four components of the Hippo pathway were discovered from genetic screens for tumor suppressor genes in *Drosophila*. They are the protein kinase Warts (Wts) (Justice et al., 1995; Xu et al., 1995), the co-factor Salvador (Sav) (Tapon et al., 2002), the protein kinase Hippo (Hpo) (Wu et al., 2003), and the adaptor protein Mob-as-tumor-suppressor (Mats) (Lai et al., 2005). These four tumor suppressors form a kinase cascade, in which Hpo in complex with Sav phosphorylates Wts and its co-factor Mats, thereby activating Wts kinase activity (Wu et al., 2003). The prime target of this kinase cascade is transcription coactivator Yorkie (Yki), which was identified as a Hippo pathway component in a yeast two-hybrid screen for Wts-binding proteins (Huang et al., 2005). Yki has oncogenic activity, when not inhibited, it translocates to the nucleus, forms an active complex with transcription factors and induces the expression of target genes, such as the cell cycle regulator *CycE*, the apoptosis inhibitor *Diap1*, the growth and cell survival-promoting miRNA *bantam* and the growth promoter *Myc*, and by doing so increases cell proliferation and inhibits apoptosis. Phosphorylation of Yki by warts prevents Yki from entering the nucleus and therefore inhibits cell proliferation and promotes apoptosis (Dong et al., 2007). In addition to the core components of the Hippo pathway, several additional tumor suppressors whose activities converge on Hpo and/or Wts have been identified. These

include Merlin (Mer) and Expanded (Ex), which were identified as upstream regulators of Hpo (Hamaratoglu et al., 2006), Kibra, another tumor suppressor that regulates Hippo signaling in conjunction with Mer and Ex (Yu et al., 2010), the transmembrane protein Fat (Ft) (Bennett & Harvey, 2006), which functions by binding to an atypical cadherin called Dachous (Ds) (Matakatsu & Blair, 2006), the kinase Discs overgrown (Dco), which phosphorylates the intracellular domain of Ft and is regulated by Ds (Sopko et al., 2009), and an apical transmembrane protein Crumbs (Crb), which regulates the Hippo signaling via binding to Ex (Robinson et al., 2010).

Although the upstream components seem complex, they converge on and signal through one downstream effector, the transcription coactivator Yki (Dong et al., 2007). Several DNA-binding partners for Yki have been reported, such as Scalloped (Sd) that regulates the expression of *Diap1* (Wu et al., 2008), and Homothorax (Hth) that regulates the expression of the microRNA *bantam* (Peng et al., 2009). The expression of three classes of genes is regulated by loss of Hippo signaling or increase of Yki activity. The first class of genes are involved in cell proliferation or survival, such as *Diap1* (Wu et al., 2008), the microRNA *bantam* (Thompson & Cohen, 2006), the cell cycle regulators *CycE* (Tapon et al., 2002) and *E2f1* (Goulev et al., 2008), and involved in cell growth control, such as ribosome biogenesis and cell growth regulator *dMyc* (Pan, 2010). The second class corresponds to genes encoding upstream regulators of the Hippo pathway, such as Kibra, Ex, Crb, which suggests the existence of a negative feedback loop involving the regulation of the expression of upstream regulators of the pathway (Pan, 2010). The third class of genes play a role in crosstalk between the Hippo pathway and other cell signaling, such as Serrate (a Notch ligand) and Wingless (Cho et al., 2006), Vein (an

EGFR ligand) (Zhang et al., 2009), and Unpaired1/2/3 (Upd1/2/3, the JAK/STAT pathway ligands) (Ren et al., 2010; Staley & Irvine, 2010). Figure 1-2 illustrates the Hippo signaling pathway in *Drosophila*.

Hippo signaling pathway in mammals

Hippo signal transduction in mammals is analogous to that seen in *Drosophila*. The core kinase cascade includes the kinases MST1 and MST2 (homologs of Hpo) and their regulatory protein WW45 (also known as SAV1, Sav homolog), which interact to form an activated complex. Activated MST1/2 can directly phosphorylate LATS1 (*large tumor suppressor kinase 1*) and LATS2 (Wts homologs) (Chan et al., 2005; Dong et al., 2007). LATS1/2 are regulated by MOB1 (homologs of Mats), which are also phosphorylated by MST1/2 to enhance binding in the LATS1/2-MOB1 complex (Praskova et al., 2008). In response to high cell densities, activated LATS1/2 phosphorylates transcriptional coactivators YAP at Ser127 and TAZ at Ser89, promoting their 14-3-3 binding and inhibiting their translocation into the nucleus (Dong et al., 2007; Zhao et al., 2007; Lei et al., 2008). Uninhibited YAP/TAZ go to the nucleus, functioning as coactivators for the TEA-domain family member (TEAD) group of transcription factors (Zhang et al., 2009). Several direct target genes of YAP-/TAZ-TEAD have been identified, such as *CTGF* and *Cyr61* (Zhao et al., 2008). Besides TEADs, YAP/TAZ may also associate with other transcription factors, such as Smad1 (Alarcon et al., 2009), Smad2/3 (Varelas et al., 2008), Smad7 (Ferrigno et al., 2002). Together, the YAP/TAZ-transcription factor complex mediates transcription of diverse genes and results in accelerated proliferation, resistance to apoptosis and massive organ overgrowth. Although the signal transduction within the core kinase cascade is well defined, the detailed mechanisms how various

upstream regulators are sensed by core kinase cascade are not as well understood (Ramos & Camargo, 2012). The known upstream components involved in the Hippo pathway include: cell polarity (apical-basal polarity, planar cell polarity), extracellular matrix and cytoskeleton to sense mechanical cues, and G-protein-coupled receptor (GPCR) signaling to sense diffusible signals. Actin cytoskeleton or cellular tension seems to be the key mediator that transmits upstream signaling to the core Hippo signaling cascade (Yu & Guan, 2013).

Hippo signaling pathway and tissue regeneration, stem cell self-renewal and expansion

Besides its roles in limiting organ size by inhibiting proliferation and promoting apoptosis, more evidence suggests roles of the Hippo pathway in stem cell and progenitor cell self-renewal and expansion. For example, YAP/TAZ controls embryonic stem cell self-renewal in response to TGF β /BMP (transforming growth factor beta/bone morphogenetic protein) signaling (Varelas et al., 2010). In addition, YAP is activated in induced pluripotent stem cells (iPS) and inactivated during mouse embryonic stem cell differentiation (Lian et al., 2010). In mouse embryonic stem cells, YAP knockdown causes loss of pluripotency, whereas ectopic expression of YAP prevents embryonic stem cell differentiation (Lian et al., 2010). The Hippo pathway is also shown to regulate tissue-specific progenitor cells. Normally YAP expression is only detected in the progenitor cells in mouse intestines. Ectopic YAP expression in mouse intestines leads to expansion of the progenitor cell compartment (Camargo et al., 2007). Similarly, YAP ectopic expression causes expansion of basal epidermal progenitors in mouse skin, while

knockout of YAP in mouse skin leads to decreased cell proliferation and failure of skin expansion (Schlegelmilch et al., 2011).

Additionally, the Hippo pathway was recently shown to regulate tissue regeneration. In the *Drosophila* midgut, Yki expression is mainly detected in intestinal stem cells (ISCs) (Karpowicz et al., 2010). Under resting conditions, inactive Yki is mostly localized to the cytoplasm. In response to injury, increased nuclear-localized Yki induces ISC proliferation cell-autonomously (Karpowicz et al., 2010). Furthermore, the Hippo pathway is inactivated in enterocytes (a differentiated cell type in the *Drosophila* midgut) in response to damage, resulting in Yki activation and subsequent expression of Upd1/2/3 (Ren et al., 2010; Staley & Irvine, 2010). This activates JAK/STAT signaling in ISCs, thereby promoting ISC proliferation in a non-cell-autonomous manner. Similarly mammalian YAP is also shown to regulate tissue regeneration. It is shown that YAP expression is required for the intestinal regeneration after dextran sodium sulfate-induced injury (Cai et al., 2010).

In conclusion, many studies have revealed the roles of the Hippo pathway in organ size control and tissue regeneration in *Drosophila* and mammals. Therefore, Hippo pathway can be a useful target in cancer therapy and regenerative medicine. Identification of the upstream regulators and downstream targets of this pathway and understanding of the mechanism of signaling regulation, are important for the therapeutic designs (Zhao et al., 2011).

Cell cycle control

Cell cycle control system in eukaryotic cells

Uncontrolled cell proliferation is a hallmark of tumorigenesis. Mechanisms controlling cell cycle progression are highly conserved due to the existence of conservatory molecules such as Cyclins, cyclin dependent kinases (Cdks), Cdk inhibitors (CKI) (Golias et al., 2004). These processes and mechanisms are deregulated in tumors.

Understanding the molecular basis of the cell cycle regulation in normal and cancer cells provides insight into potential therapeutic strategies.

It has been 63 years since Howard and Pelc first described the cell cycle and its phases in 1951 (Howard & Pelc, 1951). Their studies concluded that the cell cycle of most eukaryotic cells could be divided into four main phases: G1, S, G2, and M. G1 is the preparatory phase during which cells prepare for the process of DNA replication. During G1 phase, cells integrate growth-inducing or growth-inhibitory signals and make the decision to proceed, pause, or exit the cell cycle. S phase is the period of DNA synthesis, which is separated from mitosis by an interval of several hours, called G2. G2 is the second gap phase during which cells prepare for the process of division. M phase includes two major events: nuclear division (Mitosis) in which the replicated chromosomes are segregated into separate nuclei, and cytoplasmic division (cytokinesis). Mitosis can be subdivided into: prophase, prometaphase, metaphase, anaphase, and telophase, each with clearly distinctive features. In addition to G1, S, G2, and M, the term G0 refers to quiescent cells that have exited the cell cycle (Rieder, 2011).

Elaborate cell cycle regulation is critical to ensure normal development of multicellular organisms. Failure to coordinate such processes often leads to birth defects and cancer. Accordingly, cell cycle is tightly controlled by many regulatory events that either permit or restrain its progression (Golias et al., 2004). The eukaryotic cell cycle is primarily regulated by the periodic synthesis and destruction of Cyclins that associate with and activate Cdks, thereby causing the sequential activation and inactivation of Cdks (Johnson & Walker, 1999). Cyclins are so-named because their concentrations vary in a cyclical fashion during the cell cycle. Nine Cdks (Cdk1-9) and at least 16 Cyclins (A, B1, B2, C, D1, D2, D3, E, F, G1, G2, H, I, K, T1, and T2) have been identified in mammalian cells (Johnson & Walker, 1999). All Cyclins have a common region known as the cyclin box, which is used to bind and activate Cdks. However, not all Cyclins and Cdks regulate the cell cycle. Other functions include regulation of transcription, DNA repair, differentiation, and apoptosis (Johnson & Walker, 1999).

The D-type Cyclins are the first ones to be induced by mitogens when G0 cells enter the cell cycle (Sherr, 1994). D-type Cyclins associate with and activate Cdk4 and Cdk6. The primary substrate for Cdk4 and Cdk6 is the retinoblastoma tumor suppressor protein (Rb) (Lukas et al., 1995). The Rb protein has a critical function in regulating G1 progression, it has been shown to bind and regulate the E2F family of transcription factors (Johnson & Schneider-Broussard, 1998). E2F transcription factors regulate the expression of many genes encoding proteins required for cell cycle progression and DNA synthesis, such as Cyclins E and A, Cdk1, B-myb, dihydrofolate reductase, thymidine kinase, and DNA polymerase α . Rb binding to E2F transcription factors inhibits their activity. Phosphorylation of Rb by D-type Cyclin kinases results in the release of Rb from E2F,

which therefore activates the expression of the E2F target genes (Johnson & Walker, 1999). Then through the activation of E2F, the next Cyclin to be induced during the cell cycle progression is Cyclin E (Ohtani et al., 1995; Geng et al., 1996). Cyclin E binds to Cdk2, and Cyclin E/Cdk2 kinase complex is essential for the G1-to-S phase transition (Ohtsubo et al., 1995). Also, Cyclin E/Cdk2 is involved in maintaining Rb in the hyperphosphorylated state, and thus helps to positively accumulate active E2F (Hinds et al., 1992). Another Cyclin that accumulates during G1/S transition and S phase is Cyclin A. Cyclin A first associates with Cdk2, and then associates with Cdk1 in late S phase. Cyclin A-associated kinase activity is required for both entry into and completion of S phase, as well as entry into M phase (Lehner & O'Farrell, 1989; Girard et al., 1991; Walker & Maller, 1991). However, whereas Cyclin E positively regulates E2F activity, Cyclin A-associated kinases can inhibit the E2F DNA-binding activity through phosphorylating the E2F heterodimerization partner DP1. Then, the G2 phase has a checkpoint that responds to DNA damage, which allows DNA repair before the cell divides. Mitosis phase is regulated by Cdk1/Cyclins A, B1, and B2, whose activities phosphorylate cytoskeleton proteins (Arellano & Moreno, 1997). Cyclins A and B must be degraded for cells to exit mitosis. Cells then again enter G1 phase after mitosis, and must decide whether to exit the cell cycle or proceed into another cell cycle.

There are two families of Cdk inhibitors (CKI) that regulate CDK activity: INK4 family, such as INK4A (p16), INK4B (p15), INK4C (p18) and INK4D (p19), and the Cip/Kip family, including p21, p27 and p57 (Malumbres & Barbacid, 2009). INK4 proteins specifically bind to Cdk4 and Cdk6 and prevent the association of Cdk4 and Cdk6 with D-type Cyclins. In contrast, p21, p27, and p57 can interact with a variety of Cyclin/Cdk

complexes (Johnson & Walker, 1999). The promoter of *p21* contains a binding site for the p53 tumor suppressor protein, which allows p53 to transcriptionally activate the *p21* (el-Deiry et al., 1993). Induction of p21 inhibits cell cycle progression by inhibiting a variety of Cyclin/Cdk complexes. In addition, p21 can inhibit DNA synthesis and allow DNA repair (Li et al., 1994). Therefore, p21 is a critical mediator of p53's response to DNA damage through its ability to inhibit cell cycle progression but allow DNA repair. The p53 tumor suppressor protein is an important cell cycle check-point regulator at both G1/S and G2/M check points. It is known that the *p53* tumor-suppressor gene is the most frequently mutated gene in human cancer cells, suggesting its crucial role in normal cell cycle control. In addition, genes important for the progression of G0 cells through G1 and S phase, are often subject to genetic and epigenetic changes in many human cancers, such as *Cyclin D1*, *Cyclin D2* and *D3*, several *E2F* genes, and *Cyclin E* (Johnson & Walker, 1999).

Regulation of cell cycles in *Drosophila*

A critical aspect of cell cycle regulation is how cell growth and cell division are coordinated with developmental signals to properly pattern organisms of the appropriate size. Using *Drosophila melanogaster* as model system, considerable progress has been made to identify new cell cycle regulators that respond to developmental signals, and to define the impact of extrinsic cues on homologs of mammalian oncogenes and tumor suppressors. Most mammalian oncogenes and tumor suppressors are highly conserved. And in *Drosophila* as in mammalian cells, G1/S and G2/M transitions are controlled by Cyclin/Cdk complexes. Here I highlight several major differences from mammalian systems.

In mammalian cells, Cyclin E and Cyclin D are crucial for the G1/S cell cycle transition. Cyclin D expression is induced by growth factors, and Cyclin D/Cdk4 or Cdk6 complexes promote G1/S progression by phosphorylating and inactivating Rb tumor suppressor. However, *Drosophila* Cyclin D mainly regulates growth but does not drive G1/S progression. Cyclin E is the key regulator of the G1/S transition in *Drosophila* (Datar et al., 2000; Meyer et al., 2000). The promoter of *Cyclin E* contains many regulatory elements responsive to developmental signals (Jones et al., 2000). Thus the transcriptional regulation of *Cyclin E* provides an important way to regulate cell proliferation in tissue- and stage-specific manner.

In mammalian cells, the E2F transcription factor is a key regulator of G1/S transition. E2F associates with DP, activates transcription of *Cyclin E* and other genes encoding replication proteins. Sequential phosphorylation of Rb by Cyclin D/Cdk4 or Cdk6 and then by Cyclin E/Cdk2 leads to Rb dissociation from E2F, thereby activate E2F. In contrast, E2F plays a minor role in G1/S transition in *Drosophila* (Lee & Orr-Weaver, 2003). There are two E2F transcription factors (E2F1 and E2F2), a single DP subunit, and two Rb family proteins (RBF1 and RBF2) in *Drosophila*. dE2F1 is a transcriptional activator, whereas dE2F2 acts as a repressor (Frolov et al., 2001). dE2F1 and dE2F2 both heterodimerize with dDP and bind to the promoters of target genes *in vivo*. dE2F1 activates transcription, and the loss of *dE2f1* results in compromised cell proliferation. In contrast, dE2F2 represses gene transcription and loss of *dE2f2* results in increased gene expression. The effect of E2F on cell proliferation is a result of the interplay between two types of E2F complexes with antagonistic activities (Frolov et al., 2001).

In addition to the insights into the regulation of known cell cycle regulators in response to various developmental cues, the recovery of new cell cycle mutants in *Drosophila* will help to identify additional regulatory factors with essential roles in human cell cycle progression.

Cell apoptosis pathway

The process of programmed cell death, or apoptosis, occurs normally during development and aging, and is a homeostatic mechanism to maintain proper cell populations in tissues. Apoptosis also occurs as a defense mechanism in immune responses or when cells encounter damage. A wide variety of physiological and pathological stimuli can trigger apoptosis in specific cells. Apoptosis is a coordinated process that involves the activation of a group of cysteine proteases called “caspases”, and a cascade of events from the initiating stimuli to cell death. Three apoptotic pathways have been characterized to date: the extrinsic or death-receptor pathway, the intrinsic or mitochondrial pathway, and perforin/granzyme pathway involving T-cell mediated cytotoxicity and perforin-granzyme-dependent killing of cells. The extrinsic, intrinsic, and perforin/granzyme pathways activate their own initiator caspase (8, 9, and 10, respectively) that in turn converge on and activate the executioner caspase-3. The execution pathway results in cell shrinkage, chromatin condensation, DNA fragmentation, degradation of cytoskeletal and nuclear proteins, extensive protein cross-linking, formation of apoptotic bodies, expression of ligands for phagocytic cell receptors and finally uptake by phagocytic cells (Elmore, 2007).

Many pathological conditions involve excessive apoptosis, such as neurodegenerative disease, AIDS, and ischemia. It is thus important to look into the ways to inhibit apoptosis. The inhibitors of apoptosis proteins (IAP) is a family of proteins with the most important inhibitors of apoptosis. They can regulate both the intrinsic and extrinsic pathways (Deveraux & Reed, 1999). IAPs are highly conserved throughout evolution and eight have been identified in humans. IAP proteins have one to three conserved protein

motifs named baculovirus IAP repeat (BIR), which are important for IAPs binding to IAP-binding motifs (IBM) in the active subunits of apoptotic protease caspases (Dubrez et al., 2013).

In *Drosophila*, the induction of apoptosis needs the activity of three closely linked genes, *reaper*, *hid* and *grim* (White et al., 1994; Grether et al., 1995; Chen et al., 1996). In response to diverse death-inducing signals, *reaper*, *hid* and *grim* are transcriptionally regulated. The proteins encoded by *reaper*, *hid* and *grim* activate cell death by forming a complex with the *Drosophila* IAP1 (DIAP1) protein, thereby inhibiting its anti-apoptotic activity (Goyal et al., 2000). The double inhibition suggests that *Diap1* is required to keep the caspases and apoptosis in check. In *Drosophila*, two IAP homologs, *Diap1* and *Diap2* have been found (Hay et al., 1995; Duckett et al., 1996; Uren et al., 1996). *Diap1* is encoded by the *thread* (*th*) locus, and *Diap1* loss-of-function mutations are lethal, enhancing the cell death induced by *reaper*, *hid* and *grim* (Hay et al., 1995). In contrast, ectopic expression of *Diap1* or *Diap2* suppresses apoptosis (Hay et al., 1995).

***Drosophila* mushroom body: an excellent model to study genes essential for neuronal morphogenesis**

The early history of mushroom body research

Mushroom bodies were first described in bees and ants in 1850 by a French biologist Dujardin, who called them corps pedoncules due to their appearance being similar to the fruit bodies of lichens (Dujardin, 1850). They are a pair of prominent structures comprising thousands of densely packed parallel neurons [Kenyon cells, named after Kenyon in 1896] running on either side of the group of neuropils found along the midline of the brain of the insect called the central complex, and from back to front and downward through the protocerebrum (Heisenberg, 1998). Structures with such morphological characteristics were found in many marine annelids (such as scale worms, sabellid worms, and nereid worms) and almost all the arthropod brains, except crustaceans (Strausfeld et al., 1998). Much of what is known about mushroom bodies comes from studies of a few insect species: the honeybee, fly (*Drosophila*), cricket, grasshopper, locust, and cockroach (*Periplaneta*). The mushroom bodies of the insect brain consist of the cell bodies followed by a cup-shaped protrusion called the calyx, stalk, or peduncle and finally two lobes extending in roughly orthogonal directions (medial and vertical) (Heisenberg, 1998). The size and shape of mushroom bodies differ greatly among the insects. The number of Kenyon cells range from 2500 in *Drosophila* to 200,000 in *Periplaneta* (Heisenberg, 1998).

When Dujardin first described the mushroom bodies, he compared them to the vertebrate cerebral cortex and attributed to them a role in intelligent behavior. It took nearly 150 years to establish that mushroom bodies are indeed involved in insect learning and

memory. The comparative studies of social Hymenoptera indicate that workers and queens with relatively large mushroom bodies show the broader range of behaviors compared to drones with relatively small mushroom bodies (Strausfeld et al., 1998). Later, more studies suggested that mushroom bodies play crucial roles in learning and memory. Such studies include: lesion experiments involving the mushroom bodies of ants that perturbed their ability to negotiate a maze using olfactory cues; In *Drosophila* ablation of four mushroom body neuroblasts that generate all the postembryonic Kenyon cells by the cytostatic drug hydroxyurea (HU) resulted in flies able to perceive but not remember odors (de Belle & Heisenberg, 1994); and ablation of the pedunculus and medial lobes of *Periplaneta* affected their performance of place-memory tests, suggesting a role of mushroom bodies in spatial orientation. Studies on honeybees and *Drosophila* established that mushroom bodies harbor the cellular basis for associative memory. Studies on *Drosophila* involved mutagenesis to identify strains that are defective in odorant-driven behavior. Mutant lines with defective odorant-driven behavior were examined for neural morphology and molecular correlates and some were found to have morphologically altered mushroom bodies (Quinn et al., 1974). Another strategy involved screening for mutations resulting in structural defects of the brain, and subsequently testing them for behavioral defects. For example, *mushroom bodies deranged* and *mushroom bodies reduced* are two of the mutations in which structural defects of the mushroom bodies correlate with defects in olfactory conditioning (Heisenberg, 1980; Heisenberg et al., 1985). Actually, the intellectual momentum in learning and memory research on insects at the time of those studies has largely been from studies involving genetic and experimental induction of structural defects in

mushroom bodies, which were found to be correlated with learning and memory deficits (Strausfeld et al., 1998).

The function of the mushroom bodies in insect behavior

It has been suggested that mushroom bodies are most analogous to the vertebrate hippocampus, because both of them are involved in similar types of learning and memory, for example, place memory in mammals (Muller, 1996) and cockroaches. It has also been shown that both mammalian hippocampus and *Drosophila* mushroom bodies have elevated expression levels of various learning-related molecules (Kandel & Abel, 1995).

Remarkably, insects with malformed mushroom bodies or even without mushroom bodies, behave quite normally in many respects. They eat, defend themselves, walk, fly, court, copulate, reproduce, and learn in many situations (Wolf et al., 1998). However, loss or alteration of the mushroom bodies has been discovered to cause dramatic behavioral defects in several behavioral experimental paradigms such as olfactory discrimination (de Belle & Heisenberg, 1994), courtship conditioning (McBride et al., 1999), context generalization in visual learning (Liu et al., 1999), choice behavior (Tang & Guo, 2001), sleep regulation (Joiner et al., 2006; Pitman et al., 2006), and habit formation regulation (Brembs, 2009), as well as a non-learning function in the control of walking activity (Zars, 2000).

The olfactory systems of insects have a number of features that make them worthy models for the study of vertebrate olfaction. While the organizational logic remains similar, the olfactory system of insects is substantially reduced in scale compared to

vertebrate systems (Hildebrand & Shepherd, 1997). *Drosophila melanogaster* is particularly useful as a model because there are highly sophisticated molecular and genetic tools available. In the *Drosophila* olfactory system, olfactory information flows linearly from the site of transduction on the dendrites of the olfactory receptor neurons (ORNs) to the olfactory glomeruli of the antennal lobe (AL). There, local interneurons (LNs) mediate interactions between glomeruli, and then reformat this information pattern. The reformatted information is then transferred by projection neurons (PNs) to the dendritic region of the mushroom body (MB) and also to the lateral horn (LH) (Jefferis et al., 2002).

The cellular organization and the development of the *Drosophila* mushroom bodies

The *Drosophila* mushroom body is a paired neuropile structure in the brain. Each mushroom body is composed of about 2500 neurons called Kenyon cells. Mushroom bodies were shown to originate from four mushroom body neuroblasts per hemisphere in the embryonic brain, each giving rise to an identical set of mushroom body neurons and glia (Ito et al., 1997). Mushroom body neuroblasts exit the state of quiescence and start to divide during embryonic stage 9 (Noveen et al., 2000) and continue until the late pupal stages, giving rise to three distinct types of mushroom body neurons in succession: γ , α'/β' , and α/β neurons, respectively (Lee et al., 1999). Mushroom body neurons born in embryos and early larvae belong to the γ class, neurons born in late larvae belong to the α'/β' class, and those born after puparium formation belong to the α/β class (Lee et al., 1999). The subtype switch from γ to α'/β' neurons and from α'/β' to α/β neurons, occur abruptly and completely. In addition to Kenyon cells, the four mushroom body

neuroblasts also give rise to a small population of glia in the Kenyon cell cortex (Ito et al., 1997).

Drosophila mushroom body neuroblasts and Kenyon cells arising from them lie on the dorsoposterior surface of the brain. Each mushroom body neuron projects a neurite extending ventroanteriorly into the dendritic calyx, where it receives input from the antennal lobes via the projection neurons (Crittenden et al., 1998). An axon from each neuron is also sent in a ventro-anterior direction, fasciculating with other mushroom body axons with younger axons lying interior to older ones; this collection of axons constitutes the peduncle. From the peduncle, axons of different types of mushroom body neurons enter their distinct axonal lobes at the anterior surface of the brain. All axons bifurcate into two branches with one dorsal and one medial branch, except those of the γ neurons in adults (Jefferis et al., 2002). During metamorphosis, the early born γ neurons prune their larval-specific projections and re-extend projections only towards the midline, forming the adult γ lobe. The α'/β' neurons born during the late third instar larval stage, as well as the α/β neurons born after puparium formation, maintain both of their dorsal and medial lobes in adults (Lee et al., 1999). The significance of this morphological arrangement is poorly understood.

The gross morphology of the mushroom bodies is plastic. Rudimentary mushroom bodies that are morphologically similar to adult mushroom bodies first become apparent between embryonic stages 14 and 17. Throughout the larval stages they continue to grow by adding newly born Kenyon cells. During metamorphosis, much of the larval brain is remodeled by a process of neural degeneration and regrowth. In the case of mushroom

bodies, there are significant structural differences between the larval and adult neurons, resulting from the large-scale reorganization during metamorphosis. The γ lobe, which is projected from Kenyon cells of embryonic and larval origins, store information of relevance to both larval and adult developmental stages (Armstrong et al., 1998). And the α/β neurons that arise starting from puparium formation obviously play adult specific roles. It is interesting that α/β neurons comprise the largest volume of neurons (42%) and their axons are the most densely packed (Lee et al., 1999). The α'/β' neurons that arise in late larval stages may play important roles in the transition between the larval and adult mushroom body with respect to axon guidance, and the maintenance of the established connections with input and output neurons (Lee et al., 1999). The function of α'/β' neurons in axon guidance may be analogous to that of the subplate neurons in mammalian cerebral cortical neurons. But unlike the subplate neurons, the α'/β' neurons themselves are not pioneer neurons. Their roles are more likely to transfer the routes established by the pioneering γ neurons to the later-born α/β neurons (Lee et al., 1999). A recent study suggests that neurotransmission from mushroom body α'/β' neurons is required to acquire and stabilize aversive and appetitive odor memory. In contrast, neurotransmission from α/β neurons is exclusively required to retrieve memory (Krashes et al., 2007).

Mushroom body neuroblasts

The *Drosophila* mushroom body neuroblasts originate from a specific mitotic domain of procephalic neuroectoderm during embryogenesis. Subsequently, each mushroom body neuroblast occupies a distinct position and expresses a specific combination of transcription factors in the developing mushroom body cortex. Therefore they are

individually identifiable in the brain neuroblast map. During embryonic development, each mushroom body neuroblast produces an individual cell lineage comprising intrinsic γ neurons and other non-intrinsic neurons. This is different from the postembryonic mushroom body neuroblast development, during which four neuroblasts produce identical populations of intrinsic neurons (Kunz et al., 2012).

The *Drosophila* larval brain contains ~200 neural stem cells called neuroblasts. A neuroblast divides asymmetrically to form two distinct daughter cells that differ in size and fate. The larger cell maintains all features of a neuroblast and continues to proliferate, whereas smaller daughter cell is called the ganglion mother cell which divides either once to produce two post-mitotic neurons (type I neuroblasts) or several times to produce multiple post-mitotic neurons (type II neuroblasts) (Boone & Doe, 2008). All neurons in a mushroom body are generated from four equivalent type I neuroblasts. Most *Drosophila* neuroblasts disappear before late larval stages and generate only a few dozen neurons. However, a mushroom body neuroblast sequentially generates hundreds of neurons from the embryonic, larval, pupal, until early adult stages (Armstrong et al., 1998; Lee et al., 1999). Furthermore, the mushroom body neuroblasts are four of the five neuroblasts that are actively dividing at the time of larval hatching (Ito & Hotta, 1992). This characteristic led to the development of the chemical ablation technique for mushroom body cells by feeding the DNA-synthesis inhibitor hydroxyurea to newly hatched larvae. This technique is later widely used to examine the role of the mushroom body in various behavioral assays (de Belle & Heisenberg, 1994).

MARCM technique facilitates mushroom body studies

Mosaic analysis with a repressible cell marker (MARCM) is a genetic technique that permits the efficient creation of genetically marked clones of cells by mitotic recombination and was first developed for mushroom body studies by combining the *FLP/FRT* induced mitotic mosaic technique with a *GAL80/GAL4/UAS* mediated gene expression system (Lee & Luo, 1999). Figure 1-3 illustrates how the MARCM system works. The system starts with cells heterozygous for a transgene encoding the yeast GAL80 repressor protein that inhibits the activity of the GAL4 transcription factor. Following *FLP/FRT*-induced mitotic recombination, the GAL80 repressor gene will be absent in one of two daughter cells, thus allowing activation of GAL4-driven reporter gene expression in this daughter cell and all its progeny. If there is a mutation located on the chromosome arm *in trans* to the GAL80-containing chromosome, the uniquely labeled GAL80-negative cells will be homozygous for this mutation. When applied to the CNS of *Drosophila*, one can generate clones of different sizes depending on when mitotic recombination occurs and which cell loses the repressor. If FLP induced mitotic recombination occurs prior to the neuroblast division, half of the chance the new daughter neuroblast will be devoid of the GAL80 repressor and positively labeled. Thus, all the subsequent progeny are labeled as long as the GAL4 protein is expressed continuously in all neurons to form a large clone of labeled neurons, called a neuroblast clone. If the GMC or postmitotic neuron is devoid of the repressor transgene, only one or two neurons will be positively labeled, named single-cell or 2-cell clones (Lee & Luo, 1999).

The MARCM clone of mushroom body neuroblast generated at early developmental stages allows us to follow one mitotic neuron stem cell from embryonic to late pupal stages, which provides a fantastic model to study many aspects of neuron development,

such as neuron morphogenesis, neuron remodeling, and neuron differentiation. Since its establishment, the MARCM system has allowed researchers to identify many genes necessary for *Drosophila* neuronal morphogenesis. Through MARCM-based genetic screens, a number of genes that are required for distinct aspects of mushroom body neuronal development has been isolated. Such examples include: *Dscam* is required for normal axonal bifurcation and segregation (Wang et al., 2002; Wang et al., 2004); *TGF- β* signaling controls γ neuron remodeling (Zheng et al., 2003); and *polyhomeotic* controls neuronal identity and cell proliferation (Feng et al., 2011; Feng et al., 2012). The same kind of genetic mosaic screen described above also allowed me to reveal that JAK/STAT pathway is required for the mushroom body neurogenesis, which will be thoroughly discussed in this dissertation.

Figure 1-1. The *Drosophila* JAK/STAT signaling pathway (Adapted from (Amoyel & Bach, 2012))

The *Drosophila* JAK/STAT pathway can be activated by three ligands Unpaired (Upd) (orange). Upd binding activates the receptor Domeless (Dome) (magenta) and the associated JAK kinase Hopscotch (Hop) (green). Activated JAK leads to tyrosine phosphorylation (brown circles) of Dome, which then recruits and phosphorylates Stat92E (blue). Active Stat92E dimer translocates into nucleus, binds to TTCNNNGAA consensus site, and regulates target gene expression. The known target genes of JAK/STAT pathway include *Socs36E*, *zfh1*, and *chinmo*. Socs36E (pink) negatively regulates Dome or Hop activity. A second short receptor Eye Transformer also called Latran (Et/Lat) (red) inhibits JAK/STAT signaling by forming heterodimer with Dome.

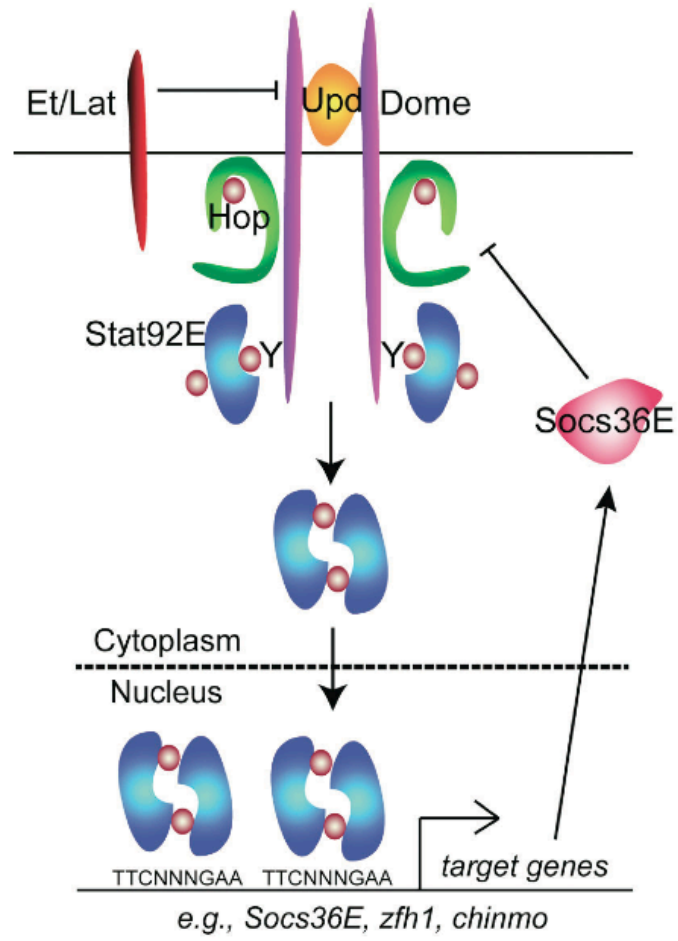


Figure 1-1

Figure 1-2. The *Drosophila* Hippo signaling pathway (Adapted from (Zhao et al., 2011))

Arrowed ends indicate activation, blunted ends indicate inhibition, and dashed lines indicate unknown mechanisms.

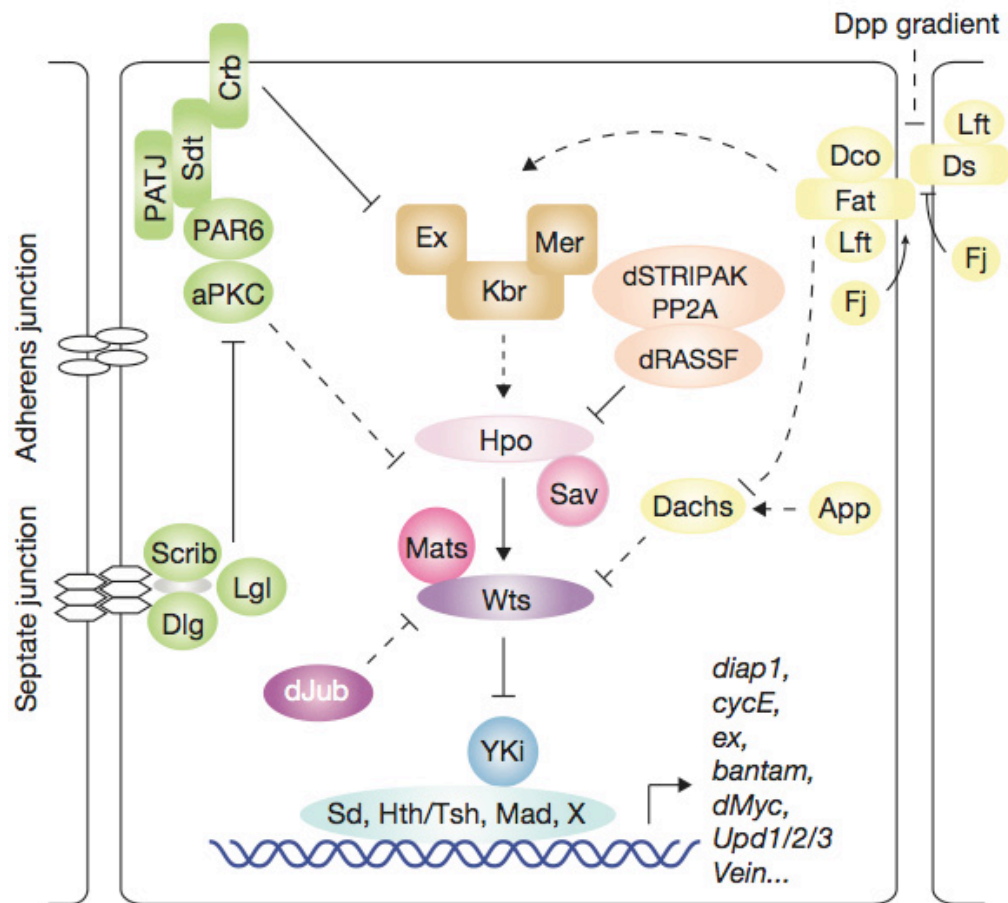


Figure 1-2

Figure 1-3. Schematic illustration of the GAL80/GAL4/UAS expression system and the MARCM system (Adapted from (Wu & Luo, 2006))

- a, In cells with the GAL80 repressor protein, GAL4 dependent expression of *UAS-GFP* is suppressed. In the absence of GAL80 repressor protein, GAL4 dependent expression of *GFP* is activated, thus the cells are positively labeled.
- b, Upon the FLP-induced mitotic recombination at *FRT* sites (black arrowhead), one type of daughter cell will be homozygous mutant that is devoid of the GAL80 repressor protein, thus the GAL4 dependent expression of *UAS-GFP* will positively label this cell and its progeny.

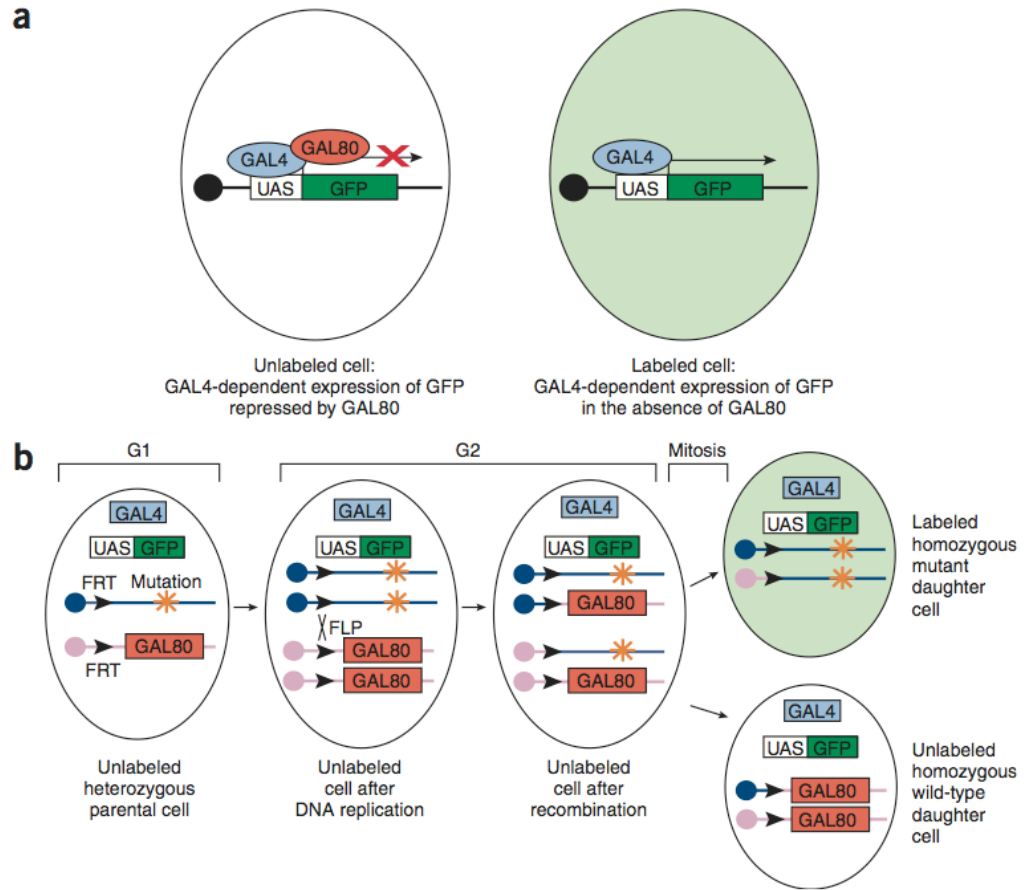


Figure 1-3

Chapter 2: A MARCM-based genetic screen for genes necessary for *Drosophila* mushroom body neuronal morphogenesis

Abstract

To identify genes important for different aspects of neuronal morphogenesis, I performed a genetic screen using the MARCM technique in the mushroom body neurons of the *Drosophila* brain. Mutations on the chromosome X or the right arm of chromosome 3 were made homozygous in the progeny of uniquely labeled mushroom body neuroblasts. ~250 independent lines were screened. 8 lines showed defects in mushroom body morphogenesis. The most frequently observed phenotypes involved the reduction or elimination of specific neuron types. Further investigation into these lines and the associated genes will surely provide insights into the functions of these genes in neurogenesis. I focused my dissertation research on a mutation line *dome*^{G0405} that caused a severe γ -only phenotype.

A small-scale genetic screen for genes required for mushroom body development

The neuronal system is extremely complex and accurate. Generation of complicated neuronal circuit involves many biological processes, such as cell proliferation, cell differentiation, cell degeneration, neuron remodeling, axon guidance and axon bifurcation. Many genes essential for neuronal morphogenesis are likely also required for similar or different processes in other cells. In a multicellular organism that is homozygous mutant for an essential gene, defects in many cell types and developmental processes are likely to occur. Development may even be arrested in early embryonic stages. The mosaic system allows for the creation of a small fraction of cells homozygous for mutations of interest in specific cells, tissues and at times of interest to the investigator so that the phenotype of insects containing those clones can be assessed and the function of the essential genes inferred.

Drosophila mushroom bodies have been used as a powerful model to investigate the molecular mechanisms underlying different aspects of neuronal development and function. I did a small-scale genetic screen to isolate genes required for *Drosophila* mushroom body neuronal morphogenesis. The MARCM technique (Lee & Luo, 1999) was used, which allows positive labeling of homozygous mutant cells in a wild-type background. I used *GAL4-OK107*, which has the *GAL4* coding region under the regulatory control of an enhancer that results expression in all mushroom body neurons, to label the mushroom body neuroblast clones (Connolly et al., 1996). The MARCM clones of mushroom body neuroblast generated at early developmental stages and labeled with *GAL4-OK107>UAS-mCD8::GFP* allow us to visualize the gross morphology of the mushroom body and to follow single neuroblasts through different developmental stages.

UAS-mCD8::GFP contains a GAL4-responsive promoter regulating the expression of the coding region of mouse CD8 fused with the green fluorescence protein (GFP).

A collection of lines with recessive lethal mutations and an appropriately located *FRT* site was obtained from the Kyoto Drosophila Genetic Resource Center (DGRC) stock center (Table 2-1). Each line has a P-element insertion resulting in recessive lethality and an *FRT* element on the X (*FRT19A*) or the 3R (*FRT82B*) chromosome arm. After examining clones homozygous for each of 250 independent P-element insertions arising from mitotic recombination in neuroblasts, I identified 8 mutations that cause defects in different aspects of mushroom body neuronal morphogenesis. In adult brains, the most frequently observed phenotypes were reduction or elimination of specific neuron lobes. We call them α/β -only (no early-born neuron lobes) or γ -only (only with early-born neurons) phenotypes. The reduction of mushroom body neurons could be due to defects in cell birth or could be caused by cell death. In order to examine whether the defects involve cell-death, rescue tests were performed by ectopically expressing *UAS-p35* in the neuroblast clones. It is known that the baculovirus gene *p35* can inhibit apoptosis in diverse animals including *Drosophila* and plays an important role in apoptotic pathway (Ohtsubo et al., 1996). Of the 8 mutant lines that cause absence of α/β neurons or γ neurons in the adult mushroom bodies, 3 could be rescued by ectopic expression of *UAS-p35*, while others failed to be rescued by ectopic expression of *UAS-p35*. These 8 mutant lines were grouped into 3 categories based on their mushroom body phenotypes and *p35* rescue results (Table 2-2). 3 mutant lines belong to the category A showing the α/β only phenotype that were rescued by *UAS-p35*, which suggests that the first born γ neuron might have died during development. 3 mutant lines belong to the category B showing

the α/β only phenotype that were not rescued by *UAS-p35*, which suggests that the absence of γ neuron was not due to cell death. 2 mutant lines belong to the category C showing the γ only phenotype that were not rescued by *UAS-p35*, which suggests that cell death is not the major cause of the absence of α/β neurons. Further investigation into these lines and the associated genes will help to reveal the functions of these genes in neurogenesis.

I focused my dissertation research on a mutation line *dome*^{G0405} that caused a severe γ -only phenotype. The line *dome*^{G0405} contains a P-element insertion in *domeless* and this mutant allele was particularly interesting for two reasons. First, the γ neurons are the first-born neuron type, so a loss of later-born α/β neurons may suggest a defect in neurogenesis or proliferation. Second, *domeless* is known to encode a JAK/STAT signaling receptor, suggesting an essential role of JAK/STAT signaling in neurogenesis. The JAK/STAT signaling pathway is one of the critical regulators of cell proliferation and stem cell self-renewal. Over-activation of JAK/STAT signaling often leads to tumorigenesis. Highly conserved regulatory and cellular functions have been identified in mammals and *Drosophila*. Compared with the complexity of the JAK/STAT pathway in mammals, the streamlined regulation of JAK/STAT in *Drosophila* makes it a perfect model to study this signaling pathway and its involvement in the regulation of cell proliferation and stem cell self-renewal.

Table 2-1. The 250 lines obtained from the Kyoto DGRC that were used for screening

Each line has a P-element insertion resulting in recessive lethality and a *FRT* element on the X (*FRT19A*, 170 lines) or the 3R (*FRT82B*, 80 lines) chromosome arm. The DGRC number and Genotype are shown for each line.

DGRC No.	Genotype
111-028	y[d2] w[1118] P{ry[+t7.2]=ey-FLP.N}2 P{GMR-lacZ.C(38.1)}TPN1; P{ry[+t7.2]=neoFRT}82B P{w[+mC]=lacW}l(3)L2100[L2100]/TM6B, P{y[+t7.7]ry[+t7.2]=Car20y}TPN1, Tb[1]
111-030	y[d2] w[1118] P{ry[+t7.2]=ey-FLP.N}2 P{GMR-lacZ.C(38.1)}TPN1; P{ry[+t7.2]=neoFRT}82B P{w[+mC]=lacW}Dhod[s3512]/TM6B, P{y[+t7.7]ry[+t7.2]=Car20y}TPN1, Tb[1]
111-031	y[d2] w[1118] P{ry[+t7.2]=ey-FLP.N}2 P{GMR-lacZ.C(38.1)}TPN1; P{ry[+t7.2]=neoFRT}82B P{w[+mC]=lacW}l(3)j1B9[j1B9]/TM6B, P{y[+t7.7]ry[+t7.2]=Car20y}TPN1, Tb[1]
111-032	y[d2] w[1118] P{ry[+t7.2]=ey-FLP.N}2 P{GMR-lacZ.C(38.1)}TPN1; P{ry[+t7.2]=neoFRT}82B P{w[+mC]=lacW}l(3)L4092[L4092]/TM6B, P{y[+t7.7]ry[+t7.2]=Car20y}TPN1, Tb[1]
111-033	y[d2] w[1118] P{ry[+t7.2]=ey-FLP.N}2 P{GMR-lacZ.C(38.1)}TPN1; P{ry[+t7.2]=neoFRT}82B P{w[+mC]=lacW}s2681, l(3)s2681[s2681]/TM6B, P{y[+t7.7]ry[+t7.2]=Car20y}TPN1, Tb[1]
111-035	y[d2] w[1118] P{ry[+t7.2]=ey-FLP.N}2 P{GMR-lacZ.C(38.1)}TPN1; P{ry[+t7.2]=neoFRT}82B P{w[+mC]=lacW}l(3)j1D8[j1D8]/TM6B, P{y[+t7.7]ry[+t7.2]=Car20y}TPN1, Tb[1]
111-036	y[d2] w[1118] P{ry[+t7.2]=ey-FLP.N}2 P{GMR-lacZ.C(38.1)}TPN1; P{ry[+t7.2]=neoFRT}82B P{w[+mC]=lacW}l(3)j5A1[j5A1]/TM6B, P{y[+t7.7]ry[+t7.2]=Car20y}TPN1, Tb[1]
111-038	y[d2] w[1118] P{ry[+t7.2]=ey-FLP.N}2 P{GMR-lacZ.C(38.1)}TPN1; P{ry[+t7.2]=neoFRT}82B P{w[+mC]=lacW}B52[s2249]/TM6B, P{y[+t7.7]ry[+t7.2]=Car20y}TPN1, Tb[1]
111-039	y[d2] w[1118] P{ry[+t7.2]=ey-FLP.N}2 P{GMR-lacZ.C(38.1)}TPN1; P{ry[+t7.2]=neoFRT}82B P{w[+mC]=lacW}l(3)L5340[L5340]/TM6B, P{y[+t7.7]ry[+t7.2]=Car20y}TPN1, Tb[1]
111-040	y[d2] w[1118] P{ry[+t7.2]=ey-FLP.N}2 P{GMR-lacZ.C(38.1)}TPN1; P{ry[+t7.2]=neoFRT}82B P{w[+mC]=lacW}Hsc70-4[L3929]/TM6B, P{y[+t7.7]ry[+t7.2]=Car20y}TPN1, Tb[1]
111-041	y[d2] w[1118] P{ry[+t7.2]=ey-FLP.N}2 P{GMR-lacZ.C(38.1)}TPN1; P{ry[+t7.2]=neoFRT}82B P{w[+mC]=lacW}MRG15[j6A3]/TM6B, P{y[+t7.7]ry[+t7.2]=Car20y}TPN1, Tb[1]
111-042	y[d2] w[1118] P{ry[+t7.2]=ey-FLP.N}2 P{GMR-lacZ.C(38.1)}TPN1; P{ry[+t7.2]=neoFRT}82B P{w[+mC]=lacW}l(3)j6A6[j6A6]/TM6B, P{y[+t7.7]ry[+t7.2]=Car20y}TPN1, Tb[1]
111-043	y[d2] w[1118] P{ry[+t7.2]=ey-FLP.N}2 P{GMR-lacZ.C(38.1)}TPN1; P{ry[+t7.2]=neoFRT}82B P{w[+mC]=lacW}l(3)L1820[L1820]/TM6B, P{y[+t7.7]ry[+t7.2]=Car20y}TPN1, Tb[1]
111-044	y[d2] w[1118] P{ry[+t7.2]=ey-FLP.N}2 P{GMR-lacZ.C(38.1)}TPN1; P{ry[+t7.2]=neoFRT}82B P{w[+mC]=lacW}CSN5[L4032]/TM6B, P{y[+t7.7]ry[+t7.2]=Car20y}TPN1, Tb[1]
111-046	y[d2] w[1118] P{ry[+t7.2]=ey-FLP.N}2 P{GMR-lacZ.C(38.1)}TPN1; P{ry[+t7.2]=neoFRT}82B P{w[+mC]=lacW}Dad[j1E4]/TM6B, P{y[+t7.7]ry[+t7.2]=Car20y}TPN1, Tb[1]
111-047	y[d2] w[1118] P{ry[+t7.2]=ey-FLP.N}2 P{GMR-lacZ.C(38.1)}TPN1; P{ry[+t7.2]=neoFRT}82B P{w[+mC]=lacW}l(3)j5A6[j7A3]/TM6B, P{y[+t7.7]ry[+t7.2]=Car20y}TPN1, Tb[1]
111-048	y[d2] w[1118] P{ry[+t7.2]=ey-FLP.N}2 P{GMR-lacZ.C(38.1)}TPN1; P{ry[+t7.2]=neoFRT}82B P{w[+mC]=lacW}mod(mdg4)[L3101]/TM6B, P{y[+t7.7]ry[+t7.2]=Car20y}TPN1, Tb[1]
111-049	y[d2] w[1118] P{ry[+t7.2]=ey-FLP.N}2 P{GMR-lacZ.C(38.1)}TPN1; P{ry[+t7.2]=neoFRT}82B P{w[+mC]=lacW}Dph5[L4910]/TM6B, P{y[+t7.7]ry[+t7.2]=Car20y}TPN1, Tb[1]

	ry[+t7.2]=Car20y}TPN1, Tb[1]
111-050	y[d2] w[1118] P{ry[+t7.2]=ey-FLP.N}2 P{GMR-lacZ.C(38.1)}TPN1; P{ry[+t7.2]=neoFRT}82B P{w[+mC]=lacW}l(3)L0580[L0580]/TM6B, P{y[+t7.7] ry[+t7.2]=Car20y}TPN1, Tb[1]
111-051	y[d2] w[1118] P{ry[+t7.2]=ey-FLP.N}2 P{GMR-lacZ.C(38.1)}TPN1; P{ry[+t7.2]=neoFRT}82B P{w[+mC]=lacW}crb[j1B5]/TM6B, P{y[+t7.7] ry[+t7.2]=Car20y}TPN1, Tb[1]
111-052	y[d2] w[1118] P{ry[+t7.2]=ey-FLP.N}2 P{GMR-lacZ.C(38.1)}TPN1; P{ry[+t7.2]=neoFRT}82B P{w[+mC]=lacW}l(3)L6710[L6710]/TM6B, P{y[+t7.7] ry[+t7.2]=Car20y}TPN1, Tb[1]
111-053	y[d2] w[1118] P{ry[+t7.2]=ey-FLP.N}2 P{GMR-lacZ.C(38.1)}TPN1; P{ry[+t7.2]=neoFRT}82B P{w[+mC]=lacW}CycB3[L6540]/TM6B, P{y[+t7.7] ry[+t7.2]=Car20y}TPN1, Tb[1]
111-054	y[d2] w[1118] P{ry[+t7.2]=ey-FLP.N}2 P{GMR-lacZ.C(38.1)}TPN1; P{ry[+t7.2]=neoFRT}82B P{w[+mC]=lacW}OstStt3[j2D9]/TM6B, P{y[+t7.7] ry[+t7.2]=Car20y}TPN1, Tb[1]
111-055	w[1118]; P{ry[+t7.2]=neoFRT}82B P{w[+mC]=lacW}l(3)j12B4[j12B4]/TM6B, P{y[+t7.7]ry[+t7.2]=Car20y}TPN1, Tb[1]
111-056	y[d2] w[1118] P{ry[+t7.2]=ey-FLP.N}2 P{GMR-lacZ.C(38.1)}TPN1; P{ry[+t7.2]=neoFRT}82B P{w[+mC]=lacW}l(3)s2784[s2784]/TM6B, P{y[+t7.7] ry[+t7.2]=Car20y}TPN1, Tb[1]
111-057	y[d2] w[1118] P{ry[+t7.2]=ey-FLP.N}2 P{GMR-lacZ.C(38.1)}TPN1; P{ry[+t7.2]=neoFRT}82B P{w[+mC]=lacW}l(3)L6241[L6241]/TM6B, P{y[+t7.7] ry[+t7.2]=Car20y}TPN1, Tb[1]
111-058	y[d2] w[1118] P{ry[+t7.2]=ey-FLP.N}2 P{GMR-lacZ.C(38.1)}TPN1; P{ry[+t7.2]=neoFRT}82B P{w[+mC]=lacW}l(3)j2D5[j2D5]/TM6B, P{y[+t7.7] ry[+t7.2]=Car20y}TPN1, Tb[1]
111-059	y[d2] w[1118] P{ry[+t7.2]=ey-FLP.N}2 P{GMR-lacZ.C(38.1)}TPN1; P{ry[+t7.2]=neoFRT}82B P{w[+mC]=lacW}l(3)j8B9[j8B9]/TM6B, P{y[+t7.7] ry[+t7.2]=Car20y}TPN1, Tb[1]
111-060	y[d2] w[1118] P{ry[+t7.2]=ey-FLP.N}2 P{GMR-lacZ.C(38.1)}TPN1; P{ry[+t7.2]=neoFRT}82B P{w[+mC]=lacW}l(3)s2500[s2500]/TM6B, P{y[+t7.7] ry[+t7.2]=Car20y}TPN1, Tb[1]
111-061	y[d2] w[1118] P{ry[+t7.2]=ey-FLP.N}2 P{GMR-lacZ.C(38.1)}TPN1; P{ry[+t7.2]=neoFRT}82B P{w[+mC]=lacW}l(3)L7321[L7321]/TM6B, P{y[+t7.7] ry[+t7.2]=Car20y}TPN1, Tb[1]
111-264	y[d2] w[1118] P{ry[+t7.2]=ey-FLP.N}2 P{GMR-lacZ.C(38.1)}TPN1; P{ry[+t7.2]=neoFRT}82B P{w[+mC]=lacW}l(3)B3-3-21[1]/TM6B, P{y[+t7.7]ry[+t7.2]=Car20y}TPN1, Tb[1]
111-268	y[d2] w[1118] P{ry[+t7.2]=ey-FLP.N}2 P{GMR-lacZ.C(38.1)}TPN1; P{ry[+t7.2]=neoFRT}82B P{w[+mC]=lacW}l(3)B7-3-32[1]/TM6B, P{y[+t7.7]ry[+t7.2]=Car20y}TPN1, Tb[1]
111-405	y[d2] w[1118] P{ry[+t7.2]=ey-FLP.N}2 P{GMR-lacZ.C(38.1)}TPN1; P{ry[+t7.2]=neoFRT}82B P{w[+mC]=lacW}l(3)j7A6[j7A6]/TM6B, P{y[+t7.7] ry[+t7.2]=Car20y}TPN1, Tb[1]
111-406	y[d2] w[1118] P{ry[+t7.2]=ey-FLP.N}2 P{GMR-lacZ.C(38.1)}TPN1; P{ry[+t7.2]=neoFRT}82B P{w[+mC]=lacW}l(3)j8C8[j8C8]/TM6B, P{y[+t7.7] ry[+t7.2]=Car20y}TPN1, Tb[1]
111-407	y[d2] w[1118] P{ry[+t7.2]=ey-FLP.N}2 P{GMR-lacZ.C(38.1)}TPN1; P{ry[+t7.2]=neoFRT}82B P{w[+mC]=lacW}neur[j6B12]/TM6B, P{y[+t7.7]ry[+t7.2]=Car20y}TPN1, Tb[1]
111-408	y[d2] w[1118] P{ry[+t7.2]=ey-FLP.N}2 P{GMR-lacZ.C(38.1)}TPN1; P{ry[+t7.2]=neoFRT}82B P{w[+mC]=lacW}Pp1-87B[j6E7]/TM6B, P{y[+t7.7] ry[+t7.2]=Car20y}TPN1, Tb[1]
111-409	y[d2] w[1118] P{ry[+t7.2]=ey-FLP.N}2 P{GMR-lacZ.C(38.1)}TPN1;

	P{ry[+t7.2]=neoFRT}82B P{w[+mC]=lacW}j2C3, l(3)j2C3[j2C3]/TM6B, P{y[+t7.7]ry[+t7.2]=Car20y}TPN1, Tb[1]
111-410	y[d2] w[1118] P{ry[+t7.2]=ey-FLP.N}2 P{GMR-lacZ.C(38.1)}TPN1; P{ry[+t7.2]=neoFRT}82B P{w[+mC]=lacW}l(3)87Eg[s2149]/TM6B, P{y[+t7.7]ry[+t7.2]=Car20y}TPN1, Tb[1]
111-413	y[d2] w[1118] P{ry[+t7.2]=ey-FLP.N}2 P{GMR-lacZ.C(38.1)}TPN1; P{ry[+t7.2]=neoFRT}82B P{w[+mC]=lacW}l(3)j1E7[j1E7]/TM6B, P{y[+t7.7]ry[+t7.2]=Car20y}TPN1, Tb[1]
111-414	y[d2] w[1118] P{ry[+t7.2]=ey-FLP.N}2 P{GMR-lacZ.C(38.1)}TPN1; P{ry[+t7.2]=neoFRT}82B P{w[+mC]=lacW}trx[j14A6]/TM6B, P{y[+t7.7]ry[+t7.2]=Car20y}TPN1, Tb[1]
111-415	y[d2] w[1118] P{ry[+t7.2]=ey-FLP.N}2 P{GMR-lacZ.C(38.1)}TPN1; P{ry[+t7.2]=neoFRT}82B P{w[+mC]=lacW}eff[s1782]/TM6B, P{y[+t7.7]ry[+t7.2]=Car20y}TPN1, Tb[1]
111-416	y[d2] w[1118] P{ry[+t7.2]=ey-FLP.N}2 P{GMR-lacZ.C(38.1)}TPN1; P{ry[+t7.2]=neoFRT}82B P{w[+mC]=lacW}14-3-3epsilon[j2B10]/TM6B, P{y[+t7.7]ry[+t7.2]=Car20y}TPN1, Tb[1]
111-417	y[d2] w[1118] P{ry[+t7.2]=ey-FLP.N}2 P{GMR-lacZ.C(38.1)}TPN1; P{ry[+t7.2]=neoFRT}82B P{w[+mC]=lacW}nos[j3B6]/TM6B, P{y[+t7.7]ry[+t7.2]=Car20y}TPN1, Tb[1]
111-418	y[d2] w[1118] P{ry[+t7.2]=ey-FLP.N}2 P{GMR-lacZ.C(38.1)}TPN1; P{ry[+t7.2]=neoFRT}82B P{w[+mC]=lacW}l(3)j5A6[j5A6]/TM6B, P{y[+t7.7]ry[+t7.2]=Car20y}TPN1, Tb[1]
111-419	y[d2] w[1118] P{ry[+t7.2]=ey-FLP.N}2 P{GMR-lacZ.C(38.1)}TPN1; P{ry[+t7.2]=neoFRT}82B P{w[+mC]=lacW}l(3)j5C7[j5C7]/TM6B, P{y[+t7.7]ry[+t7.2]=Car20y}TPN1, Tb[1]
111-420	y[d2] w[1118] P{ry[+t7.2]=ey-FLP.N}2 P{GMR-lacZ.C(38.1)}TPN1; P{ry[+t7.2]=neoFRT}82B P{w[+mC]=lacW}Rab11[j2D1]/TM6B, P{y[+t7.7]ry[+t7.2]=Car20y}TPN1, Tb[1]
111-421	y[d2] w[1118] P{ry[+t7.2]=ey-FLP.N}2 P{GMR-lacZ.C(38.1)}TPN1; P{ry[+t7.2]=neoFRT}82B P{w[+mC]=lacW}how[j5B5]/TM6B, P{y[+t7.7]ry[+t7.2]=Car20y}TPN1, Tb[1]
111-422	y[d2] w[1118] P{ry[+t7.2]=ey-FLP.N}2 P{GMR-lacZ.C(38.1)}TPN1; P{ry[+t7.2]=neoFRT}82B P{w[+mC]=lacW}scrib[j7B3]/TM6B, P{y[+t7.7]ry[+t7.2]=Car20y}TPN1, Tb[1]
111-423	y[d2] w[1118] P{ry[+t7.2]=ey-FLP.N}2 P{GMR-lacZ.C(38.1)}TPN1; P{ry[+t7.2]=neoFRT}82B P{w[+mC]=lacW}l(3)s2976[s2976]/TM6B, P{y[+t7.7]ry[+t7.2]=Car20y}TPN1, Tb[1]
111-424	y[d2] w[1118] P{ry[+t7.2]=ey-FLP.N}2 P{GMR-lacZ.C(38.1)}TPN1; P{ry[+t7.2]=neoFRT}82B P{w[+mC]=lacW}Tkr99D[s2222]/TM6B, P{y[+t7.7]ry[+t7.2]=Car20y}TPN1, Tb[1]
111-425	y[d2] w[1118] P{ry[+t7.2]=ey-FLP.N}2 P{GMR-lacZ.C(38.1)}TPN1; P{ry[+t7.2]=neoFRT}82B P{w[+mC]=lacW}l(3)j11B7[j11B7]/TM6B, P{y[+t7.7]ry[+t7.2]=Car20y}TPN1, Tb[1]
111-427	y[d2] w[1118] P{ry[+t7.2]=ey-FLP.N}2 P{GMR-lacZ.C(38.1)}TPN1; P{ry[+t7.2]=neoFRT}82B P{w[+mC]=lacW}l(3)s1921[s1921]/TM6B, P{y[+t7.7]ry[+t7.2]=Car20y}TPN1, Tb[1]
111-428	y[d2] w[1118] P{ry[+t7.2]=ey-FLP.N}2 P{GMR-lacZ.C(38.1)}TPN1; P{ry[+t7.2]=neoFRT}82B P{w[+mC]=lacW}awd[j2A4]/TM6B, P{y[+t7.7]ry[+t7.2]=Car20y}TPN1, Tb[1]
111-459	y[d2] w[1118] P{ry[+t7.2]=ey-FLP.N}2 P{GMR-lacZ.C(38.1)}TPN1; P{ry[+t7.2]=neoFRT}82B P{w[+mC]=lacW}l(3)06536[j2E5]/TM6B, P{y[+t7.7]ry[+t7.2]=Car20y}TPN1, Tb[1]
111-464	y[d2] w[1118] P{ry[+t7.2]=ey-FLP.N}2 P{GMR-lacZ.C(38.1)}TPN1; P{ry[+t7.2]=neoFRT}82B P{w[+mC]=W82}l(3)W33B[1]/TM6B, P{y[+t7.7]

	ry[+t7.2]=Car20y}TPN1, Tb[1]
111-479	y[d2] w[1118] P{ry[+t7.2]=ey-FLP.N}2 P{GMR-lacZ.C(38.1)}TPN1; P{ry[+t7.2]=neoFRT}82B P{w[+mGT]=GT1}hdc[BG00237]/TM6B, P{y[+t7.7] ry[+t7.2]=Car20y}TPN1, Tb[1]
111-496	y[d2] w[1118] P{ry[+t7.2]=ey-FLP.N}2 P{GMR-lacZ.C(38.1)}TPN1; P{ry[+t7.2]=neoFRT}82B P{w[+mGT]=GT1}BG02810/TM6B, P{y[+t7.7] ry[+t7.2]=Car20y}TPN1, Tb[1]
111-505	y[d2] w[1118] P{ry[+t7.2]=ey-FLP.N}2 P{GMR-lacZ.C(38.1)}TPN1; P{ry[+t7.2]=neoFRT}82B P{y[+mDint2] w[BR.E.BR]=SUPor-P}KG02920/TM6B, P{y[+t7.7] ry[+t7.2]=Car20y}TPN1, Tb[1]
111-511	y[d2] w[1118] P{ry[+t7.2]=ey-FLP.N}2 P{GMR-lacZ.C(38.1)}TPN1; P{ry[+t7.2]=neoFRT}82B P{y[+mDint2] w[BR.E.BR]=SUPor-P}bnl[KG00157]/TM6B, P{y[+t7.7] ry[+t7.2]=Car20y}TPN1, Tb[1]
111-532	y[d2] w[1118] P{ry[+t7.2]=ey-FLP.N}2 P{GMR-lacZ.C(38.1)}TPN1; P{ry[+t7.2]=neoFRT}82B P{y[+mDint2] w[BR.E.BR]=SUPor-P}trx[KG04195]/TM6B, P{y[+t7.7] ry[+t7.2]=Car20y}TPN1, Tb[1]
111-535	y[d2] w[1118] P{ry[+t7.2]=ey-FLP.N}2 P{GMR-lacZ.C(38.1)}TPN1; P{ry[+t7.2]=neoFRT}82B P{y[+mDint2] w[BR.E.BR]=SUPor-P}KG02255/TM6B, P{y[+t7.7] ry[+t7.2]=Car20y}TPN1, Tb[1]
111-546	y[d2] w[1118] P{ry[+t7.2]=ey-FLP.N}2 P{GMR-lacZ.C(38.1)}TPN1; P{ry[+t7.2]=neoFRT}82B P{y[+mDint2] w[BR.E.BR]=SUPor- P}CG5802[KG01634]/TM6B, P{y[+t7.7] ry[+t7.2]=Car20y}TPN1, Tb[1]
111-552	y[d2] w[1118] P{ry[+t7.2]=ey-FLP.N}2 P{GMR-lacZ.C(38.1)}TPN1; P{ry[+t7.2]=neoFRT}82B P{y[+mDint2] w[BR.E.BR]=SUPor-P}pnt[KG04968]/TM6B, P{y[+t7.7] ry[+t7.2]=Car20y}TPN1, Tb[1]
111-568	y[d2] w[1118] P{ry[+t7.2]=ey-FLP.N}2 P{GMR-lacZ.C(38.1)}TPN1; P{ry[+t7.2]=neoFRT}82B P{y[+mDint2] w[BR.E.BR]=SUPor-P}KG01914/TM6B, P{y[+t7.7] ry[+t7.2]=Car20y}TPN1, Tb[1]
111-582	y[d2] w[1118] P{ry[+t7.2]=ey-FLP.N}2 P{GMR-lacZ.C(38.1)}TPN1; P{ry[+t7.2]=neoFRT}82B P{y[+mDint2] w[BR.E.BR]=SUPor-P}crb[KG05098]/TM6B, P{y[+t7.7] ry[+t7.2]=Car20y}TPN1, Tb[1]
111-588	y[d2] w[1118] P{ry[+t7.2]=ey-FLP.N}2 P{GMR-lacZ.C(38.1)}TPN1; P{ry[+t7.2]=neoFRT}82B P{y[+mDint2] w[BR.E.BR]=SUPor-P}KG02008/TM6B, P{y[+t7.7] ry[+t7.2]=Car20y}TPN1, Tb[1]
111-594	y[*] w[*] ; P{ry[+t7.2]=neoFRT}82B P{y[+mDint2] w[BR.E.BR]=SUPor- P}CG14713[KG05924]/TM6C, Tb[1], Sb[1]
111-595	y[d2] w[1118] P{ry[+t7.2]=ey-FLP.N}2 P{GMR-lacZ.C(38.1)}TPN1; P{ry[+t7.2]=neoFRT}82B P{y[+mDint2] w[BR.E.BR]=SUPor- P}gammaCop[KG06383]/TM6B, P{y[+t7.7] ry[+t7.2]=Car20y}TPN1, Tb[1]
111-599	y[d2] w[1118] P{ry[+t7.2]=ey-FLP.N}2 P{GMR-lacZ.C(38.1)}TPN1; P{ry[+t7.2]=neoFRT}82B P{y[+mDint2] w[BR.E.BR]=SUPor-P}KG01953/TM6B, P{y[+t7.7]ry[+t7.2]=Car20y}TPN1, Tb[1]
111-605	y[d2] w[1118] P{ry[+t7.2]=ey-FLP.N}2 P{GMR-lacZ.C(38.1)}TPN1; P{ry[+t7.2]=neoFRT}82B P{y[+mDint2] w[BR.E.BR]=SUPor- P}CG8165[KG06444]/TM6B, P{y[+t7.7] ry[+t7.2]=Car20y}TPN1, Tb[1]
111-616	y[d2] w[1118] P{ry[+t7.2]=ey-FLP.N}2 P{GMR-lacZ.C(38.1)}TPN1; P{ry[+t7.2]=neoFRT}82B P{y[+mDint2] w[BR.E.BR]=SUPor-P}CtBP[KG07519]/TM6B, P{y[+t7.7] ry[+t7.2]=Car20y}TPN1, Tb[1]
111-617	y[*] w[*]; P{ry[+t7.2]=neoFRT}82B P{y[+mDint2] w[BR.E.BR]=SUPor- P}sima[KG07607]/TM6C, Tb[1] Sb[1]
111-625	y[d2] w[1118] P{ry[+t7.2]=ey-FLP.N}2 P{GMR-lacZ.C(38.1)}TPN1; P{ry[+t7.2]=neoFRT}82B P{y[+mDint2] w[BR.E.BR]=SUPor-P}KG08565/TM6B, P{y[+t7.7] ry[+t7.2]=Car20y}TPN1, Tb[1]
111-627	P{ry[+t7.2]=neoFRT}82B P{y[+mDint2] w[BR.E.BR]=SUPor- P}trx[KG08639]/TM6B, P{y[+t7.7] ry[+t7.2]=Car20y}TPN1, Tb[1]

111-633	y[1] w[67c23]; P{ry[+t7.2]=neoFRT}82B P{y[+mDint2] w[BR.E.BR]=SUPor- P}KG01234/TM6C, Sb[1] Tb[1]
111-639	y[d2] w[1118] P{ry[+t7.2]=ey-FLP.N}2 P{GMR-lacZ.C(38.1)}TPN1; P{ry[+t7.2]=neoFRT}82B P{y[+mDint2] w[BR.E.BR]=SUPor- P}Dlc90F[KG06855]/TM6B, P{y[+t7.7] ry[+t7.2]=Car20y}TPN1, Tb[1]
111-657	y[d2] w[1118] P{ry[+t7.2]=ey-FLP.N}2 P{GMR-lacZ.C(38.1)}TPN1; P{ry[+t7.2]=neoFRT}82B P{y[+mDint2] w[BR.E.BR]=SUPor-P}KG08575/TM6B, P{y[+t7.7] ry[+t7.2]=Car20y}TPN1, Tb[1]
111-733	y[d2] w[1118] P{ry[+t7.2]=ey-FLP.N}2 P{GMR-lacZ.C(38.1)}TPN1; P{ry[+t7.2]=neoFRT}82BP{w[+mGT]=GT1}tara[BG01673]/TM6B, P{y[+t7.7] ry[+t7.2]=Car20y}TPN1, Tb[1]
111-807	w[67c23] P{w[+mC]=lacW}l(1)G0254[G0254] P{neoFRT}19A/FM7c; P{ey-FLP.D}5
111-808	y[1] w[*] P{w[+mC]=lacW}inx2[G0317] P{neoFRT}19A/FM7c; P{ey-FLP.D}5
111-809	w[67c23] P{w[+mC]=lacW}l(1)G0155[G0155] P{neoFRT}19A/FM7c; P{ey-FLP.D}5
111-810	y[1] w[*] P{w[+mC]=lacW}Tom40[G0216] P{neoFRT}19A/FM7c; P{ey-FLP.D}5
111-811	y[1] w[*] P{w[+mC]=lacW}CG1530[G0307a] P{lacW}G0307b, l(1)G0307[G0307] P{neoFRT}19A/FM7c; P{ey-FLP.D}5
111-812	w[67c23] P{w[+mC]=lacW}mys[G0233] P{neoFRT}19A/FM7c; P{ey-FLP.D}5
111-813	y[1] w[*] P{w[+mC]=lacW}Trxr-1[G0154] P{neoFRT}19A/FM7c; P{ey-FLP.D}5
111-814	w[67c23] P{w[+mC]=lacW}l(1)G0228[G0228] P{neoFRT}19A/FM7c; P{ey-FLP.D}5
111-815	w[67c23] P{w[+mC]=lacW}l(1)G0219[G0219] P{neoFRT}19A/FM7c; P{ey-FLP.D}5
111-816	w[67c23] P{w[+mC]=lacW}l(1)G0178[G0178] P{neoFRT}19A/FM7c; P{ey-FLP.D}5
111-817	w[67c23] P{lacW}l(1)G0249[G0249] P{neoFRT}19A/FM7c; P{ey-FLP.D}5
111-818	w[67c23] P{w[+mC]=lacW}l(1)G0200[G0200] P{neoFRT}19A/FM7c; P{ey-FLP.D}5
111-832	y[1] w[*] P{w[+mC]=lacW}l(1)G0272[G0272] P{neoFRT}19A/FM7c; P{ey-FLP.D}5
111-833	y[1] w[*] P{w[+mC]=lacW}l(1)G0156[G0156] P{neoFRT}19A/FM7c; P{ey-FLP.D}5
111-834	y[1] w[*] P{w[+mC]=lacW}l(1)G0223[G0223] P{neoFRT}19A/FM7c; P{ey-FLP.D}5
111-835	w[67c23] P{w[+mC]=lacW}l(1)G0384[G0384] P{neoFRT}19A/FM7c; P{ey-FLP.D}5
111-836	y[1] w[*] P{w[+mC]=lacW}l(1)G0084[G0409] P{neoFRT}19A/FM7c; P{ey-FLP.D}5
111-837	w[67c23] P{w[+mC]=lacW}l(1)G0427[G0427] P{neoFRT}19A/FM7c; P{ey-FLP.D}5
111-838	y[1] w[*] P{w[+mC]=lacW}l(1)G0022[G0027] P{neoFRT}19A/FM7c; P{ey-FLP.D}5
111-839	w[67c23] P{w[+mC]=lacW}Tis11[G0124] P{neoFRT}19A/FM7c; P{ey-FLP.D}5
111-840	w[67c23] P{w[+mC]=lacW}G0143b P{lacW}CG12991[G0143a] P{neoFRT}19A/FM7c; P{ey-FLP.D}5
111-841	w[67c23] P{lacW}G0161a P{lacW}G0161b, l(1)G0161G0161 P{neoFRT}19A/FM7c; P{ey-FLP.D}5
111-842	w[67c23] P{w[+mC]=lacW}l(1)G0164[G0164] P{neoFRT}19A/FM7c; P{ey-FLP.D}5
111-843	y[1] w[*] P{w[+mC]=lacW}Act5C[G0177] P{neoFRT}19A/FM7c; P{ey-FLP.D}5
111-844	y[1] w[*] P{w[+mC]=lacW}beta-Spec[G0198] P{neoFRT}19A/FM7c; P{ey-FLP.D}5
111-845	y[1] w[*] P{w[+mC]=lacW}Top1[G0201] P{neoFRT}19A/FM7c; P{ey-FLP.D}5
111-846	w[67c23] P{w[+mC]=lacW}Act5C[G0330] P{neoFRT}19A/FM7c; P{ey-FLP.D}5
111-847	y[1] w[*] P{w[+mC]=lacW}l(1)G0332[G0332] P{neoFRT}19A/FM7c; P{ey-FLP.D}5
111-849	w[67c23] P{w[+mC]=lacW}ctp[G0445b] P{neoFRT}19A/FM7c; P{ey-FLP.D}5
111-850	w[67c23] P{w[+mC]=lacW}ras[G0098] P{neoFRT}19A/FM7c; P{ey-FLP.D}5
111-851	w[67c23] P{w[+mC]=lacW}l(1)G0030[G0140a] P{lacW}G0140b, l(1)G0140[G0140] P{neoFRT}19A/FM7c; P{ey-FLP.D}5
111-852	y[1] P{w[+mC]=lacW}G0151a P{lacW}G0151b P{lacW}G0151c, l(1)G0151[G0151] w[*] P{neoFRT}19A/FM7c; P{ey-FLP.D}5
111-853	y[1] P{w[+mC]=lacW}l(1)G0152[G0152] w[*] P{neoFRT}19A/FM7c; P{ey-FLP.D}5
111-854	w[67c23] P{w[+mC]=lacW}inx2[G0157] P{neoFRT}19A/FM7c; P{ey-FLP.D}5
111-855	P{w[+mC]=lacW}Unc-76[G0158] w[*] P{neoFRT}19A/FM7c; P{ey-FLP.D}5

111-856	y[1] w[*] P{w[+mC]=lacW} sog[G0160] P{neoFRT} 19A/FM7c; P{ey-FLP.D}5
111-857	w[67c23] P{w[+mC]=lacW} l(1)G0166[G0166] P{neoFRT} 19A/FM7c; P{ey-FLP.D}5
111-858	y[1] w[*] P{w[+mC]=lacW} inx2[G0173a] P{lacW} G0173b, l(1)G0173[G0173] P{neoFRT} 19A/FM7c; P{ey-FLP.D}5
111-859	P{w[+mC]=lacW} l(1)G0181[G0181] w[*] P{neoFRT} 19A/FM7c; P{ey-FLP.D}5
111-860	w[67c23] P{w[+mC]=lacW} l(1)G0182[G0182] P{neoFRT} 19A/FM7c; P{ey-FLP.D}5
111-861	w[67c23] P{w[+mC]=lacW} Dlic2[G0190] P{neoFRT} 19A/FM7c; P{ey-FLP.D}5
111-862	y[1] w[*] P{w[+mC]=lacW} G0213a P{lacW} G0213b, l(1)G0213[G0213] P{neoFRT} 19A/FM7c; P{ey-FLP.D}5
111-863	w[67c23] P{w[+mC]=lacW} dome[G0218] P{neoFRT} 19A/FM7c; P{ey-FLP.D}5
111-864	w[67c23] P{w[+mC]=lacW} l(1)G0232[G0232] P{neoFRT} 19A/FM7c; P{ey-FLP.D}5
111-865	y[1] w[*] P{w[+mC]=lacW} Ant2[G0247] sesB[G0247] P{neoFRT} 19A/FM7c; P{ey-FLP.D}5
111-866	w[67c23] P{w[+mC]=lacW} dome[G0264] P{neoFRT} 19A/FM7c; P{ey-FLP.D}5
111-867	w[67c23] P{w[+mC]=lacW} l(1)G0273[G0273] P{neoFRT} 19A/FM7c; P{ey-FLP.D}5
111-868	y[1] w[*] P{w[+mC]=lacW} mys[G0281] P{neoFRT} 19A/FM7c; P{ey-FLP.D}5
111-869	y[1] w[*] P{w[+mC]=lacW} l(1)G0334[G0334] P{neoFRT} 19A/FM7c; P{ey-FLP.D}5
111-870	P{w[+mC]=lacW} sgg[G0335] w[*] P{neoFRT} 19A/FM7c; P{ey-FLP.D}5
111-871	w[67c23] P{w[+mC]=lacW} Fas2[G0336] P{neoFRT} 19A/FM7c; P{ey-FLP.D}5
111-872	w[67c23] P{w[+mC]=lacW} dlgl[G0342]a P{lacW} dlgl[G0342]b dlgl[G0342] P{neoFRT} 19A/FM7c; P{ey-FLP.D}5
111-873	w[67c23] P{w[+mC]=lacW} ras[G0351] P{neoFRT} 19A/FM7c; P{ey-FLP.D}5
111-874	w[67c23] P{w[+mC]=lacW} l(1)G0353[G0353] P{neoFRT} 19A/FM7c; P{ey-FLP.D}5
111-875	w[67c23] P{w[+mC]=lacW} l(1)G0354[G0354] P{neoFRT} 19A/FM7c; P{ey-FLP.D}5
111-876	y[1] w[*] P{w[+mC]=lacW} l(1)G0356[G0356] P{neoFRT} 19A/FM7c; P{ey-FLP.D}5
111-877	y[1] w[*] P{w[+mC]=lacW} Smr[G0361] P{neoFRT} 19A/FM7c; P{ey-FLP.D}5
111-878	w[67c23] P{w[+mC]=lacW} Lag1[G0365] P{neoFRT} 19A/FM7c; P{ey-FLP.D}5
111-879	y[1] w[*] P{w[+mC]=lacW} dome[G0367] P{neoFRT} 19A/FM7c; P{ey-FLP.D}5
111-880	w[67c23] P{w[+mC]=lacW} ctp[G0371] P{neoFRT} 19A/FM7c; P{ey-FLP.D}5
111-881	P{w[+mC]=lacW} l(1)G0377[G0377] w[*] P{neoFRT} 19A/FM7c; P{ey-FLP.D}5
111-882	P{w[+mC]=lacW} elav[G0378a] P{lacW} G0378b, l(1)G0378[G0378] w[*] P{neoFRT} 19A/FM7c; P{ey-FLP.D}5
111-884	y[1] w[*] P{w[+mC]=lacW} l(1)G0287[G0287] P{neoFRT} 19A/FM7c; P{ey-FLP.D}5
111-885	y[1] w[*] P{w[+mC]=lacW} G0199a P{lacW} dome[G0199b], l(1)G0199[G0199] P{neoFRT} 19A/FM7c; P{ey-FLP.D}5
111-887	w[67c23] P{w[+mC]=lacW} l(1)G0289[G0289] P{neoFRT} 19A/FM7c; P{ey-FLP.D}5
111-888	w[67c23] P{w[+mC]=lacW} Trxr-1[G0379] P{neoFRT} 19A/FM7c; P{ey-FLP.D}5
111-889	y[1] w[*] P{w[+mC]=lacW} ras[G0380b] P{neoFRT} 19A/FM7c; P{ey-FLP.D}5
111-890	w[67c23] P{w[+mC]=lacW} l(1)G0084[G0381] P{neoFRT} 19A/FM7c; P{ey-FLP.D}5
111-891	y[1] w[*] P{w[+mC]=lacW} l(1)G0382[G0382] P{neoFRT} 19A/FM7c; P{ey-FLP.D}5
111-892	y[1] w[*] P{w[+mC]=lacW} l(1)G0392[G0392] P{neoFRT} 19A/FM7c; P{ey-FLP.D}5
111-893	w[67c23] P{w[+mC]=lacW} l(1)G0400[G0400] P{neoFRT} 19A/FM7c; P{ey-FLP.D}5
111-894	P{w[+mC]=lacW} br[G0401] w[*] P{neoFRT} 19A/FM7c; P{ey-FLP.D}5
111-895	y[1] w[*] P{w[+mC]=lacW} Moe[G0404] P{neoFRT} 19A/FM7c; P{ey-FLP.D}5
111-896	y[1] w[*] P{w[+mC]=lacW} dome[G0405] P{neoFRT} 19A/FM7c; P{ey-FLP.D}5
111-897	P{w[+mC]=lacW} l(1)G0412[G0412] w[*] P{neoFRT} 19A/FM7c; P{ey-FLP.D}5
111-898	w[67c23] P{w[+mC]=lacW} l(1)G0007[G0416] P{neoFRT} 19A/FM7c; P{ey-FLP.D}5
111-899	w[67c23] P{w[+mC]=lacW} G0417a P{lacW} G0417b, l(1)G0417[G0417] P{neoFRT} 19A/FM7c; P{ey-FLP.D}5
111-900	w[67c23] P{w[+mC]=lacW} l(1)G0419[G0419] P{neoFRT} 19A/FM7c; P{ey-FLP.D}5

111-901	w[67c23] P{w[+mC]=lacW} Act5C[G0420] P{neoFRT} 19A/FM7c; P{ey-FLP.D}5
111-902	w[67c23] P{w[+mC]=lacW} l(1)G0424[G0424] P{neoFRT} 19A/FM7c; P{ey-FLP.D}5
111-903	y[1] w[*] P{w[+mC]=lacW} mew[G0429] P{neoFRT} 19A/FM7c; P{ey-FLP.D}5
111-904	y[1] w[*] P{w[+mC]=lacW} l(1)G0430[G0430] P{neoFRT} 19A/FM7c; P{ey-FLP.D}5
111-905	P{w[+mC]=lacW} l(1)G0431[G0431] w[*] P{neoFRT} 19A/FM7c; P{ey-FLP.D}5
111-906	w[67c23] P{w[+mC]=lacW} l(1)G0437[G0437] P{neoFRT} 19A/FM7c; P{ey-FLP.D}5
111-907	w[67c23] P{w[+mC]=lacW} Chc[G0438] P{neoFRT} 19A/FM7c; P{ey-FLP.D}5
111-908	w[67c23] P{w[+mC]=lacW} ras[G0002] P{neoFRT} 19A/FM7c; P{ey-FLP.D}5
111-910	P{w[+mC]=lacW} elav[G0031] arg[G0031] w[*] P{neoFRT} 19A/FM7c; P{ey-FLP.D}5
111-911	y[1] w[*] P{w[+mC]=lacW} Fas2[G0032] P{neoFRT} 19A/FM7c; P{ey-FLP.D}5
111-913	y[1] w[*] P{w[+mC]=lacW} l(1)dd4[G0122] P{neoFRT} 19A/FM7c; P{ey-FLP.D}5
111-914	y[1] w[*] P{w[+mC]=lacW} l(1)G0007[G0176] P{neoFRT} 19A/FM7c; P{ey-FLP.D}5
111-915	P{w[+mC]=lacW} G0184a P{lacW} Rph[G0184b], l(1)G0184[G0184] w[*] P{neoFRT} 19A/FM7c; P{ey-FLP.D}5
111-916	w[67c23] P{w[+mC]=lacW} l(1)G0185[G0185] P{neoFRT} 19A/FM7c; P{ey-FLP.D}5
111-917	w[67c23] P{w[+mC]=lacW} l(1)G0279[G0279] P{neoFRT} 19A/FM7c; P{ey-FLP.D}5
111-918	y[1] w[*] P{w[+mC]=lacW} l(1)G0003[G0297] P{neoFRT} 19A/FM7c; P{ey-FLP.D}5
111-919	y[1] w[*] P{w[+mC]=lacW} l(1)G0007[G0308] P{neoFRT} 19A/FM7c; P{ey-FLP.D}5
111-920	P{w[+mC]=lacW} elav[G0319] arg[G0319] w[*] P{neoFRT} 19A/FM7c; P{ey-FLP.D}5
111-921	w[67c23] P{w[+mC]=lacW} l(1)G0376[G0376] P{neoFRT} 19A/FM7c; P{ey-FLP.D}5
111-922	w[67c23] P{w[+mC]=lacW} Ant2[G0386] sesB[G0386] P{neoFRT} 19A/FM7c; P{ey-FLP.D}5
111-923	w[67c23] P{w[+mC]=lacW} Nrg[G0413] P{neoFRT} 19A/FM7c; P{ey-FLP.D}5
111-924	y[1] w[*] P{w[+mC]=lacW} l(1)G0425[G0425] P{neoFRT} 19A/FM7c; P{ey-FLP.D}5
111-925	y[1] w[*] P{w[+mC]=lacW} l(1)G0442[G0442] P{neoFRT} 19A/FM7c; P{ey-FLP.D}5
111-926	y[1] w[*] P{w[+mC]=lacW} mew[G0443] P{neoFRT} 19A/FM7c; P{ey-FLP.D}5
111-927	w[67c23] P{w[+mC]=lacW} l(1)G0148[G0461] P{neoFRT} 19A/FM7c; P{ey-FLP.D}5
111-928	y[1] w[*] P{w[+mC]=lacW} l(1)G0464[G0464] P{neoFRT} 19A/FM7c; P{ey-FLP.D}5
111-929	y[1] w[*] P{w[+mC]=lacW} l(1)G0467[G0467] P{neoFRT} 19A/FM7c; P{ey-FLP.D}5
111-930	y[1] w[*] P{w[+mC]=lacW} l(1)G0469[G0469] P{neoFRT} 19A/FM7c; P{ey-FLP.D}5
111-931	w[67c23] P{w[+mC]=lacW} Trxr-1[G0477] P{neoFRT} 19A/FM7c; P{ey-FLP.D}5
111-932	y[1] w[*] P{w[+mC]=lacW} G0478a P{lacW} Clic[G0478b], l(1)G0478[G0478] P{neoFRT} 19A/FM7c; P{ey-FLP.D}5
111-933	w[67c23] P{w[+mC]=lacW} sd[G0483] P{neoFRT} 19A/FM7c; P{ey-FLP.D}5
111-934	y[1] w[*] P{w[+mC]=lacW} baz[G0484] P{neoFRT} 19A/FM7c; P{ey-FLP.D}5
111-935	w[67c23] P{w[+mC]=lacW} Nrg[G0488b] P{neoFRT} 19A/FM7c; P{ey-FLP.D}5
111-936	y[1] w[*] P{w[+mC]=lacW} Lag1[G0489] P{neoFRT} 19A/FM7c; P{ey-FLP.D}5
111-937	y[1] w[*] P{w[+mC]=lacW} fs(1)h[G0495] P{neoFRT} 19A/FM7c; P{ey-FLP.D}5
111-938	w[67c23] P{w[+mC]=lacW} Rala[G0501] P{neoFRT} 19A/FM7c; P{ey-FLP.D}5
111-939	y[1] w[*] P{w[+mC]=lacW} flw[G0172] P{neoFRT} 19A/FM7c; P{ey-FLP.D}5
111-940	P{w[+mC]=lacW} G0280a P{lacW} G0280b, l(1)G0280[G0280] w[*] P{neoFRT} 19A/FM7c; P{ey-FLP.D}5
111-941	P{w[+mC]=lacW} Unc-76[G0333] w[*] P{neoFRT} 19A/FM7c; P{ey-FLP.D}5
111-942	P{w[+mC]=lacW} l(1)G0399[G0399] w[*] P{neoFRT} 19A/FM7c; P{ey-FLP.D}5
111-943	w[67c23] P{w[+mC]=lacW} rap[G0418] P{neoFRT} 19A/FM7c; P{ey-FLP.D}5
111-944	y[1] w[*] P{w[+mC]=lacW} l(1)G0435[G0435] P{neoFRT} 19A/FM7c; P{ey-FLP.D}5
111-945	P{w[+mC]=lacW} sta[G0448] w[*] P{neoFRT} 19A/FM7c; P{ey-FLP.D}5
111-946	w[1118] P{w[+mGT]=GT1} CG1789[BG02603] P{neoFRT} 19A/FM7c; P{ey-FLP.D}5
111-947	y[1] w[1118] P{w[+mGT]=GT1} mRpL33[BG01040] P{neoFRT} 19A/FM7c; P{ey-FLP.D}5

111-948	y[1] w[1118] P{y[+mDint2] w[BR.E.BR]=SUPor-P}shi[KG03690] P{neoFRT}19A/FM7c; P{ey- FLP.D}5
111-949	y[1] w[1118] P{y[+mDint2] w[BR.E.BR]=SUPor-P}beta-Spec[KG02312] P{neoFRT}19A/FM7c; P{ey-FLP.D}5
111-950	y[1] w[1118] P{y[+mDint2] w[BR.E.BR]=SUPor- P}l(1)G0003[KG02485] P{neoFRT}19A/FM7c; P{ey-FLP.D}5
111-951	y[1] w[1118] P{y[+mDint2] w[BR.E.BR]=SUPor-P}CG32666[KG03058] P{neoFRT}19A/FM7c; P{ey-FLP.D}5
111-952	y[1] P{y[+mDint2] w[BR.E.BR]=SUPor-P}KG01741 w[1118] P{neoFRT}19A/FM7c; P{ey- FLP.D}5
111-953	y[1] w[1118] P{y[+mDint2] w[BR.E.BR]=SUPor- P}l(1)G0030[KG04873] P{neoFRT}19A/FM7c; P{ey-FLP.D}5
111-954	y[1] w[1118] P{y[+mDint2] w[BR.E.BR]=SUPor-P}KG06588 P{neoFRT}19A/FM7c; P{ey- FLP.D}5
111-955	y[1] w[1118] P{y[+mDint2] w[BR.E.BR]=SUPor-P}KG08470 P{neoFRT}19A/FM7c; P{ey- FLP.D}5
111-956	P{y[+mDint2] w[BR.E.BR]=SUPor-P}Pgdl[KG08676] w[*] P{neoFRT}19A/FM7c; P{ey- FLP.D}5
111-957	y[1] w[*] P{w[+mC] y[+mDint2]=EPgy2}l(1)G0255[EY00709] P{neoFRT}19A/FM7c; P{ey- FLP.D}5
111-958	y[1] P{y[+mDint2] w[BR.E.BR]=SUPor-P}RpL22[KG09650] w[*] P{neoFRT}19A/FM7c; P{ey- FLP.D}5
111-959	y[1] P{w[+mC] y[+mDint2]=EPgy2}east[EY05235] w[*] P{neoFRT}19A/FM7c; P{ey- FLP.D}5
111-960	y[1] w[*] P{w[+mC] y[+mDint2]=EPgy2}CG15738[EY02706] P{neoFRT}19A/FM7c; P{ey- FLP.D}5
111-961	y[1] w[*] P{w[+mC] y[+mDint2]=EPgy2}sqh[EY09875] P{neoFRT}19A/FM7c; P{ey- FLP.D}5
111-962	w[1118] PBac{w[+mC]=RB}CG3564[e04526] P{neoFRT}19A/FM7c; P{ey-FLP.D}5
111-963	w[1118] PBac{w[+mC]=RB}AP-1gamma[e04546] P{neoFRT}19A/FM7c; P{ey-FLP.D}5
111-964	w[1118] PBac{w[+mC]=RB}Aats-lys[e04554] P{neoFRT}19A/FM7c; P{ey-FLP.D}5
111-965	w[1118] PBac{w[+mC]=RB}CG2467[e04564] PBac{RB}fw[e04564] P{neoFRT}19A/FM7c; P{ey-FLP.D}5
111-966	w[1118] PBac{w[+mC]=RB}l(1)10Bb[e04588] P{neoFRT}19A/FM7c; P{ey-FLP.D}5
111-967	w[1118] PBac{w[+mC]=WH}Lim1[f04087] P{neoFRT}19A/FM7c; P{ey-FLP.D}5
111-968	PBac{w[+mC]=WH}cin[f05298] w[1118] P{neoFRT}19A/FM7c; P{ey-FLP.D}5
111-969	w[1118] P{w[+mC]=XP}CG1677[d02937] P{neoFRT}19A/FM7c; P{ey-FLP.D}5
114-354	P{w[+mC]=lacW}deltaCOP[G0051] w[*] P{neoFRT}19A/FM7c; P{ey-FLP.D}5
114-355	w[67c23] P{w[+mC]=lacW}l(1)G0003[G0070] P{neoFRT}19A/FM7c; P{ey-FLP.D}5
114-356	y[1] w[*] P{w[+mC]=lacW}l(1)G0191[G0191] P{neoFRT}19A/FM7c; P{ey-FLP.D}5
114-357	w[67c23] P{w[+mC]=lacW}l(1)G0209[G0209] P{neoFRT}19A/FM7c; P{ey-FLP.D}5
114-358	P{w[+mC]=lacW}Unc-76[G0360] w[*] P{neoFRT}19A/FM7c; P{ey-FLP.D}5
114-359	w[67c23] P{w[+mC]=lacW}l(1)G0148[G0148] P{neoFRT}19A/FM7c; P{ey-FLP.D}5
114-360	y[1] w[*] P{w[+mC]=lacW}Aats-his[G0358] P{neoFRT}19A/FM7c; P{ey-FLP.D}5
114-361	y[1] w[*] P{w[+mC]=lacW}l(1)G0369[G0369] P{neoFRT}19A/FM7c; P{ey-FLP.D}5
114-362	P{w[+mC]=lacW}elav[G0378a] P{lacW}G0378b, l(1)G0378[G0378] w[*] P{neoFRT}19A/FM7c; P{ey-FLP.D}5
114-364	y[1] w[*] P{w[+mC]=lacW}G0091a P{lacW}mys[G0091b] P{neoFRT}19A/FM7c; P{ey- FLP.D}5
114-367	y[1] P{w[+mC]=lacW}l(1)G0362[G0362] w[*] P{neoFRT}19A/FM7c; P{ey-FLP.D}5
114-369	y[1] w[*] P{lacW}l(1)G0462[G0462] P{neoFRT}19A/FM7c; P{ey-FLP.D}5
114-487	y[d2] w[1118] P{ry[+t7.2]=ey-FLP.N}2 P{GMR-lacZ.C(38.1)}TPN1;

	P{ry[+t7.2]=neoFRT}82B PBac{w[+mC]=RB}CG1607[e00971]/TM6B, P{y[+t7.7]ry[+t7.2]=Car20y}TPN1, Tb[1]
114-488	y[d2] w[1118] P{ry[+t7.2]=ey-FLP.N}2 P{GMR-lacZ.C(38.1)}TPN1; P{ry[+t7.2]=neoFRT}82B PBac{w[+mC]=RB}sds22[e00975]/TM6B, P{y[+t7.7]ry[+t7.2]=Car20y}TPN1, Tb[1]
114-534	y[d2] w[1118] P{ry[+t7.2]=ey-FLP.N}2 P{GMR-lacZ.C(38.1)}TPN1; P{ry[+t7.2]=neoFRT}82B PBac{w[+mC]=WH}CG5451[f03090]/TM6B, P{y[+t7.7]ry[+t7.2]=Car20y}TPN1, Tb[1]
114-556	w[1118] PBac{w[+mC]=WH}CG12659[f07899] Crag[f07899] P{neoFRT}19A/FM7c; P{ey-FLP.D}5
114-561	y[d2] w[1118] P{ry[+t7.2]=ey-FLP.N}2 P{GMR-lacZ.C(38.1)}TPN1; P{ry[+t7.2]=neoFRT}82B P{w[+mC]=XP}htl[d07110]/TM6B, P{y[+t7.7]ry[+t7.2]=Car20y}TPN1, Tb[1]
114-604	y[1] w[*] P{w[+mC]=lacW}sd[G0309] P{neoFRT}19A/FM7c; P{ey-FLP.D}5
114-607	w[67c23] P{w[+mC]=lacW}l(1)G0076[G0076] P{neoFRT}19A/FM7c; P{ey-FLP.D}5
114-608	P{w[+mC]=lacW}l(1)G0144[G0144] w[*] P{neoFRT}19A/FM7c; P{ey-FLP.D}5
114-609	w[67c23] P{w[+mC]=lacW}inx2[G0059] P{neoFRT}19A/FM7c; P{ey-FLP.D}5
114-610	w[67c23] P{w[+mC]=lacW}l(1)G0150[G0150] P{neoFRT}19A/FM7c; P{ey-FLP.D}5
114-612	y[1] w[*] P{w[+mC]=lacW}l(1)G0175[G0175] P{neoFRT}19A/FM7c; P{ey-FLP.D}5
114-614	w[67c23] P{w[+mC]=lacW}ras[G0391] P{neoFRT}19A/FM7c; P{ey-FLP.D}5
114-615	w[67c23] P{w[+mC]=lacW}l(1)G0414[G0414] P{neoFRT}19A/FM7c; P{ey-FLP.D}5
114-636	y[d2] w[1118] P{ry[+t7.2]=ey-FLP.N}2; P{ry[+t7.2]=neoFRT}42D P{w[+mC]=EP}EP882a P(Hildebrand & Shepherd)EP882b /CyO y[+]
114-660	y[d2] w[1118] P{ry[+t7.2]=ey-FLP.N}2 P{GMR-lacZ.C(38.1)}TPN1; P{ry[+t7.2]=neoFRT}82B PBac{w[+mC]=WH}CG31004[f04955]/TM6B, P{y[+t7.7]ry[+t7.2]=Car20y}TPN1, Tb[1]

Table 2-1

Table 2-2. A list of mutant lines causing abnormalities in mushroom body morphogenesis that were identified from the mosaic genetic screen

As shown here are 8 mutant lines that cause absence of α/β neurons or γ neurons in the adult mushroom bodies. These 8 lines are grouped into 3 categories based on their mushroom body phenotypes and *p35* rescue results. The DGRC Number, associated gene(s), the allele name(s) are also shown for each line. Representative images for each category are also shown.

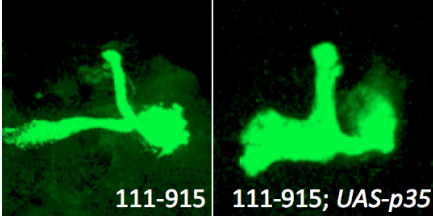
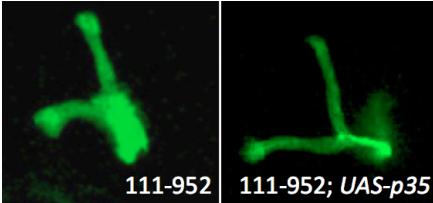
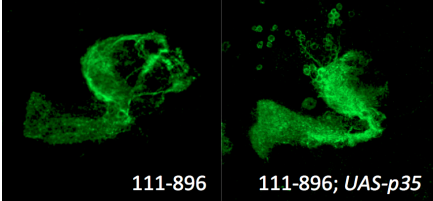
DGRC No.	associated gene(s)	allele name(s)
Category A: mutant showing the α/β only phenotype that were rescued by ectopic expression of <i>UAS-p35</i>		
111-853	<i>l(1)G0152</i>	<i>l(1)G0152^{G0152}</i>
111-882	<i>elav, l(1)G0378</i>	<i>elav^{G0378a}, l(1)G0378^{G0378}</i>
111-915	<i>Rph, l(1)G0184</i>	<i>Rph^{G0184b}, l(1)G0184^{G0184}</i>
		
Category B: mutant showing the α/β only phenotype that were not rescued by ectopic expression of <i>UAS-p35</i>		
111-890	<i>e(y)3</i>	<i>e(y)3^{G0381}</i>
111-897	<i>l(1)G0412</i>	<i>l(1)G0412^{G0412}</i>
111-952	<i>gt</i>	<i>gt^{KG01741}</i>
		
Category C: mutant showing the γ only phenotype that were not rescued by ectopic expression of <i>UAS-p35</i>		
111-840	<i>CG12991</i>	<i>CG12991^{G0143a}</i>
111-896	<i>dome</i>	<i>dome^{G0405}</i>
		

Table 2-2

Chapter 3: JAK/STAT signaling prevents neuroblast termination and promotes neuroblast division in *Drosophila* mushroom bodies

Abstract

Through a MARCM-based genetic screen, I found that mutations in *Drosophila* receptor of the Janus Kinase (JAK) / Signal Transducer and Activator of Transcription (STAT) pathway *domeless* (*dome*) led to significantly reduced number of neurons that are all γ type. And loss of JAK/STAT downstream kinase *hopscotch* (*hop*) caused the similar phenotype in mushroom body. The mutant phenotype could be perfectly rescued by ectopic expression of *UAS-dome* or a dominant-active form of *Stat92E* (*Stat92E^{ΔNΔC}*) in the *dome* mutant mushroom body neuroblast clones. Therefore, I conclude that the mutant phenotype is caused by loss of JAK/STAT signaling. More evidence suggests that the loss of JAK/STAT pathway does not affect the morphogenesis and survival of post-mitotic γ neurons, nor the subtype differentiation of mushroom body neurons. Furthermore, by performing a time-course study and neuroblast-specific antibody staining, I found that loss of *dome* caused precocious disappearance of mushroom body neuroblasts, and ectopic expression of *Stat92E^{ΔNΔC}* led to neuronal overgrowth. Based on these results, I confirmed that JAK/STAT signaling is required for the neuroblast maintenance and cell proliferation in mushroom bodies.

Loss of *dome* function leads to defects in mushroom body neurogenesis

When generated in newly hatched larvae (NHL) and examined in adult brains, each wild type mushroom body neuroblast generated all three subtypes of neurons: γ , α'/β' , and α/β (Fig. 3-1A). However, mushroom body neuroblast clones homozygous for the mutant JAK/STAT pathway receptor gene *domeless* (*dome*) exhibit significantly reduced number of neurons that are all γ type (Fig. 3-1B). This is a recessive lethal mutant named *dome*^{G0405} in the flybase that is induced by P element insertion in the 5' untranslated region of *dome* gene. It is a hypomorphic allele, the lethality occurs during the first and second larval instars. To confirm it is the mutation in *dome* gene responsible for this γ -only phenotype, another *dome* mutant allele named *dome*⁴⁶⁸ was tested using MARCM analysis. *dome*⁴⁶⁸ is a loss of function allele which is also induced by P element insertion in the 5' untranslated region of *dome*. Mutant animals are lethal at the first instar larval stage (Brown et al., 2001). The similar mushroom body abnormalities were observed (Fig. 3-1C), although some wild-type clones were seen occasionally. So *dome*^{G0405} causes more severe phenotype in mushroom bodies than *dome*⁴⁶⁸. This is different from the case in posterior spiracles, with the latter showing stronger phenotypes than the former (Brown et al., 2001). Next, the rescue test was performed by specifically overexpressing *UAS-dome* in the *dome* mutant clones. I found that expression of *UAS-dome* in the *dome* mutant mushroom body clones fully rescues the γ -only phenotype (Fig. 3-1D). Altogether, these results suggest that the loss of *dome* function cause the γ -only phenotype in mushroom bodies.

Figure 3-1. Loss of *dome* function causes γ -only phenotype in adult mushroom bodies

A-D shown are composite confocal images of mushroom body neuroblast clones induced in newly hatched larvae and examined in adult brains. All mushroom body neurons are labeled due to *GAL4-OK107*-driven expression of *mCD8::GFP*. Midline of the brain is at the left side of the image in this and all subsequent images. In wild-type mushroom body neuroblast clone (A), all five axon lobes of three neuron subtypes, γ , α'/β' , and α/β lobes were observed. In *dome*^{G0405} mushroom body neuroblast clone (B), only the first-born γ neurons were observed, and the number of neurons was greatly reduced. In *dome*⁴⁶⁸ mushroom body neuroblast clone (C), the phenotype is similar to that of *dome*^{G0405}. In (D), the expression of *UAS-dome* in the *dome* mutant clone rescued the γ -only phenotype.

Genotype: (A) *FRT19A, UAS-mCD8::GFP/FRT19A, hs-FLP, tubP-GAL80; UAS-mCD8::GFP/+; GAL4-OK107/+*; (B) *FRT19A, dome*^{G0405}*/FRT19A, hs-FLP, tubP-GAL80; UAS-mCD8::GFP/+; GAL4-OK107/+*; (C) *FRT19A, dome*⁴⁶⁸*/FRT19A, hs-FLP, tubP-GAL80; UAS-mCD8::GFP/+; GAL4-OK107/+*; (D) *FRT19A, dome*^{G0405}*/FRT19A, hs-FLP, tubP-GAL80; UAS-mCD8::GFP/UAS-dome; GAL4-OK107/+*.

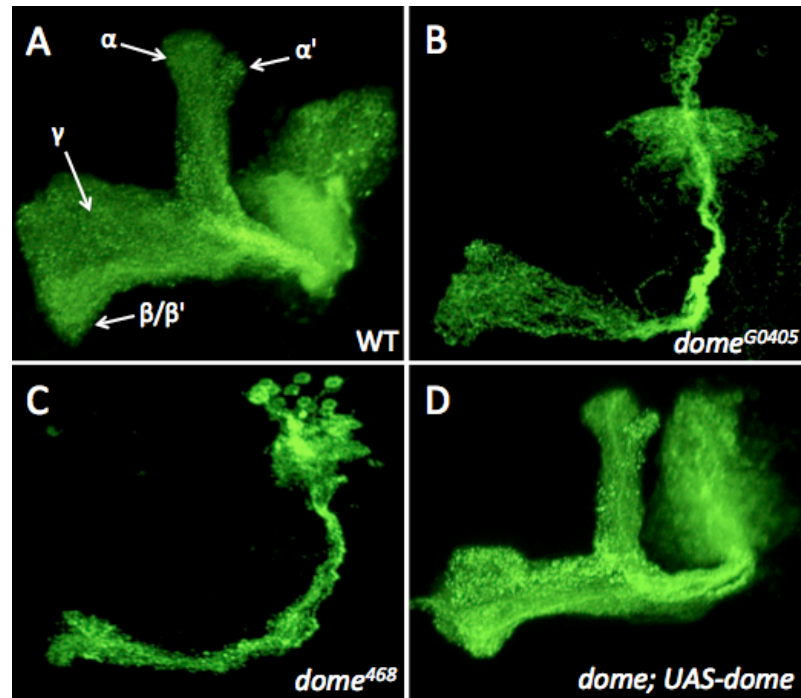


Figure 3-1

Lack of JAK/STAT signaling causes the γ -only phenotype in adult mushroom bodies

Dome is the receptor for *Drosophila* JAK/STAT signaling pathway. Loss of *dome* function causes γ -only phenotype in adult mushroom bodies. To test if this phenotype is caused by loss of JAK/STAT signaling, I examined the effect of loss of JAK kinase (*hop*) in adult mushroom body. *hop*² is a loss of function allele, which was induced by X ray to delete about 300bp of genomic DNA (Binari & Perrimon, 1994). I performed MARCM analysis for *hop*² in the mushroom body. The similar phenotype was observed as that in *dome* mutant clones, which is the significantly reduced number of neurons that are nearly all γ type (Fig. 3-2C).

Next, I examined the effect of the gain-of-function of the downstream transcriptional factor Stat92E. The expression of a dominant-active form of *Stat92E* in *dome* mutant clones was performed for MARCM analysis. The dominant-active form of *Stat92E* resulted from the removal of both the N- and C-terminal domains in *Stat92E*, named *Stat92E* ^{Δ NAC} (Ekas et al., 2010). It has been shown that neither the first 133 nor the last 36 amino acids are required for Stat92E function, and the removal of both of these domains resulted in a constitutively active form of Stat92E. It was also shown that the dominant-active abilities of *Stat92E* ^{Δ NAC} require phosphorylation of Tyr⁷¹¹ as well as the formation of the endogenous Stat92E: *Stat92E* ^{Δ NAC} dimers (Ekas et al., 2010). I found that the expression of *UAS-Stat92E* ^{Δ NAC} fully rescued the γ -only phenotype in *dome* mutant clones (Fig. 3-2D), suggesting the requirement of activation of JAK/STAT signaling in mushroom body normal development. With all these results, I come to the conclusion

that loss of JAK/STAT signaling activity causes the γ -only phenotype in the mushroom bodies.

Figure 3-2. Lack of JAK/STAT signaling causes the γ -only phenotype in adult mushroom bodies

A-D shown are composite confocal images of mushroom body neuroblast clones induced in newly hatched larvae and examined in adult brains. All mushroom body neurons are labeled due to *GAL4-OK107*-driven expression of *mCD8::GFP*. In wild-type (A), full γ , α'/β' , and α/β lobes were observed. In *dome*^{G0405} mutant clone (B), only the first-born γ neurons were observed, and the number of neurons was greatly reduced. In *hop*² mutant clone (C), very similar phenotype was observed as that in *dome* mutant clones. Most of the neurons are early-born γ neurons, and the number of neurons was greatly reduced. In (D), the expression of *UAS-Stat92E*^{ANAC} in the *dome*^{G0405} mutant clones rescued the γ -only phenotype. Genotype: (A) *FRT19A, UAS-mCD8::GFP/FRT19A, hs-FLP, tubP-GAL80; UAS-mCD8::GFP/+; GAL4-OK107/+*; (B) *FRT19A, dome*^{G0405}/*FRT19A, hs-FLP, tubP-GAL80; UAS-mCD8::GFP/+; GAL4-OK107/+*; (C) *FRT19A, hop*²/*FRT19A, hs-FLP, tubP-GAL80; UAS-mCD8::GFP/+; GAL4-OK107/+*; (D) *FRT19A, dome*^{G0405}/*FRT19A, hs-FLP, tubP-GAL80; UAS-mCD8::GFP/UAS-Stat92E*^{ANAC}; *GAL4-OK107/+*.

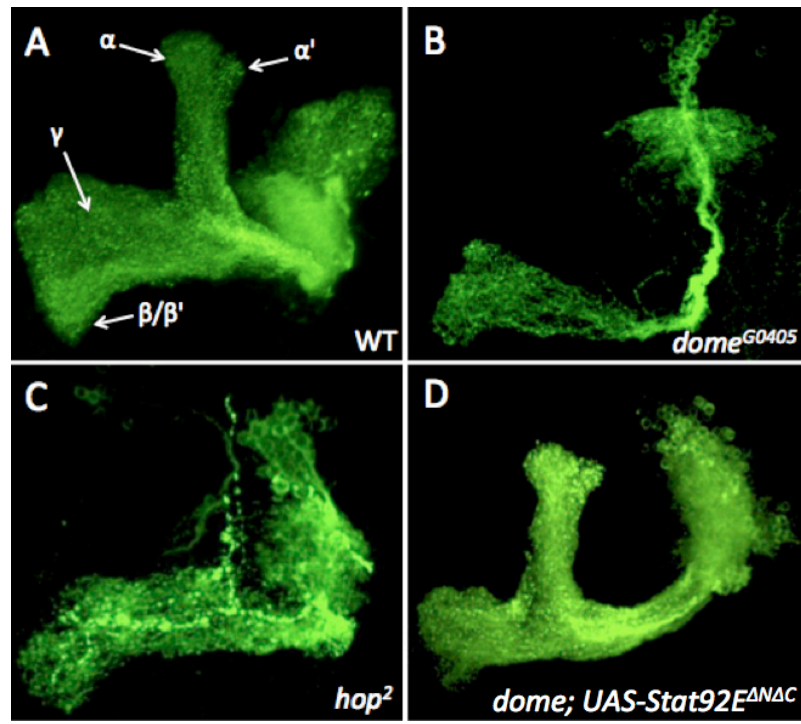


Figure 3-2

JAK/STAT pathway activity is not required for the survival and cell fate specification of mushroom body neurons

Reduction in mushroom body neurons could be due to decreased neuron generation or increased post-mitotic neuron death. Moreover, the γ -only phenotype of *dome* or *hop* mushroom body could be the result of either cell fate specification failure or premature neuroblast termination. To clarify the cellular basis of *dome* or *hop* mushroom body phenotype, I first test whether the JAK/STAT signaling affects post-mitotic neuron survival and cell fate specification of mushroom body neurons.

When generated in newly hatched larvae and examined at different developmental stages, the number of neurons in the *dome* mushroom body neuroblast clones are comparable at newly emerged and 4-week-old adults (Fig. 3-3A, c and d), indicating that JAK/STAT is not required for the long-term survival of post-mitotic mushroom body neurons.

Furthermore, neurons generated by *dome* mushroom body neuroblast clones were of normal γ neuron morphology at the wandering larval stage (Fig. 3-3A, a) and underwent remodeling at the pupal stage (Fig. 3-3A, b), which resulted in WT-like adult γ neurons (Fig. 3-3A, c and d). This indicates that loss of JAK/STAT does not affect morphology, remodeling and survival of mushroom body γ neurons, and the reduced neuron number is not caused by the death of postmitotic neurons. Thus, JAK/STAT signaling is not required for the long-term survival of mushroom body neurons. Alternatively, it is needed to generate neurons.

I then generated *dome* mushroom body neuroblast clones at different developmental stages and examined them in adult brains. Whenever the clones were created, I invariably observed fewer neurons generated by *dome* mushroom body neuroblast clones (Fig. 3-

3B). However, the γ to α'/β' or α'/β' to α/β subtype switch of mushroom body neurons wasn't affected. For example, when created in early 2nd instar larva (24 hrs ALH), *dome* mushroom body neuroblast clones produced γ plus a few α'/β' neurons (Fig. 3-3B, e); when created in the early 3rd instar larva (48 hrs ALH), *dome* mushroom body neuroblast clones mainly produced α'/β' and a few γ and α/β neurons (Fig. 3-3B, f); *dome* mushroom body neuroblast clones induced at the middle 3rd instar (72 hrs ALH) produced α'/β' and α/β neurons (Fig. 3-3B, g); and *dome* mushroom body neuroblast clones induced at early pupa (96 hrs ALH) produced only α/β neurons (Fig. 3-3B, h). I invariably observed a premature arrest of neuroblast proliferation when the *dome* mutant clones were induced at different larval stages, indicating that JAK/STAT signaling is required for neuroblast proliferation during these early developmental stages. Altogether these results indicate that the JAK/STAT pathway does not affect the morphogenesis and survival of post-mitotic γ neurons or the subtype differentiation of mushroom body neurons.

Figure 3-3. Loss of *dome* does not affect differentiation and survival of the post-mitotic neurons

Confocal images of *dome*^{G0405} mushroom body neuroblast clones induced/examined at the indicated developmental stages. All clones were labeled by *GAL4-OK107>UAS-mCD8::GFP*.

Figure 3-3A: Confocal images of *dome*^{G0405} mushroom body neuroblast clones induced in the newly hatched larvae and examined at different developmental stages, showing normal morphology (a) and remodeling (b) of larval γ neurons and the survival of γ adult neurons till 4 weeks after eclosion (comparing d to c). Loss of *dome* does not affect morphology, remodeling and survival of mushroom body γ neurons.

Figure 3-3B: Confocal images of *dome*^{G0405} mushroom body neuroblast clones induced at different developmental stages and examined at one-week adult brains, showing that loss of *dome* does not affect γ to α'/β' or α'/β' to α/β subtype-switch of mushroom body neurons. e, *dome* clones induced in early 2nd instar larva (24 hrs ALH), showing γ plus a few α'/β' neurons were produced; f, *dome* clones induced in early 3rd instar larva (48 hrs ALH), showing γ and α'/β' plus a few α/β neurons were produced; g, *dome* clones induced at middle 3rd instar (72 hrs ALH), showing α'/β' and α/β neurons were produced; and h, *dome* clones induced at early pupa (96 hrs ALH), showing only α/β neurons were produced.

Genotype: *FRT19A, dome*^{G0405}/*FRT19A, hs-FLP, tubP-GAL80; UAS-mCD8::GFP/+; GAL4-OK107/+*.

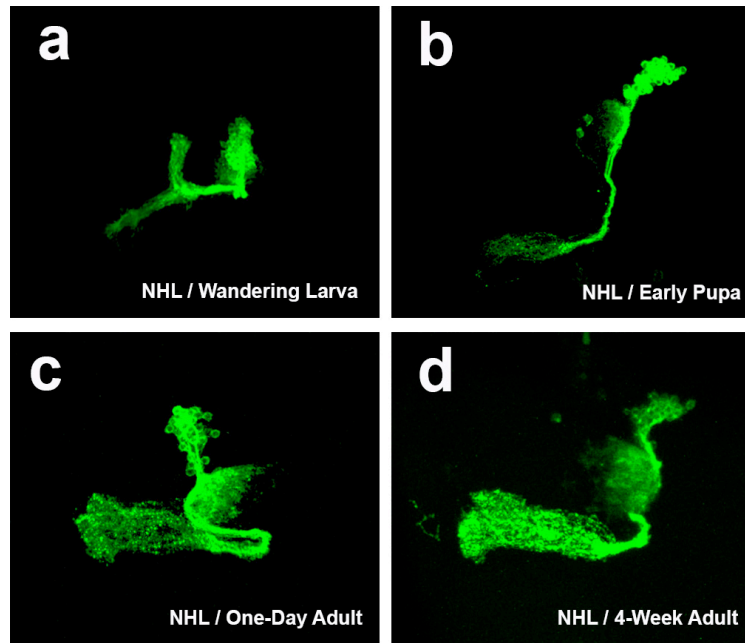


Figure 3-3A

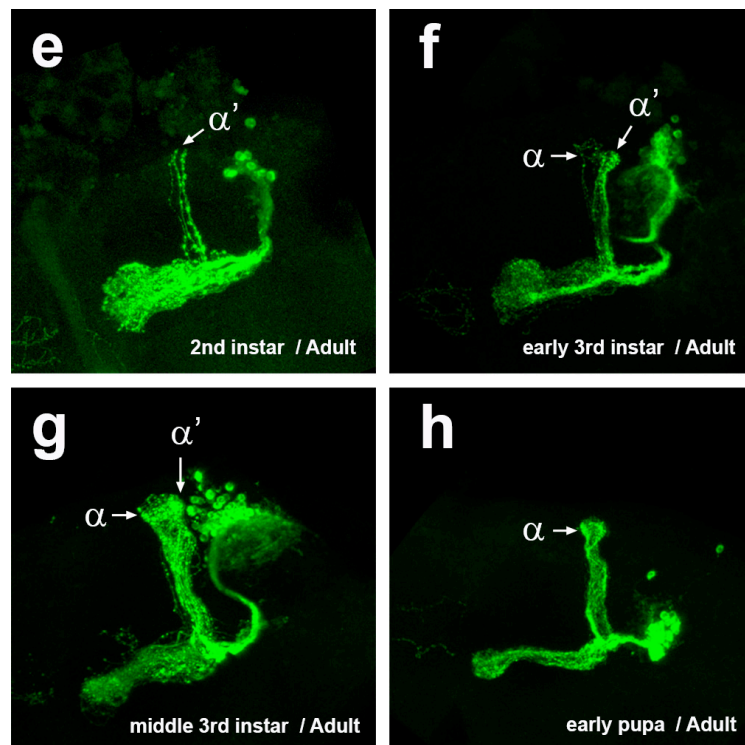


Figure 3-3B

JAK/STAT signaling prevents premature neuroblast termination and promotes cell division of mushroom body neuroblasts

Neuroblast clones homozygous for *dome*, as well as for *hop*, exhibit significantly reduced cell number, with most or all neurons are early-born γ neurons, suggesting a defect in the continuous generation of new neurons from the neuroblasts. To clarify the cellular basis of the γ -only phenotype, I performed a time-course study to quantify the neurons generated by wild type, *dome* mutant, and *Stat92E* gain-of-function mushroom body neuroblasts at different developmental stages. Using the MARCM technique, I induced neuroblast clones in NHL. Brains are collected at 48h-, 72h-, 96h-ALH, 24h-, 60h-APF (after pupa formation), and 1-day-, 1-week-, 2-week-adults and processed for mCD8 (clone marker) antibody staining. Images were collected using confocal microscopy. Individual neuroblast lineage sizes were determined by counting the number of neurons in each clone.

Loss of *dome* results in significantly smaller mutant clones, in which the neuroblasts fail to generate new neurons starting from the wandering larval (WL) stages. On the other side, expression of dominant-active *Stat92E* (*Stat92E DA*) in the wild-type clones leads to neuronal overgrowth. In WL, wild-type clones had an average of 104 ± 10.2 cells ($n=12$ clones), compared with 19.9 ± 3.5 cells ($n=9$ clones) in *dome* mutant clones, and 193.9 ± 20.1 cells ($n=15$) in *Stat92E DA* clones ($P < 0.0001$) (Fig. 3-4, a). At 24h APF (Fig. 3-4, b), the average number of cells is 32.3 ± 5.6 ($n=27$) in *dome* mutant clones, 264.4 ± 10.7 ($n=13$) in *Stat92E DA* clones, compared with 190.2 ± 20.1 ($n=11$) in wild-type clones ($P < 0.0001$). At later pupa stage (60h APF) (Fig. 3-4, b), the average number of cells is 25.3 ± 4.0 ($n=12$) in *dome* mutant clones, 296.1 ± 30.8 ($n=9$) in *Stat92E DA* clones,

compared with 139.8 ± 26.8 (n=12) in wild-type clones ($P < 0.0001$). In 1-day adults (Fig. 3-4, c), the average number of cells is 23.1 ± 1.4 (n=14) in *dome* mutant clones, 414.1 ± 38.4 (n=20) in *Stat92E DA* clones, compared with 191.1 ± 17.7 (n=13) in wild-type clones ($P < 0.0001$). In 1-week adults (Fig. 3-4c), the average number of cells is 21.5 ± 3.2 (n=14) in *dome* mutant clones, 509.1 ± 49.2 (n=12) in *Stat92E DA* clones, compared with 228.9 ± 38.5 (n=12) in wild-type clones ($P < 0.0001$).

In summary, as shown in (Figure. 3-4, d), from 48 hours after larval hatching (ALH) to the early pupal stage, the number of neurons generated by a wild type mushroom body neuroblast continuously increased. It then moderately decreased during metamorphosis and increased again to over 200 neurons at the adult stage. However, the number of neurons generated by a *dome* mutant mushroom body neuroblast stopped increasing at the early 3rd larval stage and remained at ~20 hereafter. By contrast, when *Stat92E^{ΔNΔC}*, a dominant-active form of *Stat92E* (named *Stat92E DA* here), was expressed in a wild-type mushroom body neuroblast clone, the number of neurons generated overpassed that generated by wild type neuroblasts at all developmental stages and resulted in more than 500 neurons, a two-fold increase.

I further labeled mushroom body neuroblasts using a neuroblast-specific marker, Dpn antibody (Boone & Doe, 2008), at the early pupal stage. Mushroom body neuroblast clones are induced in NHL, and brains are collected and processed for Dpn antibody staining. Images are collected using confocal microscopy. The brain hemisphere with a wild-type clone has four mushroom body neuroblasts (Fig. 3-4, e, left panel). That with a *dome* mutant clone has only three mushroom body neuroblasts (Fig. 3-4, e, middle panel),

implying that the *dome* mutant neuroblasts prematurely disappeared. The neuroblast premature disappearance could be due to either death or defects in self-renewal, which is usually called neuroblast termination. However, the brain hemisphere with a *Stat92E* gain-of-function clone also has only four mushroom body neuroblasts (Fig. 3-4, e, right panel), indicating that the supernumerary neurons in *Stat92E* gain-of-function clones are a result of faster cell division from a single neuroblast.

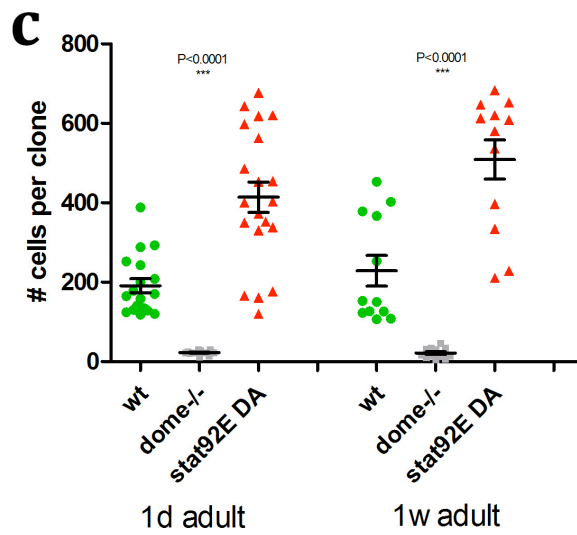
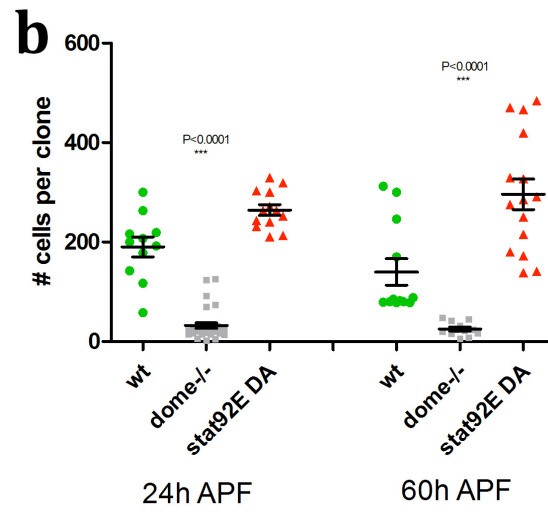
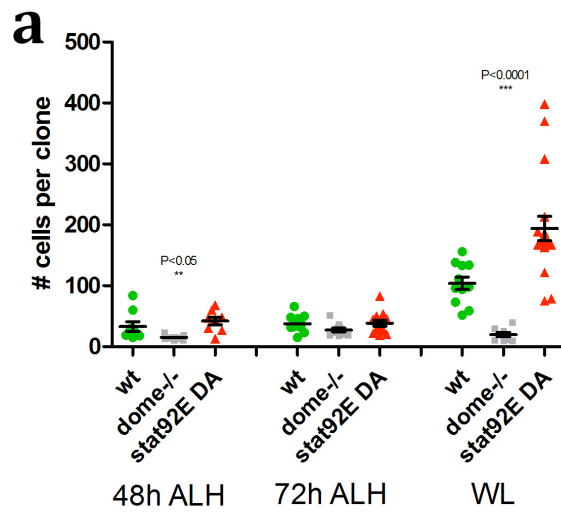
All together, these results demonstrate that the JAK/STAT pathway plays two major roles in the mushroom body neurogenesis: preventing premature neuroblast termination and promoting neuroblast division.

Figure 3-4. JAK/STAT signaling promotes division and prevents premature termination of mushroom body neuroblasts

a-c, Quantification of neurons generated by wild-type, *dome* mutant, and *Stat92E* gain-of-function mushroom body neuroblasts. Mushroom body neuroblast clones were induced in newly hatched larvae and examined at different developmental stages. Individual clone sizes were quantified by counting cells within each clone, grouped by developmental stages: (a) for larval stages, (b) for pupa stages, and (c) for adults. Data represent average of 10-27 clones. Statistical significance was calculated using One way ANOVA. Error bars indicate standard error of the mean. Genotypes and *P*-values as indicated.

d, Line plot of average cells per neuroblast clone at different developmental stages based on data in a-c. Wild type represented in blue line, *dome* mutant represented in red line, and *Stat92E* gain-of-function represented in green line.

e, Confocal images of the mushroom body region of early pupa brains. Only cell bodies are presented to show MARCM neuroblast clones induced in the newly hatched larvae (green, *GAL4-OK107>UAS-mCD8::GFP*) and neuroblasts (red, Dpn antibody staining). Genotypes as indicated.



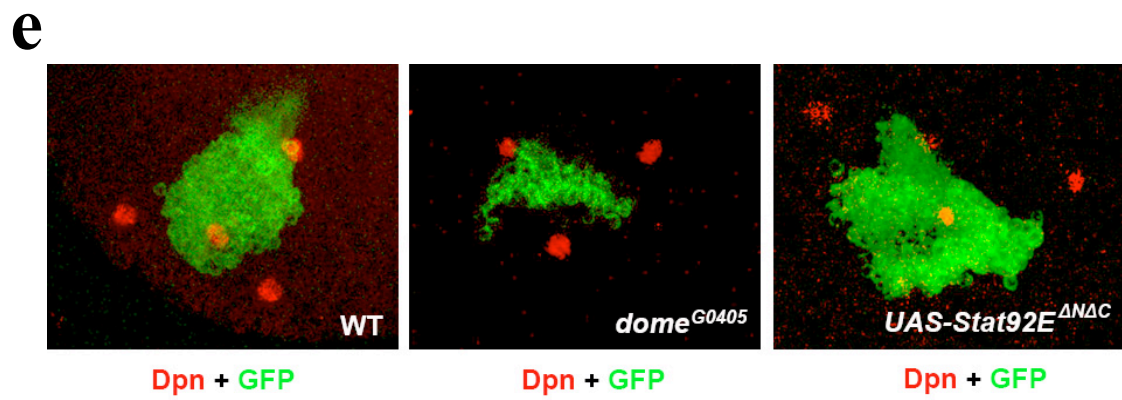
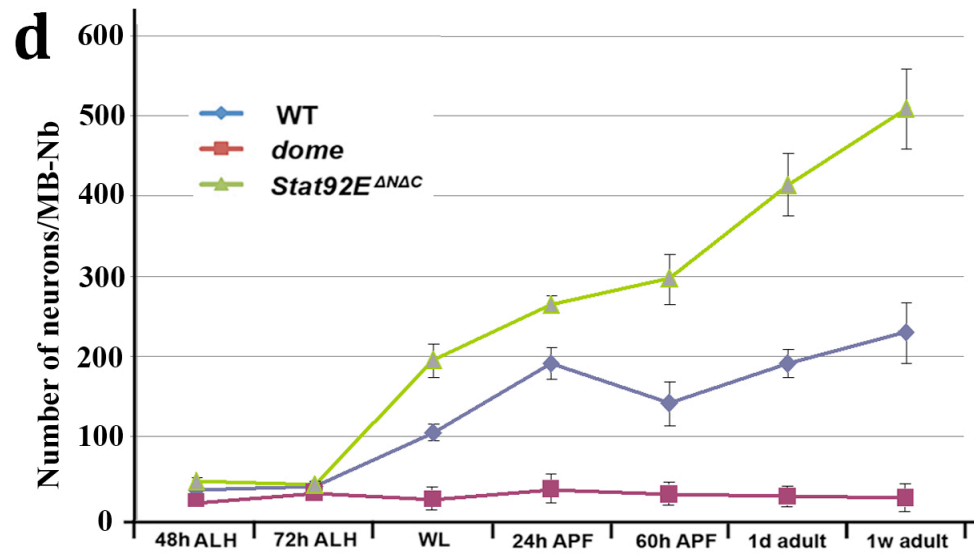


Figure 3-4

Chapter 4: Both JAK/STAT signaling activity and Hippo pathway effector Yki activity are required for mushroom body neurogenesis, and higher activation of one can compensate for lack of the other

Abstract

To identify JAK/STAT signaling downstream targets that are crucial for mediating mushroom body neurogenesis, I tested a group of genes that are well characterized to be involved in the control of cell proliferation or cell death. Overexpression of Hippo pathway effector *yorkie* (*yki*) fully and overexpression of *CycE* and/or *Diap1*, the downstream target genes of Yki, partially rescues the phenotype of *dome* mutant mushroom body neuroblast clones. In order to investigate whether Yki function is required for the normal development of mushroom bodies, loss-of-function phenotypes of *yki* were analyzed. In adult brains, MARCM neuroblast clones mutant for *yki* exhibit the similar mutant phenotype, although with a lower penetrance. I further examined whether over-activation of JAK/STAT can rescue *yki* mutant phenotypes. And I found that ectopic expression of *UAS-Stat92E^{ΔNΔC}*, *UAS-CycE* or/and *UAS-Diap1* in the *yki* mutant neuroblast clones significantly rescued the mutant phenotype. Therefore, I conclude that loss of JAK/STAT signaling activity and loss of Hippo pathway downstream effector *yki* cause similar cell proliferation defects in mushroom body, which can be mutually rescued by higher level of each other and by overexpression of *CycE* or *Diap1*.

***yorkie* (*yki*) overexpression rescues the phenotype resulting from the loss of JAK/STAT signaling in mushroom bodies**

JAK/STAT signaling might function through *Death-associated inhibitor of apoptosis protein 1* (*Diap1*) to prevent neuroblast termination, because *Diap1* is a direct target of Stat92E (Betz et al., 2008). In contrast, its downstream target(s) of promoting neuroblast division is unclear. JAK/STAT signaling was reported to facilitate cells progressing through G1/S and G2/M cell cycle checkpoints in the *Drosophila* eye and wing imaginal discs (Bach et al., 2003; Rodrigues et al., 2012). However, multiple independent genetic and RNAi screens failed to identify the target genes that are required for cell-cycle progression (Zoranovic et al., 2013). Because a *Stat92E* gain-of-function neuroblast generates more neurons than a wild-type one without producing excess neuroblasts (Fig. 3-4, d and e), I believe that JAK/STAT signaling does not regulate neuroblast asymmetrical division. Instead, it works through a general mechanism to control cell division and death.

To identify JAK/STAT signaling downstream targets that are crucial for mediating mushroom body neurogenesis, I set out to test a group of genes that are well characterized to be involved in the control of either cell proliferation or cell death. Taking advantage of a collection of *UAS* transgenic lines (see Table 4-1), including *UAS-CycD*, *UAS-Cdk4*, *UAS-CycE*, *UAS-Myc*, *UAS-E2f1*, *UAS-Dp*, *UAS-yorkie* (*yki*), *UAS-shg*, *UAS-Pi3K92E*, and *UAS-Diap1*, I overexpressed these genes in the *dome* mutant mushroom body clones, respectively, and tested whether they could rescue the γ -only phenotype of *dome* mutant mushroom body. Studies in vertebrates suggest *Cyclin D* (*CycD*) and *c-Myc* as JAK/STAT downstream target genes to promote cell-cycle progression (Bowman et al.,

2000; Calo et al., 2003). Here, I found that overexpression of *CycD* or *Myc* failed to rescue the γ -only phenotype of *dome* mutant mushroom body (Fig. 4-1). Instead, of 11 genes examined, overexpression of Hippo pathway downstream effector *yorkie* (*yki*) fully rescued the γ -only phenotype of *dome* mushroom body neuroblast clones (Fig. 4-2, a) and overexpression of *CycE* or *Diap1* partially but significantly rescues this phenotype (Fig. 4-2, b and c). Moreover, overexpression of *CycE* and *Diap1* together resulted in more complete rescue than either of them separately (Fig. 4-2, d). Therefore, I propose that JAK/STAT signaling acts through *Diap1* to prevent neuroblast termination and through *CycE* to promote neuroblast division.

Table 4-1. List of genes tested as potential downstream mediators for the JAK/STAT signaling pathway in mushroom body neurogenesis

As shown here is a collection of *UAS*-transgene lines of genes involved in the control of either cell proliferation or cell death. *UAS*-transgenes were expressed in *dome*^{G0405} mutant mushroom body neuroblast clones that were induced in newly hatched larvae, and the rescue effects were examined in adult brains. The gene encoding protein name in *Drosophila*, the efficiency to rescue *dome* mutant phenotype in mushroom body, the known function of gene in *Drosophila*, and the orthologs in mammals are listed.

<i>UAS</i> -transgene	Encoding protein name	Rescue Efficiency	Function in <i>Drosophila</i>	Orthologs in Mammals
<i>UAS-Diap1</i>	Death-associated inhibitor of apoptosis 1, also known as Thread	significant rescue	cell apoptosis inhibitor	XIAP, MIHB, MIHC, NAIP, Survivin
<i>UAS-CycD</i>	Cyclin D	none	promote cellular growth in complex with Cdk4 (Datar et al., 2000)	Cyclin D1, D2, and D3
<i>UAS-Cdk4</i>	Cyclin-dependent kinase 4	none	promote cellular growth in complex with CycD (Datar et al., 2000)	Cdk4
<i>UAS-CycE</i>	Cyclin E	significant rescue	the G1 cyclin essential and rate limiting for progression into S phase (Jones et al., 2000)	CycE1 and E2
<i>UAS-Myc</i>	v-Myc myelocytomatosis viral oncogene homolog	none	transcription factor regulates cell growth, proliferation and apoptosis (Benassayag et al., 2005)	C-Myc, and L-Myc
<i>UAS-E2f1</i>	E2F1 transcription factor	none	promote transcription of a large set of cell cycle genes by interacting with DP (Du et al., 1996)	E2F-1, -2, -3, -4, and -5
<i>UAS-Dp</i>	DP transcription factor	none	promote transcription of a large set of cell cycle genes by interacting with E2F (Du et al., 1996)	DP-1 and DP-2
<i>UAS-yki</i>	Yorkie	full rescue	transcriptional coactivator and major downstream effector of Hippo signaling pathway	YAP and TAZ
<i>UAS-shg</i>	Shotgun, also known as DE-cadherin	weak rescue	critical for cell adhesion (Dumstrei et al., 2002)	E-cadherin
<i>UAS-Pi3K92E</i>	Phosphatidylinositol 3-kinase at 92E	weak rescue	intracellular signal transducer enzyme involved in cell growth, proliferation, and differentiation	PI3K

Table 4-1

Figure 4-1. Excess *CycD.Cdk4* or *Myc* in the *dome* mutant mushroom body neuroblasts failed to rescue the γ -only phenotype

a-d, Confocal images of *dome* mushroom body neuroblast clones induced in newly

hatched larvae and examined in the adult brains. All mushroom body neurons are labeled

due to *GAL4-OK107*-driven expression of *mCD8::GFP*. Overexpression of either *UAS-*

CycD.Cdk4 (a) or *UAS-Myc* (b) failed to rescue *dome*^{G0405} phenotypes. Genotype: (a)

FRT19A, dome^{G0405}/*FRT19A, hs-FLP, tubP-GAL80; UAS-mCD8::GFP/+; UAS-*

CycD.Cdk4/+; GAL4-OK107/+; (b) FRT19A, dome^{G0405}/*FRT19A, hs-FLP, tubP-GAL80;*

UAS-mCD8::GFP/+; UAS-Myc/+; GAL4-OK107.

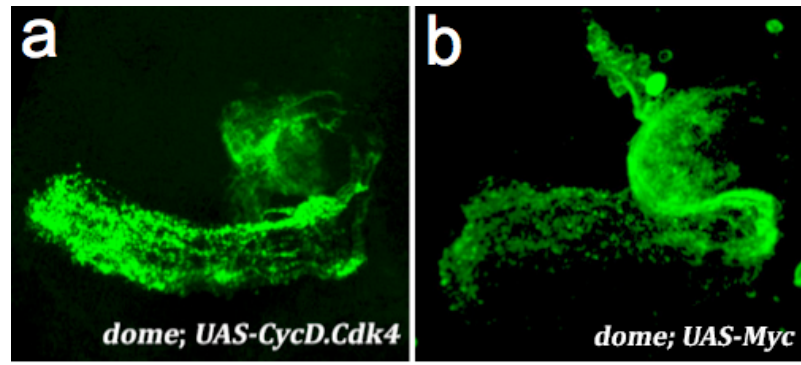


Figure. 4-1

Figure 4-2. The cell proliferation defects of *dome* mushroom bodies are rescued by excess of *yki*, *CycE*, or *Diap1*

a-d, Confocal images of *dome* mushroom body neuroblast clones induced in newly hatched larvae and examined in adult brains, showing rescue efficiencies of *yki*, *CycE*, *Diap1* and *CycE* plus *Diap1* on *dome* mutant phenotypes. All mushroom body neurons are labeled due to *GAL4-OK107*-driven expression of *mCD8::GFP*. In (a), a full rescue was observed by ectopic expression of *yki* in *dome* mutant clones. In (b) and (c), only partial rescue was observed by ectopic expression of *CycE* or *Diap1* in *dome* mutant clones. In (d), overexpression of *CycE* and *Diap1* together in the *dome* mutant clones resulted in more complete rescue than either of them separately. Genotype: (a) *FRT19A, dome^{G0405}/FRT19A, hs-FLP, tubP-GAL80; UAS-mCD8::GFP/+; UAS-yki/+; GAL4-OK107/+*; (b) *FRT19A, dome^{G0405}/FRT19A, hs-FLP, tubP-GAL80; UAS-mCD8::GFP/+; UAS-CycE/+; GAL4-OK107/+*; (c) *FRT19A, dome^{G0405}/FRT19A, hs-FLP, tubP-GAL80; UAS-mCD8::GFP/+; UAS-Diap1/+; GAL4-OK107/+*; and (d) *FRT19A, dome^{G0405}/FRT19A, hs-FLP, tubP-GAL80; UAS-mCD8::GFP/+; UAS-CycE, UAS-Diap1/+; GAL4-OK107/+*.

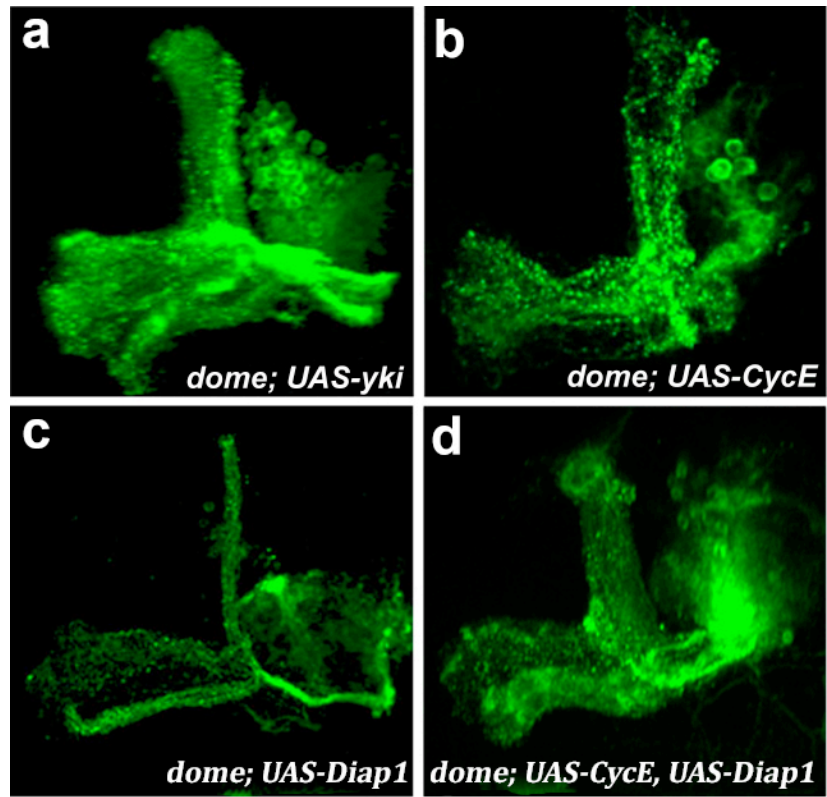


Figure 4-2

Loss of *yki* expression also causes a phenotype similar to that caused by the loss of JAK/STAT signaling in mushroom bodies, and ectopic expression of *Stat92E*^{*ΔNAC*} rescues this phenotype

Interestingly, *CycE* and *Diap1* are also the major target genes of Yki, the downstream effector of the Hippo signaling pathway, in regulating cell division and apoptosis (Tapon et al., 2002; Wu et al., 2003; Wu et al., 2008), which perfectly interprets why *yki* rescues *dome* mutant phenotypes (Fig. 4-2a). However, it is not necessary that Yki function is also required for normal mushroom body neurogenesis. To test this, I next analyzed loss-of-function phenotypes of *yki*. MARCM neuroblast clones homozygous for *yki*^{*B5*}, an *yki* null allele (Bennett & Harvey, 2006), were induced in newly hatched larvae and examined in adult brains. I found that ~43% *yki* mutant neuroblast clones showed cell proliferation defects to different extents, such as reduced α'/β' or α/β lobes (Fig. 4-3, a and b), suggesting premature neuroblast termination, while other clones had WT-like morphology (Fig. 4-3, c). Thus, loss of *yki* in mushroom body neuroblasts caused phenotypes similar to but less severe than loss of the JAK/STAT pathway activity (Fig. 3-2).

As *yki* overexpression rescues JAK/STAT mutant phenotypes, next I tested whether higher JAK/STAT pathway activity could also rescue *yki* mutant phenotypes. When *UAS-Stat92E*^{*ΔNAC*}, *UAS-Diap1*, *UAS-CycE*, and *UAS-Diap1* plus *UAS-CycE*, was expressed in the *yki*-null mutant mushroom body neuroblast clones, overexpression of *UAS-Stat92E*^{*ΔNAC*} fully rescued *yki* mutant phenotypes, whereas overexpression of *Diap1* or/and *CycE* partially but significantly rescued *yki* mutant phenotypes (see Fig. 4-3d, bar graph). Therefore, loss of JAK/STAT pathway activity and loss of Hippo pathway downstream effector *yki* cause similar cell proliferation defects in mushroom body, which

can be mutually rescued by higher level of each other and by overexpression of *CycE* or *Diap1*.

Figure 4-3. Loss of *yki* also causes the cell proliferation defects similar to that caused by loss of JAK/STAT signaling in mushroom bodies, and ectopic expression of *Stat92E^{ΔNΔC}* can rescue this phenotype

a-c, Confocal images of *yki^{B5}* neuroblast clones induced in newly hatched larvae and examined in adult brains. Mainly, the lobe region is presented to show *yki^{B5}* phenotypes of different degrees. ~43% *yki* neuroblast clones showed cell proliferation defects to different extents, such as reduced α' or α' lobes. a, weak α' lobes were shown in some clones, and b, weak α lobes were shown in some clones, suggesting premature neuroblast termination, while in c, WT-like phenotype was observed in ~57% of the *yki^{B5}* clones. Thus, loss of *yki* in mushroom body neuroblasts caused phenotypes similar to but less severe than loss of the JAK/STAT pathway activity.

d, Penetrance of *yki^{B5}* mushroom body neuroblast clones showing phenotypes of the reduced α or α' lobes under overexpression of *Stat92E^{ΔNΔC}*, *CycE*, *Diap1*, and *CycE* plus *Diap1*. The percentage is calculated based on 23-40 neuroblast clones for each genotype. *Stat92E^{ΔNΔC}* fully rescued *yki* phenotypes, whereas *CycE* and/or *Diap1* partially but significantly rescued *yki* mutant phenotypes. Therefore, loss of JAK/STAT pathway activity and loss of Hippo pathway downstream effector *yki* cause similar cell proliferation defects in mushroom body, which can be mutually rescued by higher level of each other and by overexpression of *CycE* or *Diap1*.

Genotype: (a-c) *hs-FLP, UAS-mCD8::GFP/+; FRTG13, yki^{B5}/FRTG13, tubP-GAL80; GAL4-OK107/+;*

(d, WT) *hs-FLP, UAS-mCD8::GFP/+; FRTG13/FRTG13, tubP-GAL80; GAL4-OK107/+;*

(d, *yki^{B5}*; *UAS-CycE*) *hs-FLP, UAS-mCD8::GFP/+; FRTG13, yki^{B5}/FRTG13, tubP-GAL80; UAS-CycE/+; GAL4-OK107/+;*

(d, yki^{B5} ; *UAS-Diap1*) *hs-FLP*, *UAS-mCD8::GFP/+*; *FRTG13*, $yki^{B5}/FRTG13$, *tubP-GAL80*; *UAS-Diap1/+*; *GAL4-OK107/+*;

(d, yki^{B5} ; *UAS-CycE+Diap1*) *hs-FLP*, *UAS-mCD8::GFP/+*; *FRTG13*, $yki^{B5}/FRTG13$, *tubP-GAL80*; *UAS-CycE*, *UAS-Diap1/+*; *GAL4-OK107/+*;

(d, yki^{B5} ; *UAS-Stat92E^{ΔNΔC}*) *hs-FLP*, *UAS-mCD8::GFP/+*; *FRTG13*, $yki^{B5}/FRTG13$, *tubP-GAL80*; *UAS-Stat92E^{ΔNΔC}/+*; *GAL4-OK107/+*;

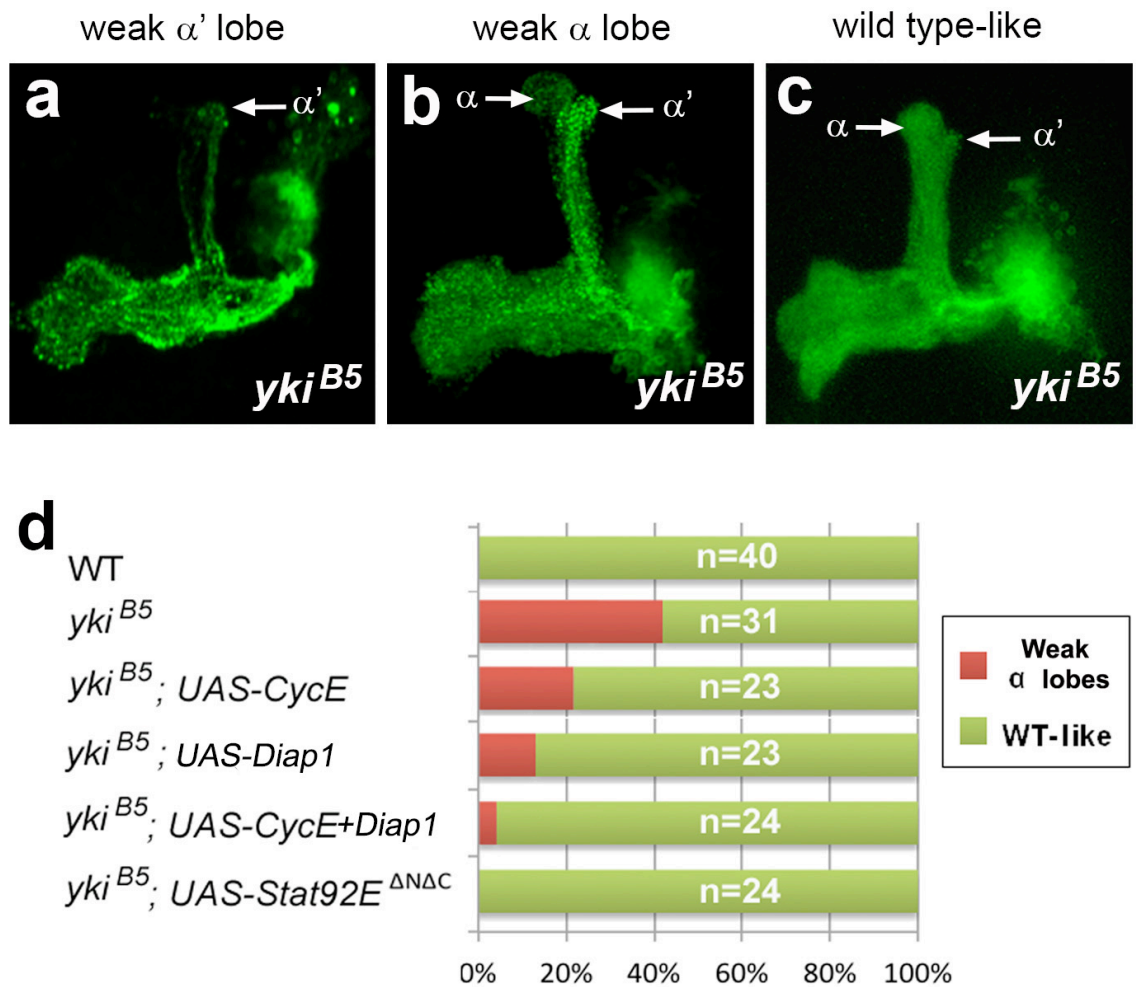


Figure 4-3

Chapter 5: Stat92E directly activates *CycE* expression in mushroom body neuroblasts, and Stat92E and Yki regulate the *CycE* transcription by each interacting with an independent enhancer on *CycE*

Abstract

A consensus Stat92E-binding site is located in the regulatory region of *CycE* locus. To reveal whether JAK/STAT signaling directly regulates *CycE* expression, *lacZ* reporter transgenic studies were performed. I found that expression of *CycE* in the wing disc and mushroom body is activated by Stat92E via the consensus STAT-binding site.

Furthermore, loss-of-function phenotypes of *CycE* in the mushroom body neuroblast clones mimic those of lacking of JAK/STAT pathway activities. And excess *CycE* leads to neuronal overgrowth to the same extend as Stat92E gain-of-function in mushroom body neuroblasts. Together these results suggest that *CycE* is transcriptionally regulated by STAT92E and required for mediating cell proliferation. Therefore, besides *Diap1*, *CycE* is another direct target of JAK/STAT signaling in *Drosophila*, which contribute to the proliferative activity of JAK/STAT. Moreover, by dividing the 16.4kb *cis*-regulatory region of *CycE* into seven fragments and generating seven *lacZ* reporter transgenic flies, I found that Stat92E and Yki regulate the transcription of *CycE* by interacting with two independent *cis*-regulatory elements on *CycE*.

The Stat92E DNA-binding sequence at the *CycE* locus is required for full *CycE* transcriptional activity in wing imaginal discs

My rescue results in mushroom bodies suggest potential interactions between JAK/STAT, Yki, *CycE*, and *Diap1*. Death-associated inhibitor of apoptosis protein 1 (Diap1), also known as Thread, is a key regulator of apoptosis (Hay et al., 1995). The Yki/Scalloped complex binds the Scalloped-binding motif (CATTCCA) in *Diap1* to mediate its transcription (Wu et al., 2003; Wu et al., 2008). Moreover, *Diap1* is also a direct target of the JAK/STAT pathway to protect against apoptosis. Two consensus Stat92E-binding sites (TTCCNNGAA) in the *Diap1* locus are required for Stat92E-dependent *Diap1* expression (Betz et al., 2008). Therefore, both the Hippo and JAK/STAT pathways directly regulate *Diap1* transcription by binding to different enhancers in the *Diap1 cis*-regulatory region. It's well known that Hippo signaling controls cell proliferation mainly through the regulation of *Diap1* and *CycE* (Tapon et al., 2002; Wu et al., 2003). In this study, I found that overexpression of *Diap1* sufficiently rescued the premature termination of *dome* mushroom body neuroblasts. As shown in Fig. 4-2c, though a *dome*, *UAS-Diap1* mushroom body neuroblast clone still generated much fewer neurons than the WT ones, I observed obvious α and β lobes. Therefore, JAK/STAT signaling might act through *Diap1* to prevent mushroom body neuroblast termination. As overexpression of *CycE* substantially rescued the proliferation defects of *dome* neuroblasts (Fig. 4-2b), I was wondering whether JAK/STAT signaling also regulates *CycE* expression.

A consensus STAT-binding sequence, TTCNNNGAA, is found in the first intron of *CycE* gene. It is located at 2L: 15,744,093-15,744,102 (Fig. 5-1a shown in green), which perfectly matched one of 105 Stat92E-binding sites detected by ChIP-chip in the whole

genome, 2L: 15,743,596-15744,299 (Fig. 5-1a shown in red). The same Stat92E ChIP-chip assay has successfully detected known JAK/STAT target genes, such as *Diap1* and *Stat92E* (modENCODE_616). Moreover, this potential Stat92E binding sequence TTCCAAGAA is perfectly conserved across the 12 *Drosophilidae* genomes. Together with my earlier results that *dome* mutant phenotypes can be rescued by overexpression of *CycE*, I propose that *CycE* is a direct target of Stat92E. To test whether the predicted Stat92E-binding site is functional *in vivo*, I produced a *lacZ* reporter transgenic fly line, *CycE(Stat92E-WT)-lacZ*, using an ~ 1-kb genomic DNA fragment that contains this Stat92E-binding site (Fig. 5-1c). The 1-kb DNA fragment containing the predicted Stat92-binding site was subcloned into *pH-Pelican*, an insulated *lacZ* reporter vector designed specifically for enhancer analysis (Barolo et al., 2000). The transgenic fly line was generated by germline injection. *CycE(Stat92E-WT)-lacZ* expression was detected in the wing disc hinge, margin and pouch regions (Fig. 5-1e), which closely resembles the expression pattern of *STAT-GFP*, a Stat92E activity reporter (Bach et al., 2007).

To test whether the Stat92E-binding site in this fragment is responsible for the *lacZ* expression in wing disc, I generated another *lacZ* reporter transgenic fly line, *CycE(Stat92E-MT)-lacZ*, that carries a mutant Stat92E-binding site (TTCCAAGAA to TTCCAAGTT) (Rivas et al., 2008). *CycE(Stat92E-MT)-lacZ* reporter was only weakly expressed in the hinge and margin regions (Fig. 5-1f). These results indicate that the Stat92E DNA-binding site is required for the full *CycE* expression in the wing imaginal discs. To further test the specificity of the Stat92E DNA-binding site, I compared the response of *CycE(Stat92E-WT)-lacZ* and *CycE(Stat92E-MT)-lacZ* to *Stat92E* overexpression in the posterior wing disc domain driven by an *en-GAL4* (Neufeld et al.,

1998) (Fig. 5-1, g and h). *CycE(Stat92E-WT)-lacZ* expression (Fig. 5-1g), but not *CycE(Stat92E-MT)-lacZ* expression (Fig. 5-1h), was increased in response to *en>Stat92E*. Together these data indicate that signals from the *lacZ* reporter highly depend on Stat92E, and that the conserved Stat92E DNA-binding site in the *CycE* locus is required for full *CycE* transcriptional activity *in vivo*.

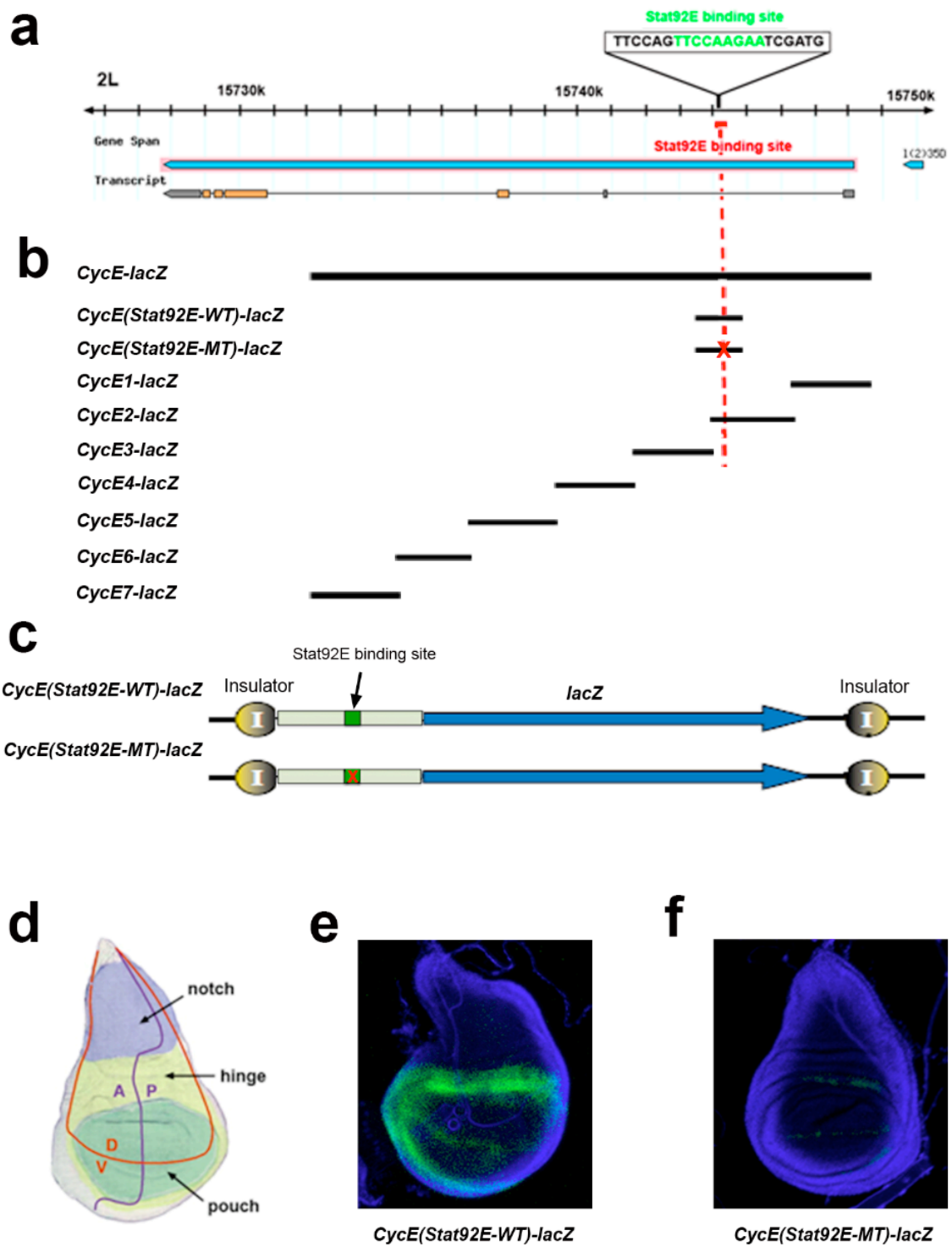
Figure 5-1. Stat92E directly regulate *CycE* transcription in the wing imaginal discs by binding to a consensus STAT DNA-binding site

a-c, *CycE* gene structure and *CycE-lacZ* reporter transgenic lines. a, The structure of *CycE* locus showing the consensus Stat92E-binding site (green; 2L: 15,744,093-15,744,102; TTCCAAGAA), which perfectly matches the Stat92E-binding site detected by CHIP-chip (red; 2L: 15,743,596-15,744,299). b, Diagram showing different *lacZ* reporter transgenic lines that were generated for the *CycE* cis-regulatory element analysis. From top to bottom, they are *CycE-lacZ* carrying a 16.4kb upstream cis-regulatory region of *CycE* gene (Jones et al., 2000); *CycE(Stat92E-WT)-lacZ*; *CycE(Stat92E-MT)-lacZ*; and *CycE1-lacZ* to *CycE7-lacZ*, seven *lacZ* transgenic lines generated by dividing the 16.4kb cis-regulatory DNA into seven fragments. c, Constructs for the *lacZ* reporter transgenic lines of *CycE(Stat92E-WT)-lacZ* and *CycE(Stat92E-MT)-lacZ*. A 1kb DNA segment that contains the predicted *CycE* Stat92E-binding site was isolated by PCR and cloned into *pH-Pelican lacZ* reporter vector to produce *CycE(Stat92E-WT)-lacZ* construct. The predicted *CycE* Stat92E-binding site was mutated from TTCCAAGAA to TTCCAAGTT in *CycE(Stat92E-MT)-lacZ* construct. The vector contains a basal *hs* promoter and insulator elements to prevent position effects. Transgenic lines were generated by germline injection.

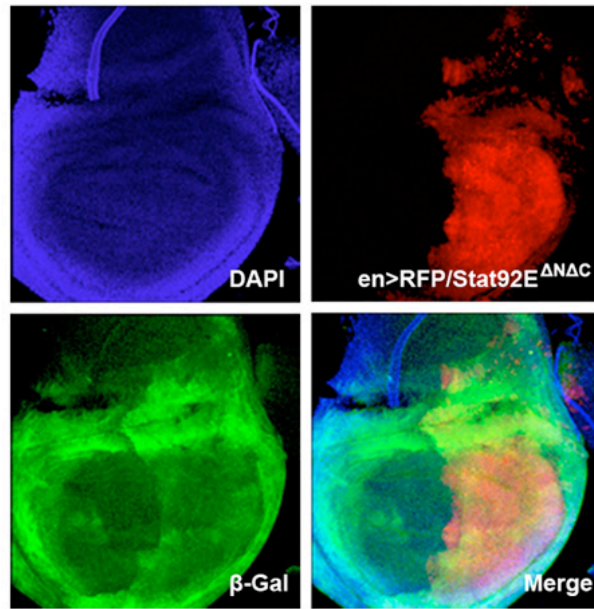
d, A diagram of *Drosophila* wing imaginal disc modified from Butler et al., (2003) Development 130: 659-670.

e-f, Expression of *CycE(Stat92E-WT)-lacZ* and *CycE(Stat92E-MT)-lacZ* in wing discs assessed by β -galactosidase antibody staining, showing that *CycE(Stat92E-WT)-lacZ* highly and *CycE(Stat92E-MT)-lacZ* weakly expressed in the hinge and pouch of wing discs.

g-h, Confocal images of wing discs showing *CycE(Stat92E-WT)-lacZ* or *CycE(Stat92E-MT)-lacZ* expression (green, β -galactosidase antibody staining) in the *en-Gal4*, *UAS-Stat92E^{ΔNΔC}*, *UAS-RFP* (red) genetic background, DAPI (blue) is used to label nuclei. It's shown that *CycE(Stat92E-WT)-lacZ* activity requires the wild-type Stat92E DNA-binding sites. Overexpressed *Stat92E* in the posterior wing disc activates *CycE(Stat92E-WT)-lacZ* (g) but not the *CycE(Stat92E-MT)-lacZ* reporter (h).

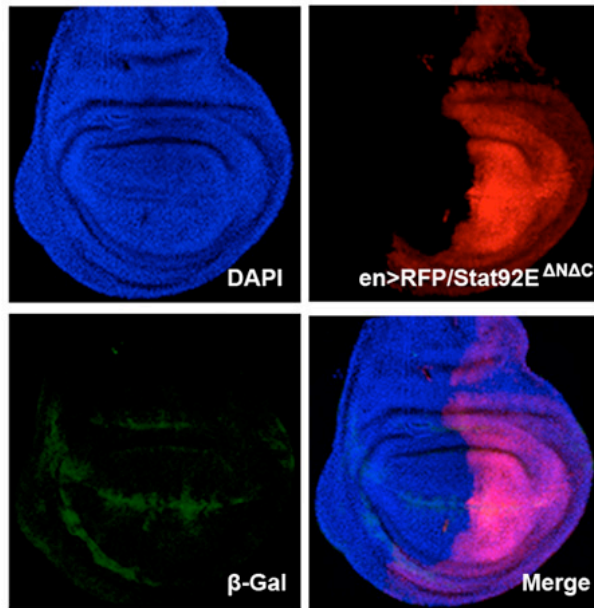


g



CycE(Stat92E-WT)-lacZ

h



CycE(Stat92E-MT)-lacZ

Figure 5-1

Stat92E regulates the expression of *CycE* in mushroom bodies

The earlier data has shown that overexpression of *CycE* partially rescues the γ -only phenotype of *dome* mutant mushroom body neuroblast clones (Fig. 4-2b). And more experiments confirmed that *CycE* is transcriptionally regulated by Stat92E in wing discs. Next I wondered if Stat92E regulate the *CycE* expression in mushroom bodies. I first examined *CycE* and *CycE(Stat92E-WT)-lacZ* expression in the mushroom body region. Immunofluorescence staining with a CycE antibody revealed that *CycE* was broadly expressed in larval brains, and then restricted to the four mushroom body neuroblasts in each brain hemisphere during pupal stages (Fig. 5-2a). The *CycE* expression levels in mushroom bodies were high at early pupal stages and decreased at late pupal stages (Fig. 5-2a). This expression pattern correlates with the pattern of neuroblast proliferation during brain development- most neuroblasts generate neurons in the larval stages and terminate before pupa formation, but exceptionally, mushroom body neuroblasts continuously divide until the end of pupal stages (Sousa-Nunes et al., 2010). *CycE(Stat92E-WT)-lacZ* showed a similar expression pattern to that of endogenous *CycE*, but was expressed in a broader area surrounding mushroom body neuroblasts (Fig. 5-2b), which is, likely, because β -galactosidase is more stable than CycE protein. In contrast, expression of *CycE(Stat92E-MT)-lacZ* was not detected in the mushroom body area of pupal brains (Fig. 5-2c), indicating that the predicted Stat92E-binding site is critical to *CycE* expression in the mushroom body neuroblasts.

To further test the dependence of *CycE* expression on Stat92E in mushroom body neuroblasts, I performed a loss-of-function analysis using a temperature-sensitive *Stat92E* allele, *Stat92E^F/Stat92E⁰⁶³⁴⁶* (*Stat92E^{ts}*) (Baksa et al., 2002). Shifting temperature-

sensitive *Stat92E^{ts}* flies to 29°C can drastically reduce STAT function (Baksa et al., 2002). When shifted at early/mid larva stages, and kept at 29°C for different days, *Stat92E^{ts}* brains were dissected at early pupa stages and being processed for CycE antibody staining. Compared to those consistently kept at permissive temperature (25°C) (Fig. 5-2d), the *CycE* expression levels in the mushroom body neuroblasts were apparently decreased in brains 2 days after temperature shift from the permissive (25°C) to the restrictive temperature (29°C) (Fig. 5-2d), and even further decreased in brains 4 days after temperature shift (Fig. 5-2d). From the loss-of-function results, it is more convincing that JAK/STAT signaling directly regulates *CycE* expression levels in mushroom body neuroblasts.

Therefore, JAK/STAT signaling directly regulates *CycE* expression in the mushroom body neuroblasts and wing discs. As both *CycE* and *Diap1* are directly regulated by JAK/STAT and overexpression of two genes efficiently rescues loss of JAK/STAT phenotypes, we conclude that JAK/STAT signaling functions mainly through *Diap1* and *CycE* to prevent premature termination and promote division of mushroom body neuroblasts.

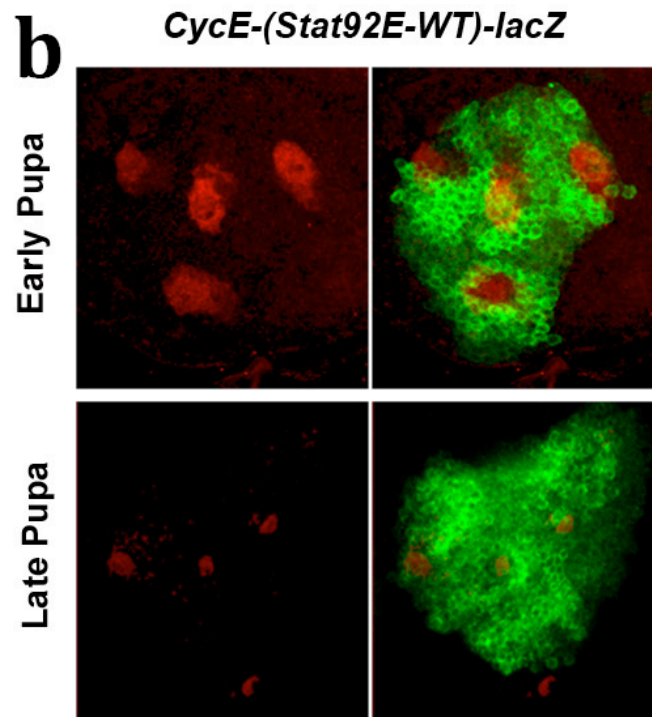
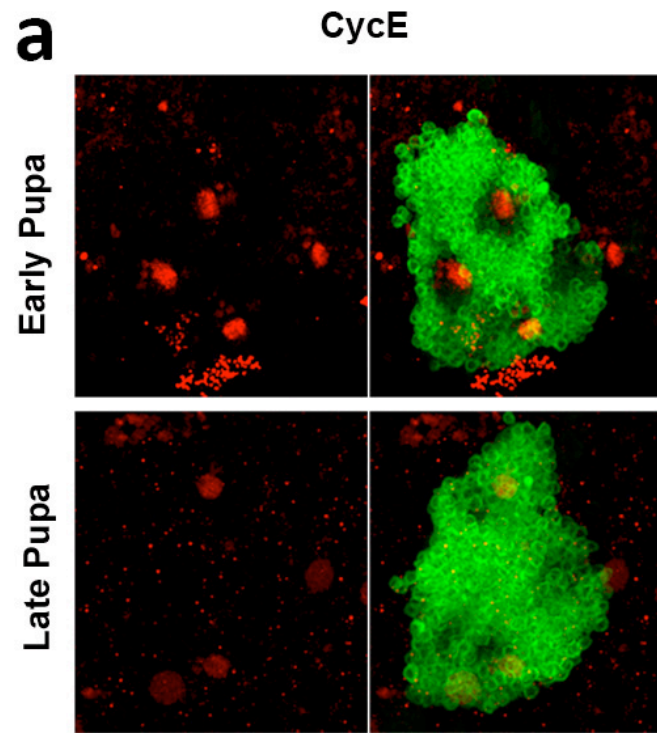
Figure 5-2. JAK/STAT signaling directly regulates *CycE* expression in the mushroom body neuroblasts

a-b, Confocal images showing cell body region of mushroom bodies at pupal stages,

CycE or *CycE(Stat92E-WT)-lacZ* expression (red, CycE or β -galactosidase antibody staining) in the wild type mushroom bodies labeled by *GAL4-OK107>UAS-mCD8::GFP* (green). The *CycE* expression levels in mushroom bodies were high at early pupal stages and decreased at late pupal stages. *CycE(Stat92E-WT)-lacZ* showed a similar expression pattern to that of endogenous *CycE*, but was expressed in a broader area surrounding mushroom body neuroblasts.

c, *CycE(Stat92E-MT)-lacZ* expression (red, β -galactosidase antibody staining) in the wild type mushroom bodies labeled by *GAL4-OK107>UAS-mCD8::GFP* (green). In contrast with *CycE(Stat92E-WT)-lacZ*, expression of *CycE(Stat92E-MT)-lacZ* was not high enough to be detected in the mushroom body area.

d, *CycE* expression (red, CycE antibody staining) in the *Stat92E^{ts}* mushroom bodies at early pupal stage. CycE levels in the mushroom body neuroblasts of first-day pupae decreased 2-4 days after the *Stat92E^{ts}* larvae were shifted from the permissive (25°C) to the restrictive temperature (29°C). Temperature and days after switch are shown. The observations are based on at least 20 mushroom bodies for each time point.



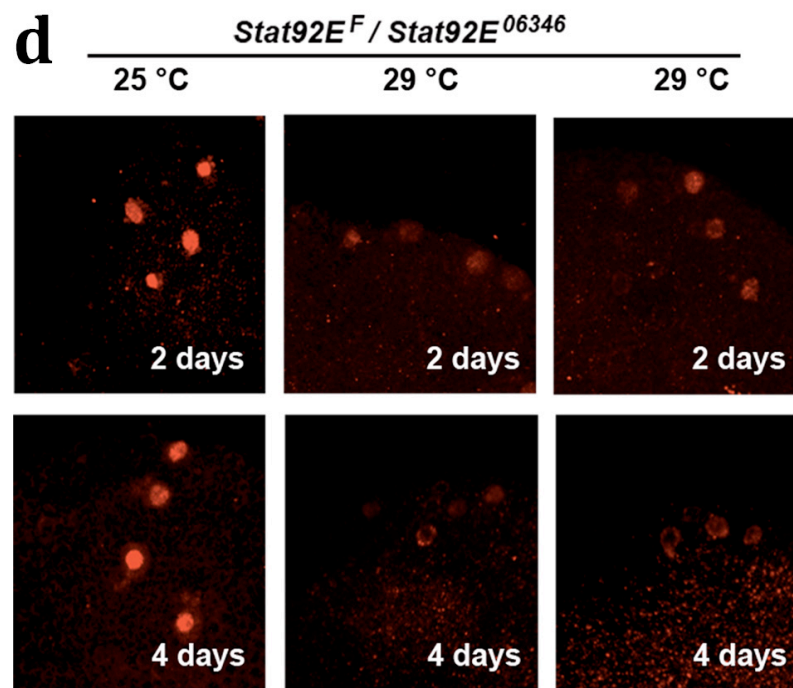
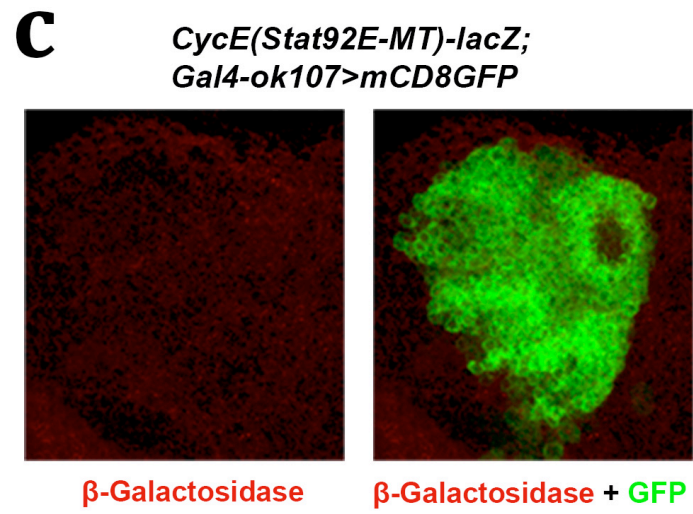


Figure 5-2

Clones of mushroom body neuroblasts either lacking *CycE* expression or with elevated *CycE* expression phenocopy clones with decreased or increased JAK/STAT signaling activities, respectively

Previous data has well established an important role of JAK/STAT signaling in mushroom body neurogenesis. It is also convincing that Stat92E controls *CycE* expression in mushroom body neuroblasts, and excess *CycE* substantially rescued the proliferation defects in *dome* mutant mushroom body neuroblasts. Based on these results, I reasoned that JAK/STAT functions through *CycE* to promote division of mushroom body neuroblasts. In order to test whether *CycE* is required for the normal proliferation of mushroom body neuroblasts, I examined the loss-of-function phenotypes of *CycE* in mushroom body. MARCM neuroblast clones homozygous for *CycE*^{AR95}, a *CycE* loss of function allele induced by EMS (Flybase), were induced in newly hatched larvae and examined in adult brains. Exactly the same γ -only phenotype as *dome* or *hop* mushroom body neuroblast clones was observed in most cases, occasionally some clones showed the less severe phenotype with a few α neurons (Fig. 5-3, a). This result confirms that *CycE* is required for mushroom body neurogenesis. I next analyzed whether excess *Diap1* or *Stat92E*^{ΔNΔC} could rescue the *CycE* mutant phenotype. Overexpression of *UAS-Diap1* or *UAS-Stat92E*^{ΔNΔC} was driven by *OK107-GAL4* in *CycE*^{AR95} mushroom body neuroblast clones. MARCM clones were induced in NHL, and examined in adult brains. Even with excess *Diap1* or *Stat92E*^{ΔNΔC}, most of the clones showed the γ -only phenotype, with a few exceptions showed less severe phenotype with α ' neurons (Fig. 5-3, b and c). This result indicates that excess *Diap1* couldn't rescue the proliferation defects of *CycE* mushroom body neuroblasts. Also, excess *Stat92E*^{ΔNΔC} couldn't compensate for the

proliferation defects caused by loss of *CycE*, indicating that *CycE* functions downstream of JAK/STAT signaling to promote mushroom body neuroblast proliferation.

I further tested the effect of *CycE* gain-of-function in mushroom body neurogenesis.

Overexpression of *UAS-CycE* was driven by *OK107-GAL4* in wild type mushroom body neuroblast clones. I counted the number of neurons generated by wild type, *CycE* mutant, and *CycE* gain-of-function mushroom body neuroblasts at one-week adults. Using the MARCM technique, I induced neuroblast clones in NHL. Brains are collected and processed for mCD8 (clone marker) antibody staining. Images were collected using confocal microscopy. Individual neuroblast lineage sizes were determined by counting the number of neurons in each clone. Loss of *CycE* results in significantly smaller mutant clones, with 24.5 ± 2.6 cells ($n=8$ clones). On the other side, expression of excess *CycE* in the wild-type clones leads to neuronal overgrowth, with 503 ± 21.6 cells ($n=16$ clones), compared with 354 ± 24.3 cells ($n=8$) in wild type clones (Fig. 5-3, d). Note excess *CycE* leads to neuronal overgrowth to the same extent as excess *Stat92E* does (Fig. 3-4c and d).

Based on the *CycE* loss-of-function and gain-of-function results, I conclude that *CycE* is the major, if not the only, downstream target of JAK/STAT pathway in controlling mushroom body neuroblast cell proliferation.

Figure 5-3. *CycE* mushroom body neuroblast clone phenocopies loss of JAK/STAT pathway activity, and excess *CycE* leads to neuronal overgrowth to the same extent as excess *Stat92E* does

a-c, Confocal images of MARCM neuroblast clones induced in the newly hatched larvae

and examined in the adult brains. Mushroom body neurons were labeled by *OK107-*

GAL4>UAS-mCD8::GFP. In *CycE*^{AR95} mutant clones, γ -only phenotype was observed in

most cases (a, left panel), occasionally some clones showed the less severe phenotype

with a few α neurons (a, right panel). This result suggests that *CycE* caused the similar

phenotype as loss of JAK/STAT in mushroom body neuroblasts. In *CycE*^{AR95} clones with

overexpression of *UAS-Diap1*, most of the clones showed the γ -only phenotype (b, left

panel), with a few exceptions showed less severe phenotype with α ' neurons (b, right

panel). In *CycE*^{AR95} clones with overexpression of *UAS-Stat92E*^{ANAC}, most of the clones

showed the γ -only phenotype (c, left panel), with a few exceptions showed less severe

phenotype with α ' neurons (c, right panel).

d, Bar graph showing the number of neurons/mushroom body neuroblast clone in one-

week adult brains. The number of neurons generated by wild type, *CycE* mutant, and

CycE gain-of-function mushroom body neuroblasts was counted and compared. The

MARCM neuroblast clones were induced in NHL. Brains are collected in one-week

adults and processed for mCD8 (clone marker) antibody staining. Images were collected

using confocal microscopy. Individual neuroblast lineage sizes were determined by

counting the number of neurons in each clone. Loss of *CycE* results in significantly

smaller mutant clones, with 24.5 ± 2.6 cells (n=8 clones). On the other side, expression of

excess *CycE* in the wild-type clones leads to neuronal overgrowth, with 503 ± 21.6 cells

(n=16 clones), compared with 354 ± 24.3 cells (n=8) in wild type clones.

Genotype: (a) *hs-FLP, UAS-mCD8::GFP; FRT40A, CycE^{AR95}/FRTG40A, tubP-GAL80; GAL4-OK107/+*; (b) *hs-FLP, UAS-mCD8::GFP; FRT40A, CycE^{AR95}/FRTG40A, tubP-GAL80; UAS-Diap1/+; GAL4-OK107/+*; (c) *hs-FLP, UAS-mCD8::GFP; FRT40A, CycE^{AR95}/FRTG40A, tubP-GAL80; UAS-Stat92E^{ΔNΔC}/+; GAL4-OK107/+*; (d, WT) *hs-FLP, UAS-mCD8::GFP/+; FRTG13/FRTG13, tubP-GAL80; GAL4-OK107/+*; (d, *UAS-CycE*) *hs-FLP, UAS-mCD8::GFP/+; FRTG13/FRTG13, tubP-GAL80; UAS-CycE/+; GAL4-OK107/+*.

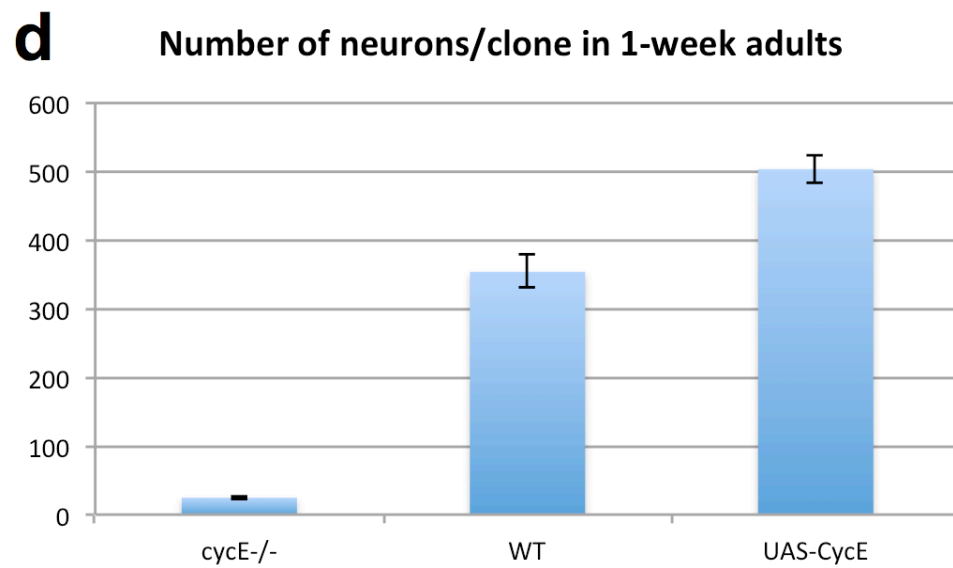
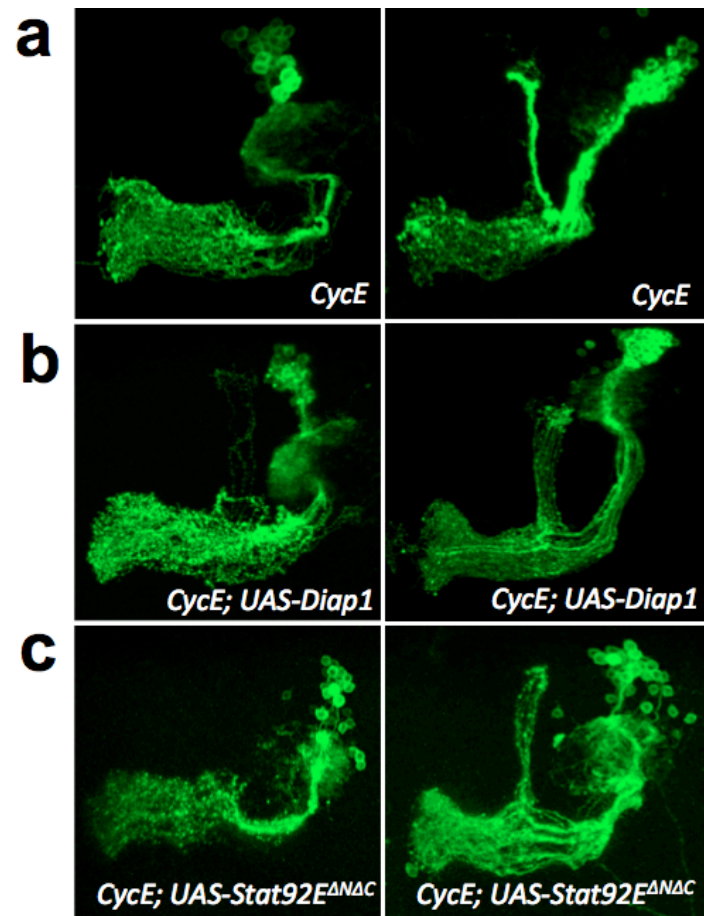


Figure 5-3

Stat92E and Yki regulate the transcription of *CycE* by interacting with two independent enhancers in the *CycE* cis-regulatory region

Previous data confirmed that *CycE* is a direct target of Stat92E, and the Stat92E DNA-binding site in the *CycE* locus is required for Stat92E-dependent *CycE* production. It's well known that *CycE* is also transcriptionally activated by Yki (Huang et al., 2005), but it is not known if this transcriptional regulation is direct or indirect. Next I want to identify the *cis*-regulatory element in the *CycE* gene response for Yki stimulation.

Expression of a *CycE-lacZ* reporter, which contains 16.4kb of the 5' regulatory sequence of *CycE* (Jones et al., 2000) including the consensus Stat92E-binding site described above, was reported increased in *yki*-overexpressing clones of eye imaginal discs (Huang et al., 2005). To determine where the Yki-responsive *cis*-regulatory element of *CycE* is localized, I divided this 16.4kb region into seven fragments and generated seven *lacZ* transgenic lines, named *CycE1-lacZ* to *CycE7-lacZ* (Fig. 5-1b). *lacZ* expression was examined with β -galactosidase antibody staining in the wing discs of either *en-GAL4/UAS-Stat92E^{ΔNΔC}* or *en-GAL4/UAS-yki* larvae. Consistent with *CycE(Stat92E-WT)-lacZ* (Fig. 5-1g), only *CycE2-lacZ*, which carries the consensus Stat92E-binding site, showed increased expression in the posterior domain of *en> Stat92E^{ΔNΔC}* wing discs (Fig. 5-4a). On the other hand, only *CycE3-lacZ* showed increased expression in the posterior domain of *en>yki* wing discs (Fig. 5-4b).

Together these results indicate that the *cis*-regulatory element on *CycE* response for Yki stimulation is within the fragment 3, and Stat92E and Yki regulate *CycE* transcription through different *cis*-regulatory elements. Therefore, JAK/STAT and Hippo signaling

pathways coordinately regulate cell proliferation and survival by targeting the same set of downstream genes, such as *CycE* and *Diap1*.

Figure 5-4. Stat92E and Yki regulate the transcription of *CycE* by interacting with two independent enhancers

a-b, Confocal images of wing discs showing *CycE2-lacZ* or *CycE3-lacZ* expression

(green, β -galactosidase antibody staining) in the *en-Gal4*, *UAS-Stat92E^{ΔNΔC}*, *UAS-RFP* (red) or *en-GAL4*, *UAS-yki*, *UAS-RFP* (red) genetic backgrounds. DAPI (blue) is used to label nuclei. *CycE1-lacZ* to *CycE7-lacZ* expression was examined with β -galactosidase antibody staining in the wing discs of either *en-Gal4/UAS-Stat92E^{ΔNΔC}* or *en-Gal4/UAS-yki* larvae. The observations are based on 3 independent transgenic lines for each construct.

a, Only *CycE2-lacZ*, which carries the consensus Stat92E-binding site, showed increased expression in the posterior wing disc domain in response to *en>Stat92E^{ΔNΔC}*.

b, Only *CycE3-lacZ* showed increased expression in the posterior wing disc domain in response to *en>yki*.

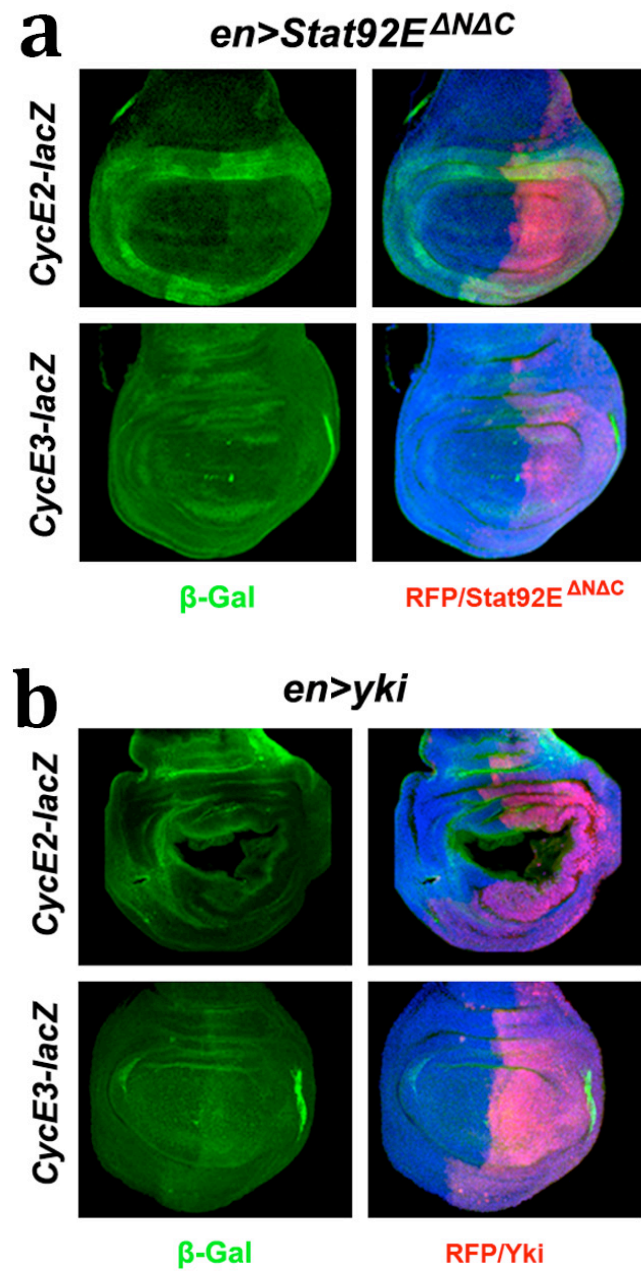


Figure 5-4

Chapter 6: Stat92E directly regulates the expression of the cell-cycle regulatory gene *E2f1*, another common target gene of Stat92E and Yki

Abstract

Two consensus STAT DNA-binding sequences TTCNNNGAA are found next to each other within the *E2f1* gene loci. To reveal whether these are functional Stat92E-binding sites *in vivo*, *lacZ* reporter transgenic studies were performed. I found that expression of *E2f1* in the wing disc and brain is dependent on Stat92E-binding sites. Therefore, besides *Diap1* and *CycE*, *E2f1* is another direct target of JAK/STAT signaling in *Drosophila*, which might also contribute to the proliferative activity of JAK/STAT. Together with previous report that Yki overexpression induced *E2f1* expression in wing imaginal discs, *E2f1* might be another common downstream target of Stat92E and Yki.

Conserved STAT DNA-binding sites in the *E2f1* locus are required for *E2f1* transcriptional activity in vivo

It is known that both Stat92E and Yki (Yki/Scalloped complex) directly regulate *Diap1* transcription by interacting with two independent enhancers in the *Diap1* cis-regulatory region, respectively (Betz et al., 2008; Wu et al., 2008). Here, my results showed that Stat92E and Yki also regulate the transcription of *CycE*, another major downstream target of Hippo pathway, by interacting with two independent enhancers in the *CycE* cis-regulatory region. In addition to *CycE*, another cell-cycle regulator *E2f1* could be the third candidate for the common targets of the two signaling pathways. This is because, on the one hand, it has been reported Yki overexpression induces *E2F1* expression in wing imaginal discs (Goulev et al., 2008). On the other hand, two consensus STAT DNA-binding sequences TTCNNNGAA are found next to each other within the *E2F1* gene loci (TTCACGGAATTCCTGGAA), which perfectly match one of 105 Stat92E-binding sites detected by ChIP-chip in the whole genome, 3R: 17,466,843-17,468,306. The same Stat92E ChIP-chip assay has successfully detected other JAK/STAT target genes, such as *Diap1* and *CycE* (modENCODE_616). These two predicted Stat92E-binding sequences are also highly conserved across 12 *Drosophila* genomes.

To test whether these are functional Stat92E-binding sites *in vivo*, I produced a *lacZ* reporter transgenic fly line, *E2f1(Stat92E-WT)-lacZ*, using an ~800bp genomic DNA fragment that contains these two STAT-binding sites (Fig. 6-1a). The 800bp DNA fragment containing the two predicted Stat92-binding sites was subcloned into *pH-Pelican*. The transgenic fly line was generated by germline injection. *E2f1(Stat92E-WT)-lacZ* expression was examined in various larval tissues. *lacZ* expression was detected

mainly in the optic lobe region of the larval brain (Fig. 6-1b), and in some of the hinge region of the wing imaginal disc (Fig. 6-1d).

To test whether the two Stat92E binding sites in this fragment are responsible for the *lacZ* expression in brain and wing disc, I generated another *lacZ* reporter transgenic fly line, *E2f1(Stat92E-MT)-lacZ*, that carries mutation in both Stat92E binding sites (TTCACGGAATTCCTGGAA to TTCACGGTTTTCCTGGTT). *E2f1(Stat92E-MT)-lacZ* reporter failed to be detected in either brain (Fig. 6-1c) or wing imaginal disc (Fig. 6-1e). These results indicate that these two STAT DNA-binding sites are required for the *E2f1* expression in the brain and wing imaginal disc.

To further test the specificity of the STAT DNA-binding sites, I examined the response of *E2f1(Stat92E-WT)-lacZ* to *Stat92E* overexpression in the posterior wing disc domain driven by an *en-GAL4* (Fig. 6-1f). *E2f1(Stat92E-WT)-lacZ* expression was increased in the posterior domain in response to *en>Stat92E*. Together these data indicate that signals from the *lacZ* reporter highly depended on Stat92E, and that the conserved STAT DNA-binding sites in the *E2f1* locus are required for *E2f1* transcriptional activity *in vivo*.

Therefore, based on my results here and other's finding that Yki regulates *E2f1* expression in wing disc, *E2f1* is another common downstream target gene of Stat92E and Yki activity, which may contribute to the proliferative activity of JAK/STAT pathway and the anti-proliferative activity of Hippo pathway.

Figure 6-1. Stat92E directly regulate *E2f1* transcription by binding to two STAT DNA-binding sequences

a, Diagram showing the constructs for the *lacZ* reporter transgenic lines of *E2f1(Stat92E-*

WT)-lacZ and *E2f1(Stat92E-MT)-lacZ*. A 800bp DNA segment that contains the two

predicted *E2f1* STAT DNA-binding sites was isolated by PCR and cloned into *pH-*

Pelican lacZ reporter vector to produce *E2f1(Stat92E-WT)-lacZ* construct. Both of the

two predicted *E2f1* STAT DNA-binding sites were mutated in *E2f1(Stat92E-MT)-lacZ*

construct (TTCACGGAAATTCCTGGAA to TTCACGGTTTCCTGGTT). The vector

contains a basal *hs* promoter and insulator elements to prevent position effects.

Transgenic lines were generated by germline injection. At least 3 independent transgenic fly lines were produced for each construct.

b-c, Expression of *E2f1(Stat92E-WT)-lacZ* and *E2f1(Stat92E-MT)-lacZ* in wondering

larval brain assessed by β -galactosidase antibody staining, showing that *E2f1(Stat92E-*

WT)-lacZ highly expressed in the optic lobe region, whereas no *E2f1(Stat92E-MT)-lacZ*

expression detected. The observations are consistent among 3 independent transgenic

lines for each construct.

d-e, Expression of *E2f1(Stat92E-WT)-lacZ* and *E2f1(Stat92E-MT)-lacZ* in wondering

larval wing imaginal disc assessed by β -galactosidase antibody staining, showing that

E2f1(Stat92E-WT)-lacZ highly expressed in some of the hinge region, whereas no

E2f1(Stat92E-MT)-lacZ expression detected. The observations are consistent among 3

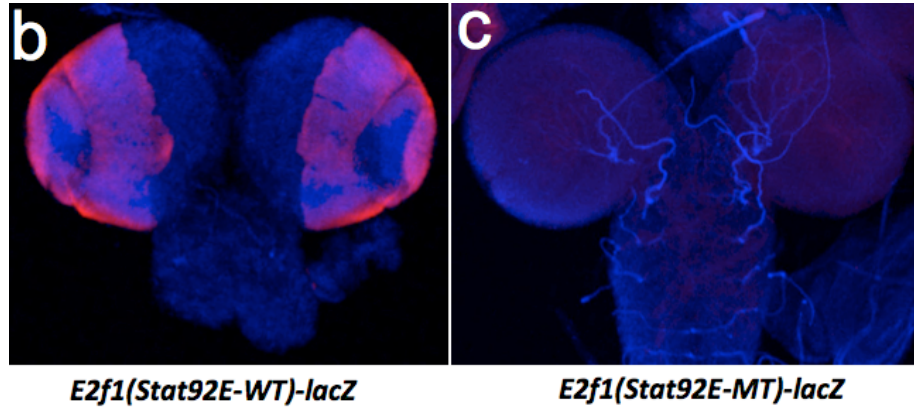
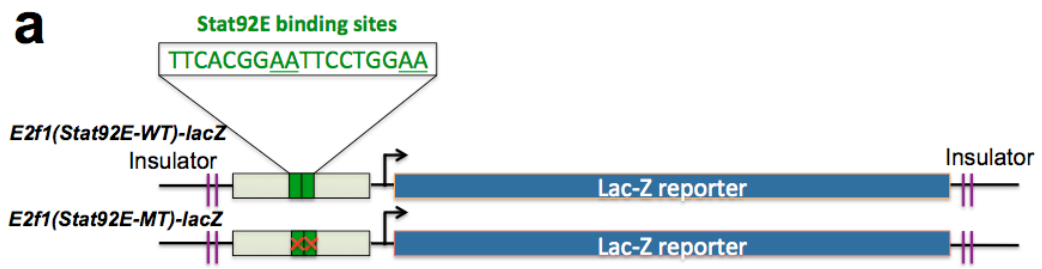
independent transgenic lines for each construct.

f, Confocal images of wing discs showing *E2f1(Stat92E-WT)-lacZ* expression (green, β -

galactosidase antibody staining) in the *en-Gal4*, *UAS-Stat92E^{ΔNAC}*, *UAS-RFP* (red)

genetic background, DAPI (blue) is used to label nuclei. It's shown that overexpressed

Stat92E in the posterior wing disc increases *E2f1(Stat92E-WT)-lacZ* reporter expression specifically in the posterior half. The observations are based on 3 independent transgenic lines.



f

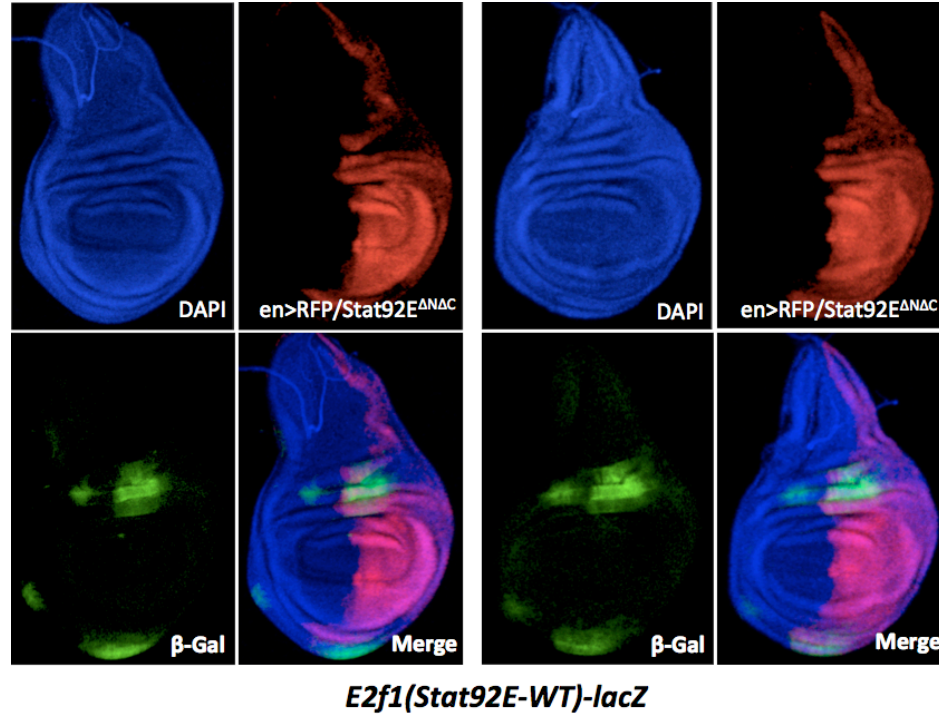


Figure 6-1

Chapter 7: Conclusions and Scientific impacts

The JAK/STAT and Hippo pathways are two major cell-proliferation-controlling signaling pathways in both vertebrates and invertebrates. Dysregulation of either JAK/STAT or Hippo signaling is linked to the development of various human diseases. Over-activation of JAK/STAT or down-regulation of Hippo signaling may lead to human cancers, including blood malignancies and solid tumors. Otherwise, loss of JAK/STAT or over-activation of Hippo signaling causes organ degeneration. In this project, I propose to investigate the relationship between the JAK/STAT and Hippo signaling pathways and their roles in controlling mushroom body neurogenesis.

From a MARCM-based genetic screen, I found that loss of *Drosophila* JAK/STAT pathway receptor *domeless* (*dome*) function led to significantly reduced number of neurons that are all γ type. And loss of JAK/STAT downstream kinase *hopscotch* (*hop*) caused the similar phenotype in mushroom body. The mutant phenotype could be perfectly rescued by ectopic expression of *UAS-dome* or a dominant-active form of *Stat92E* (*Stat92E^{ΔNΔC}*) in the *dome* mutant mushroom body neuroblast clones. Therefore, I conclude that the mutant phenotype is caused by loss of JAK/STAT signaling. More evidence suggests that the loss of JAK/STAT pathway does not affect the morphogenesis and survival of post-mitotic γ neurons, nor the subtype differentiation of mushroom body neurons. Furthermore, by performing a time-course study and neuroblast-specific antibody staining, I found that loss of *dome* caused precocious disappearance of mushroom body neuroblasts, and ectopic expression of *Stat92E^{ΔNΔC}* led to neuronal overgrowth. Based on these results, I concluded that JAK/STAT signaling is required for the neuroblast maintenance and cell proliferation in mushroom bodies.

Then to identify JAK/STAT signaling downstream targets that are crucial for mediating mushroom body neurogenesis, I tested a group of genes that are well characterized to be involved in the control of cell proliferation or cell death. Overexpression of Hippo pathway effector *yorkie* (*yki*) fully and overexpression of *CycE* and/or *Diap1*, the downstream target genes of Yki, partially rescues the phenotype of *dome* mutant mushroom body neuroblast clones. Moreover, MARCM neuroblast clones mutant for *yki* exhibit the similar cell proliferation defect as loss of JAK/STAT, although with a lower penetrance. I further found that ectopic expression of *UAS-Stat92E^{ΔNΔC}*, *UAS-CycE* or/and *UAS-Diap1* in the *yki* mutant neuroblast clones significantly rescued the mutant phenotype. Therefore, I conclude that loss of JAK/STAT signaling activity and loss of Hippo pathway downstream effector *yki* cause similar cell proliferation defects in mushroom body, which can be mutually rescued by higher activation of each other and by overexpression of *CycE* or *Diap1*.

A consensus Stat92E-binding site is located in the regulatory region of *CycE* locus. I found that expression of *CycE* in the wing disc and mushroom body is activated by Stat92E via the consensus Stat92E-binding site. Therefore, besides *Diap1*, *CycE* is another direct target of JAK/STAT signaling in *Drosophila*, which contributes to the proliferative activity of JAK/STAT. Furthermore, I found that Stat92E and Yki regulate the transcription of *CycE* by interacting with two independent *cis*-regulatory elements on *CycE*.

Two consensus STAT DNA-binding sequences TTCNNNGAA are found next to each other within the *E2f1* gene loci. From the *lacZ* reporter transgenic analysis, I found that

expression of *E2f1* in the wing disc and brain is dependent on Stat92E-binding sites. Therefore, besides *Diap1* and *CycE*, *E2f1* is another direct target of JAK/STAT signaling in *Drosophila*, which might also contribute to the proliferative activity of JAK/STAT. Together with previous report that *yki* overexpression induced *E2f1* expression in wing imaginal discs, *E2f1* might be another common downstream target of Stat92E and Yki to control proliferation.

Together with others' finding that *Diap1* is a direct target of STAT92E as well as of Yki (Yki/Scalloped complex), my dissertation research firstly propose that JAK/STAT and Hippo signaling pathways are integrated to control development in *Drosophila* by independently regulating common transcriptional targets, such as *CycE* and *E2f1* to control cell proliferation, and *Diap1* to control cell survival. The results collected in this study will not only provide new insight into the downstream targets of the JAK/STAT and Hippo pathways but also shed light onto the means by which distinct pathways converge to regulate the same biological process. This is especially important since both the JAK/STAT and Hippo signaling pathways are key regulators of normal growth and proper development from insects to mammals. Each of the two pathways coordinately regulates cell proliferation and apoptosis. Thus, the coordination between these two pathways is extremely critical to ensure proper growth.

My dissertation research represents three novel findings:

***CycE* as the direct target of the JAK/STAT signaling pathway and promotes cell-cycle progression**

Although its function in promoting cell-cycle progression is well documented, how

JAK/STAT pathway interacts with cell cycle regulators to promote cell cycle progression

is poorly understood. Here in this dissertation project, I identify a solid connection between JAK/STAT signaling and *CycE*, an essential G1 cyclin rate-limiting for progression into S phase, by evidencing that JAK/STAT controls cell proliferation through the direct regulation of *CycE* transcription.

A previous study finds that *Drosophila Cyclin B (CycB)* is elevated in a cell autonomous manner in clones with increased JAK-STAT pathway activity (Mukherjee et al., 2005). But, it is not clear whether *CycB* is a target of JAK-STAT signaling. Here, I report that Stat92E mediates *CycE* expression to accelerate cell proliferation. Mushroom body neuroblasts lacking of JAK/STAT pathway activity produce much fewer neurons than WT ones. Conversely, those with excess JAK/STAT signaling activity generate double number of neurons without generating supernumerary neuroblasts. Importantly, I find that excess *CycE* significantly rescues *dome* mutant phenotypes and Stat92E directly stimulate *CycE* expression in both wing discs and mushroom body neuroblasts through binding a consensus STAT-binding site in the *CycE cis*-regulatory region. Finally, loss-of-function phenotypes of *CycE* in the mushroom body neuroblast clones mimic those of lacking of JAK/STAT pathway activities. And excess *CycE* leads to neuronal overgrowth to the same extend as Stat92E gain-of-function in mushroom body neuroblasts. Together these results suggest that *CycE* is transcriptionally regulated by STAT92E and required for mediating cell proliferation.

This finding is different from, but not contradicts to, the previous report that Cyclin D-Cdk4, as well as Cyclin E-Cdk2, binds and regulates Stat92E protein stability (Chen et al., 2003). In that study, the authors discovered that excess JAK/STAT signaling activity

specifically synergizes with CycD-Cdk4, not CycE-Cdk2, to promote the formation of an enlarged eye with extra ommatidia. Now, this phenomenon can be perfectly interpreted. CycD-Cdk4 promotes cellular growth through mitochondrial biogenesis and is dispensable for cell proliferation (Meyer et al., 2000) and JAK-STAT signaling promotes cell proliferation through CycE-Cdk2, so that cooperation of the two signals results in a dramatically outgrown tumor-like eye. This interpretation is further evidenced by the fact that loss of JAK/STAT signaling phenotype is rescued by excess *CycE*, but not *CycD-Cdk4*. Thus, my study has great significance in current understanding of JAK/STAT regulation of proliferation in *Drosophila*. Also, it will be worthwhile to investigate the possibility of an evolutionarily conserved STAT-*CycE* connection.

Interestingly, *CycE* is expressed broadly in larva brains, and then restricted to four mushroom body neuroblasts, with the expression levels from high to low from early to late pupa stages. No *CycE* expression could be detected in adulthood. This *CycE* expression pattern fits perfectly with neuroblast division rate in mushroom bodies. Four mushroom body neuroblasts continue dividing throughout the larval and pupal stages, with the division rate from high to low until the neuroblast termination at the late pupal stage. Here I provide evidence that JAK/STAT signaling regulates neuroblast proliferation at least partially by controlling *CycE* expression in mushroom bodies. Based on these results, our working model for roles of JAK/STAT signaling in mushroom body development is that JAK/STAT pathway activity in the mushroom body neuroblasts is high during the early developmental stages, which promotes cell division and prevents cell death; it is reduced or eliminated during the late developmental stages, which induces neuroblast termination (Fig. 7-1).

Novel function of JAK/STAT signaling pathway in neurogenesis

The *Drosophila* central nervous system (CNS) develops from a bilateral neuroectoderm that contains a cluster of neuroepithelial (NE) cells. Selected NE cells differentiate into a few number of neuroblasts, which undergo asymmetric division producing a daughter neuroblast that self-renews, and a smaller ganglion mother cell (GMC) that gives rise to a variety of neuronal and glial cells. Previous studies in the optic lobe reveal that JAK/STAT pathway is required for NE cell maintenance and proliferation (Wang et al., 2011) and represses the transition of NE cells to neuroblasts (Yasugi et al., 2008; Ngo et al., 2010). Here, I report that JAK/STAT pathway also plays important roles in neuroblast to promote its cell-cycle progression and prevent its premature termination.

The new mechanism of the interaction between JAK/STAT and Hippo signaling pathways

The JAK/STAT and Hippo pathways are two major cell-proliferation-controlling signaling pathways in both vertebrates and invertebrates (Arbouzova & Zeidler, 2006; Pan, 2010). My dissertation research reveals the similar functions of the two signaling pathways in the control of mushroom body development: promoting cell division and preventing cell death. In *Drosophila*, Stat92E and Yki are the prime effectors of JAK/STAT and Hippo signaling pathways, respectively. They are directly involved in the transcriptional regulation of downstream target genes of the two pathways. It was reported that activation of Yki could induce expression of *upd* cytokines and then activate JAK/STAT signaling to regulate intestine stem cells (ISCs) proliferation (Ren et al., 2010). Here I find that gain-of-function of *Stat92E* and *yki* mutually rescue the mutant phenotypes of each other. This explains against the model that Yki activate JAK/STAT,

because overexpression of *yki* also fully rescues *dome*-null phenotypes, indicating that the rescuing effect of *yki* to *JAK/STAT* mutant phenotypes is JAK/STAT-independent.

There are two models left to interpret the relationship between JAK/STAT and Hippo signaling pathways in mediating mushroom body development. One is that the two pathways regulate different sets of cell proliferation-related genes, but functions of the two gene sets are similar to each other. Another is that the two pathways work in parallel to regulate the same set of target genes (Fig. 7-2). Multiple lines of evidence support the model that Stat92E and Yki act combinatorially to regulate common transcriptional targets. First, both Stat92E and Yki (Yki/Scalloped complex) directly regulate *Diap1* transcription by interacting with two independent enhancers in the *Diap1* cis-regulatory region, respectively (Betz et al., 2008; Wu et al., 2008). Second, I demonstrate here that Stat92E and Yki also regulate the transcription of *CycE*, another major downstream target of Hippo pathway, by interacting with two independent enhancers in the *CycE* cis-regulatory region. Third, in addition to *CycE*, another cell-cycle regulator *E2f1* is the third common target gene of the two signaling pathways. This is because, on the one hand, it has been reported *yki* overexpression induces *E2f1* expression in wing imaginal discs (Goulev et al., 2008). On the other hand, my transgenic analysis indicates that the two consensus STAT DNA-binding sequences within the *E2f1* gene loci are required for *E2f1* expression in brain and wing imaginal disc. Taken together, I propose that JAK/STAT and Hippo signaling pathways coordinately control cell proliferation and cell death by independently regulating the same set of downstream genes.

This notion is further supported by the fact that excess *yki* or the combination of *CycE* and *Diap1* has higher rescue efficiency than *CycE* alone. This finding not only provides novel insights regarding the molecules that are downstream of the JAK/STAT signaling pathway in cell proliferation, but also sheds light on the means by which distinct pathways converge to regulate the same biological process. Why do organisms need two signaling pathways to control the same biological process through regulating the same cluster of genes? With respect to JAK/STAT and Hippo pathways in the control of cell proliferation, our explanations range from function diversity to tissue specificity. Functionally, the activity of the JAK/STAT pathway promotes cell division and suppresses apoptosis, whereas the activity of Hippo pathway restrains cell division and induces apoptosis. Another reasonable explanation for the existence of these parallel pathways is that JAK/STAT and Hippo pathways differentially regulate downstream genes in different tissues, providing another level of regulation to cell proliferation and tissue homeostasis. As an example, my study here shows that JAK/STAT pathway is more important than Hippo pathway in controlling mushroom body development.

Future directions and implications

The development of multicellular organisms requires the coordination of cell proliferation and growth with developmental signals to produce properly patterned organisms of the appropriate size. The regulators that intrinsically control cell cycle progression have been well studied in eukaryotic system. Also, considerable progress has been made in defining the impact of extrinsic signals on cell proliferation and growth. The links between developmental signals and the cell cycle control are being elucidated.

The JAK/STAT and Hippo signaling pathways are two major cell proliferation-controlling pathways. Here in this dissertation research, I propose that JAK/STAT and Hippo pathways converge on common downstream targets, such as *Diap1* to control cell death, *CycE* and *E2f1* to control cell cycle progression. It is interesting to identify whether there are other common targets of JAK/STAT and Hippo pathways, besides *Diap1*, *CycE*, and *E2f1*. Moreover, it is worthwhile to study the *cis*-regulatory elements of these essential cell death and cell cycle genes such as *Diap1*, *CycE* and *E2f1*, which will facilitate the identification of other signaling pathways that might also be involved in the regulation of their expression. These will help to build up the network linking various developmental signals and intrinsic cell cycle regulators. Furthermore, it is important to investigate how different signaling pathways collaborate and divide work to maintain the proper growth and homeostasis of various tissues in multicellular organisms.

Figure 7-1. Working model for roles of JAK/STAT signaling in mushroom body development

The *CycE* expression pattern revealed in this study fits perfectly with neuroblast division rate in mushroom bodies. Four mushroom body neuroblasts continue dividing throughout the larval and pupal stages, with the division rate from high to low until the neuroblast termination at the late pupal stage. In this thesis I provide evidence that JAK/STAT signaling regulates neuroblast proliferation at least partially by controlling *CycE* expression in mushroom bodies. Based on these results, our working model for roles of JAK/STAT signaling in mushroom body development is that JAK/STAT pathway activity in the mushroom body neuroblasts is high during the early developmental stages, which promotes cell division and prevents cell death; it is reduced or eliminated during the late developmental stages, which induces neuroblast termination.

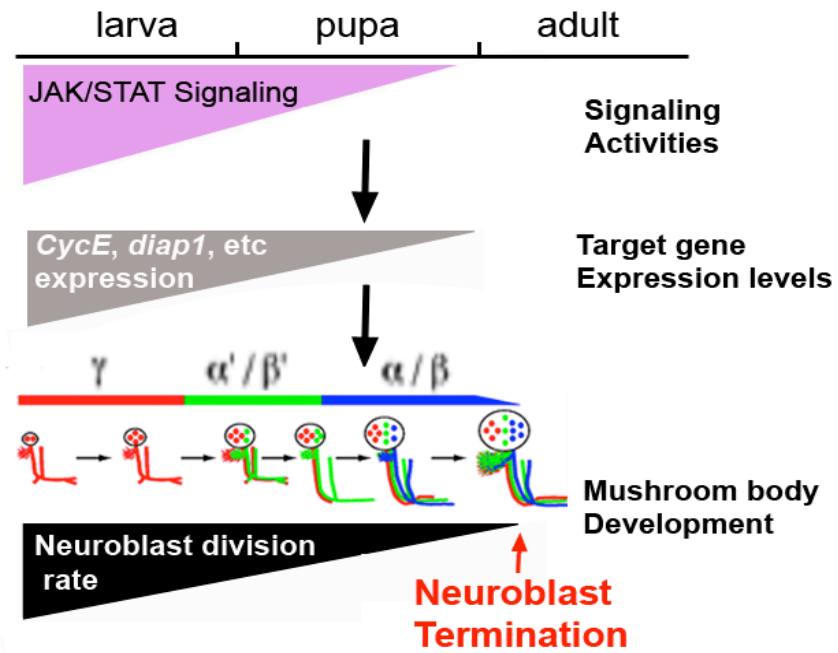


Figure 7-1

Figure 7-2. Working model for the relationship between JAK/STAT and Hippo pathways in controlling cell proliferation and cell survival

Stat92E and Yki are the prime downstream effectors of JAK/STAT and Hippo signaling

pathways, respectively. Upon the activation of JAK/STAT pathway, Stat92E dimers

translocate into nucleus and activate target gene expression. However, the activation of

Hippo signaling phosphorylates and restrains Yki in cytoplasm. Only unphosphorylated

Yki can go into nucleus and associate with different transcription factors to activate target

gene expression. “X” represents the transcription factor associates with Yki. In my thesis

study, I find that Stat92E and Yki/X independently regulate *CycE* transcription by

interacting with different enhancers. According to others’ studies about *Diap1*, it is

convincing that Stat92E and Yki/X regulate *Diap1* expression by binding to different *cis*-

regulatory elements. In addition, based on my and other’s results, *E2f1* is another

common downstream target of Stat92E and Yki/X. My working model suggests that

JAK/STAT and Hippo signaling pathways coordinately regulate common downstream

genes, such as *CycE*, *E2f1*, and *Diap1* to control cell proliferation and cell death.

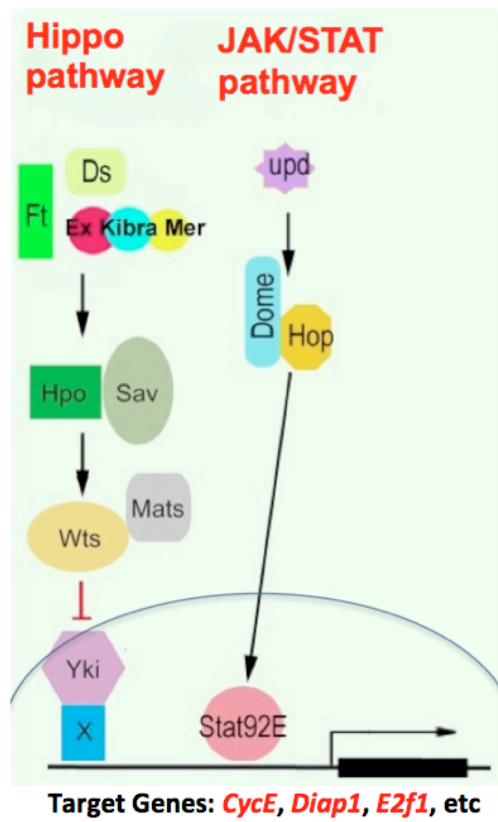


Figure 7-2

Chapter 8: Materials and methods

Materials

Fly strains. *UAS-dome* was a gift from Steven Hou. *UAS-Stat92E^{ΔNAC}* was a gift from Erika Bach. *CycE^{AR95}*, *UAS-CycE*, *UAS-Diap1*, and *UAS-yorkie* were gifts from Jianhua Huang. *yki^{B5}* was a gift from Duoqia Pan. *CycE(Stat92E-WT)-lacZ*, *CycE(Stat92E-MT)-lacZ*, *CycE(1-7)-lacZ* and *E2f1(Stat92E-WT)-lacZ*, *E2f1(Stat92E-MT)-lacZ* transgenic reporter lines were produced by germline injection. Other fly strains were collected from the Bloomington *Drosophila* Stock Center. All flies were maintained on standard cornmeal medium at 25°C.

Antibodies. The following primary antibodies were used: rat anti-Dpn antibody was a gift from Chris Doe (used at 1: 10); rabbit anti-β-Galactosidase antibody (catalog number A-11132) (used at 1: 50) was purchased from Life technologies; and rabbit anti-CycE antibody (catalog number sc-481) (used at 1:50) was purchased from Santa Cruz Biotechnology. Rat anti-mCD8 (catalog number RM2200) was purchased from Caltag Laboratories. FITC and Cy3 conjugated secondary antibodies were purchased from Jackson ImmunoResearch.

Reagents. Geneticin (catalog number 11811-031) was purchased from GIBCO. 16% paraformaldehyde was purchased from Electron Microscopy Laboratories (catalog number 15710), and mounting medium with DAPI was purchased from Vector Laboratories (catalog number H-1200).

Commercial Kits. The following commercially available kits were used: QIAquick PCR Purification Kit (250) (catalog number 28106), QIAquick Gel Extraction Kit (250)

(catalog number 28706), QIAprep Spin Miniprep Kit (250) (catalog number 27106), and QIAfilter Plasmid Midi Kit (25) (catalog number 12243) were purchased from QIAGEN.

Methods

Mushroom body MARCM screening. Cross 20-30 MARCM-ready virgin females (*GAL4-201Y, hs-FLP, UAS-mCD8::GFP; FRT82B, tubP-GAL80*) to 5-10 males carrying *FRT82B* and a P-element induced recessive lethal mutation on Chromosome 3R (*FRT82B, */TM3, Sb¹*); or cross 20-30 virgin females carrying *FRT19A* and a P-element induced recessive lethal mutation on Chromosome X (*FRT19A, */FM7c*) to 5-10 MARCM-ready males (*FRT19A, hs-FLP, tubP-GAL80/Y; UAS-mCD8::GFP; GAL4-OK107*). MARCM was performed as described (Lee and Luo, 1999). Neuroblast clones of 250 independent lines were checked in adult mushroom bodies, phenotypes were recorded and the lines showing abnormalities in mushroom body morphogenesis were kept for further analysis.

MARCM in mushroom body neuroblasts. MARCM was performed as described (Lee and Luo, 1999). To induce loss of JAK/STAT MARCM clones of mushroom body neuroblasts, *FRT19A, dome^{G0405}* virgin flies with or without specific *UAS*-transgene on the third chromosome, *FRT19A, dome⁴⁶⁸*, or *FRT19A, hop²* virgin flies were crossed to *FRT19A, hs-FLP, tubP-GAL80/Y; UAS-mCD8::GFP; GAL4-OK107* male flies. To induce *yki* loss of function MARCM clones, *FRTG13* was recombined to *yki^{B5}* line using conventional genetic techniques. 300mg/L of geneticin in fly food was used to select for larvae with *FRTG13*. *FRTG13, yki^{B5}* virgin or male flies with or without specific *UAS*-transgene on the third chromosome were crossed to *hs-FLP, UAS-mCD8::GFP; FRTG13, tubP-GAL80; GAL4-OK107* male or virgin files. To induce *CycE* loss of function neuroblast clones, *FRTG40A, CycE^{AR95}* virgin or male flies with or without specific *UAS*-transgene on the third chromosome were crossed to *hs-FLP, UAS-mCD8::GFP; FRT40A,*

tubP-GAL80; *GAL4-OK107* male or virgin flies. In all these crosses, F1 newly hatched larvae were heat-shocked at 38°C for 1h. *GAL4-OK107* was used as the source of *GAL4*, and *UAS-mCD8-GFP*, a cell membrane localized GFP was used to label the clones. After heat shocking at newly hatched larvae, brains from adult flies with the right genotype were collected for dissection. The images of MARCM clones were taken using confocal microscopy. For each MARCM analysis, at least 15 clones were observed, and the phenotype is consistent unless otherwise stated.

Generation of mutant lines with *UAS*-transgenes for the rescue tests. *FRT19A*, *dome*^{G0405}/*FM7c* virgin flies were crossed to *FM7c/Y*; *TM3,Sb*¹/*TM6b,Tb*¹ males. *FRT19A*, *dome*^{G0405}/*FM7c*; *TM3,Sb*¹/+ virgins were collected from F1 generation, and were then crossed to *FM7c/Y*; *TM3,Sb*¹/*TM6b,Tb*¹ males. *FRT19A*, *dome*^{G0405}/*FM7c*; *TM3,Sb*¹/*TM6b,Tb*¹ virgins and *FM7c/Y*; *TM3,Sb*¹/*TM6b,Tb*¹ male flies were collected from F2 generation to make a stable stock line. As the same way, *FRTG13*, *yki*^{B5}/*Cyo*; *TM3,Sb*¹/*TM6b,Tb*¹ and *FRT40A*, *CycE*^{AR95}/*Cyo*; *TM3,Sb*¹/*TM6b,Tb*¹ lines were generated. To produce *dome* mutant lines with different *UAS*-transgenes, *FRT19A*, *dome*^{G0405}/*FM7c*; *TM3,Sb*¹/*TM6b,Tb*¹ virgins were crossed to *FM7c/Y*; *UAS*-*/*TM3,Sb*¹ males. *FRT19A*, *dome*^{G0405}/*FM7c*; *UAS*-*/*TM3,Sb*¹ virgins and *FM7c/Y*; *UAS*-*/*TM3,Sb*¹ males were collected from F1 generation to make a stable stock line. * indicates the transgene to be introduced and then to be overexpressed by *GAL4/UAS* system. As the same way, *FRTG13*, *yki*^{B5}/*Cyo*; *UAS*-*/*TM3,Sb*¹ and *FRT40A*, *CycE*^{AR95}/*Cyo*; *UAS*-*/*TM3,Sb*¹ lines were generated.

Reverse genetic screen to identify JAK/STAT downstream targets. *dome*^{G0405}

neuroblast MARCM clones with overexpression of different *UAS*-transgenes were induced at the newly hatched larvae using *GAL4-OK107*. Adult brains with the right genotype were collected for dissection. The images of MARCM clones were taken using confocal microscopy.

Time-course analysis. Wild type, *dome*^{-/-}, or wild type with the overexpression of *Stat92E*^{ΔNΔC} mushroom body neuroblast clones were induced at newly hatched larvae. Brains were collected at 48h-, 72h-, 96h-ALH (after larvae hatching), 24h-, 60h-APF (after pupa formation), and 1d-, 1w-adults. Images of cell bodies were collected using confocal microscopy in 1μm section. Individual neuroblast lineage sizes were determined by counting the number of cells in each clone. 10-27 clones were counted for each time point. Statistical significance was calculated using One way ANOVA.

Generation of *lacZ* reporter transgenes. To make *CycE(Stat92E-WT)-lacZ* construct, primers designed against the *CycE* locus were used to PCR-amplify ~1kb fragment flanking the predicted STAT-binding site from genomic DNA. The fragment was subcloned into pBluescript and then subcloned into the P-element transformation vector, pH-Pelican. To make *CycE(Stat92E-MT)-lacZ* construct, site-directed mutagenesis using Pfu DNA polymerase was performed with complementary oligonucleotides and *DpnI* digestion of the parental template. Products were transformed in DNA adenine methylation-free bacteria, tested for the successful generation of the TTCCAAGAA to TTCCAAGTT mutation by sequencing before subcloning into the pH-Pelican. Primers for amplifying target sequence from genomic DNA are as follows: Forward primer:

5'GCATCTAGAGAATCCACACATATCAACTGGC3', Reverse primer:
5'ATAGGATCCACCACTCTTGCAATTAGTTGG3'. Primers for site-specific
mutagenesis are as follows:
5'GCTACTTCAAGGCCATCGAACTTGGAACGAC3', and
5'GCGTTCCAGTTCCAAGTTTCGATGGCCTTGAAGTAGC3'.

In the similar way, *E2f1(Stat92E-WT)-lacZ* and *E2f1(Stat92E-MT)-lacZ* constructs were
generated. Primers for amplifying target sequence from genomic DNA are as follows:

Forward primer: 5'GCTCTAGAGCAAGAAAAGCGAACCAGGT3', Reverse primer:
5'GGGGTACCTTCGGGCCAAGTACCAAGTA3'. Primers for site-specific
mutagenesis are as follows:

5'GATCGGCAAATAACCAGGAAAACCGTGAATGGGAAAAAC3', and
5'GTTTTTCCCATTACGGTTTTCTGGTTATTTGCCGATC3'.

To make *CycE(1-7)-lacZ* constructs, the 16.4kb *CycE cis*-regulatory element was
dissected into 7 fragments. 7 sets of primers were designed to PCR-amplify each ~2.5kb
fragment from genomic DNA. Each fragment was subcloned into pBluescript and then
subcloned into the P-element transformation vector, pH-Pelican. All the sequences were
verified by DNA sequencing before subcloning into the pH-Pelican. Primers used were as
follows: Primer F1: 5'CATCTAGAGCGATCATTGTGTTACTTTGGA3', Primer R1:
5'CGGAATTCATAAGCTGCATCTCAAGCCTTC3'. Primer F2:
5'GCGGTACCTTTCTAATGCGTAACGGGAGTT3', Primer R2:
5'GCGGATCCTACTGCAAACGAGAACAGGAAA3'. Primer F3:

5'GCTCTAGATTTCTCTGTTCTCGTTTGCAGTA3', Primer R3:
 5'CGGAATTCAGTCACGGAATGGTCATCTTTT3'. Primer F4:
 5'GCTCTAGAATCAATCGAGACTCGTGGAAAT3', Primer R4:
 5'GCGAATTCCAACCTGCACTTTAAGCAATTCG3'. Primer F5:
 5'TCCCCGCGGTTTTTCTCTCGTTCTCCTGAGC3', Primer R5:
 5'CGGGATCCTTACTCAACAAAGTTCGCCTGA3'. Primer F6:
 5'GCTCTAGATCAGGCGAACTTTGTTGAGTAA3', Primer R6:
 5'CGGGATCCGTCAAGCGTTATGGAATCACAA3'. Primer F7:
 5'GCTCTAGATTGTGATTCCATAACGCTTGAC3', Primer R7:
 5'GTCCGCGGGGCATGGAGGTAAGACAATAGC3'.

***Stat92E* loss of function analysis by using *Stat92E* temperature sensitive allele.**

Stat92E^F flies were crossed to *Stat92E⁰⁶³⁴⁶/TM3*, *GFP* flies, temperature sensitive *Stat92E^F/Stat92E⁰⁶³⁴⁶* (*Stat92E^{ts}*) early larvae were collected from F1 progeny by the absence of GFP under a fluorescence microscope. The vial#1 of collected larvae was always kept at permissive temperature 25°C. The vial#2 of collected larvae was moved to restrictive temperature 29°C at early larvae stage, and kept at 29°C for 4 days until the early pupa stage. The vial#3 of collected larvae was moved to restrictive temperature 29°C at mid larvae stage, and kept at 29°C for 2 days until the early pupa stage. Brains from 3 vials were collected for dissection at early pupa stages and being processed for CycE antibody staining. Exactly the same antibody staining treatments were conducted to ensure comparability. The *CycE* expression levels were examined based on the confocal images of at least 20 mushroom bodies for each time point. Confocal imaging was performed using exactly the same parameters.

Immunohistochemistry of brains and imaginal discs. Antibody staining was performed essentially as the following. Brains or imaginal discs at proper stages were dissected, and fixed with 4% formaldehyde in PBS for 30 minutes at room temperature. The samples were then washed in PBT (PBS containing 1% Triton X-100) for 3 times, with 30 minutes each time, followed by a blocking step with 5% normal goat serum in PBT at room temperature for 30 minutes. The samples were then incubated with the primary antibody at 4°C overnight. After washing with PBT for 3 times with 20 minutes each at room temperature, the samples were incubated with the secondary antibody at room temperature for 2-4 hours or at 4°C overnight. Samples were then washed 3 times with PBT at room temperature, with 30 minutes each, before mounting.

All images of immunofluorescent staining were collected using a Zeiss LSM710 confocal microscope and processed with Adobe Photoshop.

References

- Agaisse H, Petersen UM, Boutros M, Mathey-Prevot B, Perrimon N. (2003). Signaling role of hemocytes in *Drosophila* JAK/STAT-dependent response to septic injury. *Dev Cell*, 5(3), 441-450.
- Alarcon C, Zaromytidou AI, Xi Q, Gao S, Yu J, Fujisawa S, Barlas A, Miller AN, Manova-Todorova K, Macias MJ, Sapkota G, Pan D, Massague J. (2009). Nuclear CDKs drive Smad transcriptional activation and turnover in BMP and TGF-beta pathways. *Cell*, 139(4), 757-769.
- Amoyel M, Bach EA. (2012). Functions of the *Drosophila* JAK-STAT pathway: Lessons from stem cells. *Jakstat*, 1(3), 176-183.
- Arbouzova NI, Bach EA, Zeidler MP. (2006). Ken & barbie selectively regulates the expression of a subset of Jak/STAT pathway target genes. *Curr Biol*, 16(1), 80-88.
- Arbouzova NI, Zeidler MP. (2006). JAK/STAT signalling in *Drosophila*: insights into conserved regulatory and cellular functions. *Development*, 133(14), 2605-2616.
- Arellano M, Moreno S. (1997). Regulation of CDK/cyclin complexes during the cell cycle. *Int J Biochem Cell Biol*, 29(4), 559-573.
- Armstrong JD, de Belle JS, Wang Z, Kaiser K. (1998). Metamorphosis of the mushroom bodies; large-scale rearrangements of the neural substrates for associative learning and memory in *Drosophila*. *Learn Mem*, 5(1-2), 102-114.
- Bach EA, Ekas LA, Ayala-Camargo A, Flaherty MS, Lee H, Perrimon N, Baeg GH. (2007). GFP reporters detect the activation of the *Drosophila* JAK/STAT pathway in vivo. *Gene Expr Patterns*, 7(3), 323-331.
- Bach EA, Vincent S, Zeidler MP, Perrimon N. (2003). A sensitized genetic screen to identify novel regulators and components of the *Drosophila* janus kinase/signal transducer and activator of transcription pathway. *Genetics*, 165(3), 1149-1166.
- Baeg GH, Zhou R, Perrimon N. (2005). Genome-wide RNAi analysis of JAK/STAT signaling components in *Drosophila*. *Genes Dev*, 19(16), 1861-1870.
- Baksa K, Parke T, Dobens LL, Dearolf CR. (2002). The *Drosophila* STAT protein, stat92E, regulates follicle cell differentiation during oogenesis. *Dev Biol*, 243(1), 166-175.

- Barolo S, Carver LA, Posakony JW. (2000). GFP and beta-galactosidase transformation vectors for promoter/enhancer analysis in *Drosophila*. *Biotechniques*, 29(4), 726, 728, 730, 732.
- Bennett FC, Harvey KF. (2006). Fat cadherin modulates organ size in *Drosophila* via the Salvador/Warts/Hippo signaling pathway. *Curr Biol*, 16(21), 2101-2110.
- Betz A, Lampen N, Martinek S, Young MW, Darnell JE, Jr. (2001). A *Drosophila* PIAS homologue negatively regulates stat92E. *Proc Natl Acad Sci U S A*, 98(17), 9563-9568.
- Betz A, Ryoo HD, Steller H, Darnell JE, Jr. (2008). STAT92E is a positive regulator of *Drosophila* inhibitor of apoptosis 1 (DIAP/1) and protects against radiation-induced apoptosis. *Proc Natl Acad Sci U S A*, 105(37), 13805-13810.
- Binari R, Perrimon N. (1994). Stripe-specific regulation of pair-rule genes by hopscotch, a putative Jak family tyrosine kinase in *Drosophila*. *Genes Dev*, 8(3), 300-312.
- Boone JQ, Doe CQ. (2008). Identification of *Drosophila* type II neuroblast lineages containing transit amplifying ganglion mother cells. *Dev Neurobiol*, 68(9), 1185-1195.
- Bowman T, Garcia R, Turkson J, Jove R. (2000). STATs in oncogenesis. *Oncogene*, 19(21), 2474-2488.
- Brembs B. (2009). Mushroom bodies regulate habit formation in *Drosophila*. *Curr Biol*, 19(16), 1351-1355.
- Brown S, Hu N, Hombria JC. (2001). Identification of the first invertebrate interleukin JAK/STAT receptor, the *Drosophila* gene domeless. *Curr Biol*, 11(21), 1700-1705.
- Cai J, Zhang N, Zheng Y, de Wilde RF, Maitra A, Pan D. (2010). The Hippo signaling pathway restricts the oncogenic potential of an intestinal regeneration program. *Genes Dev*, 24(21), 2383-2388.
- Calo V, Migliavacca M, Bazan V, Macaluso M, Buscemi M, Gebbia N, Russo A. (2003). STAT proteins: from normal control of cellular events to tumorigenesis. *J Cell Physiol*, 197(2), 157-168.
- Camargo FD, Gokhale S, Johnnidis JB, Fu D, Bell GW, Jaenisch R, Brummelkamp TR. (2007). YAP1 increases organ size and expands undifferentiated progenitor cells. *Curr Biol*, 17(23), 2054-2060.

- Chan EH, Nousiainen M, Chalamalasetty RB, Schafer A, Nigg EA, Sillje HH. (2005). The Ste20-like kinase Mst2 activates the human large tumor suppressor kinase Lats1. *Oncogene*, 24(12), 2076-2086.
- Chao JL, Tsai YC, Chiu SJ, Sun YH. (2004). Localized Notch signal acts through eyg and upd to promote global growth in Drosophila eye. *Development*, 131(16), 3839-3847.
- Chen HW, Chen X, Oh SW, Marinissen MJ, Gutkind JS, Hou SX. (2002). mom identifies a receptor for the Drosophila JAK/STAT signal transduction pathway and encodes a protein distantly related to the mammalian cytokine receptor family. *Genes Dev*, 16(3), 388-398.
- Chen P, Nordstrom W, Gish B, Abrams JM. (1996). grim, a novel cell death gene in Drosophila. *Genes Dev*, 10(14), 1773-1782.
- Chen X, Oh SW, Zheng Z, Chen HW, Shin HH, Hou SX. (2003). Cyclin D-Cdk4 and cyclin E-Cdk2 regulate the Jak/STAT signal transduction pathway in Drosophila. *Dev Cell*, 4(2), 179-190.
- Chiba T, Yamada M, Aiso S. (2009). Targeting the JAK2/STAT3 axis in Alzheimer's disease. *Expert Opin Ther Targets*, 13(10), 1155-1167.
- Cho E, Feng Y, Rauskolb C, Maitra S, Fehon R, Irvine KD. (2006). Delineation of a Fat tumor suppressor pathway. *Nat Genet*, 38(10), 1142-1150.
- Connolly JB, Roberts IJ, Armstrong JD, Kaiser K, Forte M, Tully T, O'Kane CJ. (1996). Associative learning disrupted by impaired Gs signaling in Drosophila mushroom bodies. *Science*, 274(5295), 2104-2107.
- Crittenden JR, Skoulakis EM, Han KA, Kalderon D, Davis RL. (1998). Tripartite mushroom body architecture revealed by antigenic markers. *Learn Mem*, 5(1-2), 38-51.
- Darnell JE, Jr., Kerr IM, Stark GR. (1994). Jak-STAT pathways and transcriptional activation in response to IFNs and other extracellular signaling proteins. *Science*, 264(5164), 1415-1421.
- Datar SA, Jacobs HW, de la Cruz AF, Lehner CF, Edgar BA. (2000). The Drosophila cyclin D-Cdk4 complex promotes cellular growth. *Embo j*, 19(17), 4543-4554.
- de Belle JS, Heisenberg M. (1994). Associative odor learning in Drosophila abolished by chemical ablation of mushroom bodies. *Science*, 263(5147), 692-695.

- Decker T. (1999). Introduction: STATs as essential intracellular mediators of cytokine responses. *Cell Mol Life Sci*, 55(12), 1505-1508.
- Decotto E, Spradling AC. (2005). The Drosophila ovarian and testis stem cell niches: similar somatic stem cells and signals. *Dev Cell*, 9(4), 501-510.
- Deveraux QL, Reed JC. (1999). IAP family proteins--suppressors of apoptosis. *Genes Dev*, 13(3), 239-252.
- Dong J, Feldmann G, Huang J, Wu S, Zhang N, Comerford SA, Gayyed MF, Anders RA, Maitra A, Pan D. (2007). Elucidation of a universal size-control mechanism in Drosophila and mammals. *Cell*, 130(6), 1120-1133.
- Dubrez L, Berthelet J, Glorian V. (2013). IAP proteins as targets for drug development in oncology. *Onco Targets Ther*, 9, 1285-1304.
- Duckett CS, Nava VE, Gedrich RW, Clem RJ, Van Dongen JL, Gilfillan MC, Shiels H, Hardwick JM, Thompson CB. (1996). A conserved family of cellular genes related to the baculovirus iap gene and encoding apoptosis inhibitors. *Embo j*, 15(11), 2685-2694.
- Dumon S, Santos SC, Debierre-Grockiego F, Gouilleux-Gruart V, Cocault L, Boucheron C, Mollat P, Gisselbrecht S, Gouilleux F. (1999). IL-3 dependent regulation of Bcl-xL gene expression by STAT5 in a bone marrow derived cell line. *Oncogene*, 18(29), 4191-4199.
- Ehret GB, Reichenbach P, Schindler U, Horvath CM, Fritz S, Nabholz M, Bucher P. (2001). DNA binding specificity of different STAT proteins. Comparison of in vitro specificity with natural target sites. *J Biol Chem*, 276(9), 6675-6688.
- Ekas LA, Cardozo TJ, Flaherty MS, McMillan EA, Gonsalves FC, Bach EA. (2010). Characterization of a dominant-active STAT that promotes tumorigenesis in Drosophila. *Dev Biol*, 344(2), 621-636.
- el-Deiry WS, Tokino T, Velculescu VE, Levy DB, Parsons R, Trent JM, Lin D, Mercer WE, Kinzler KW, Vogelstein B. (1993). WAF1, a potential mediator of p53 tumor suppression. *Cell*, 75(4), 817-825.
- Elmore S. (2007). Apoptosis: a review of programmed cell death. *Toxicol Pathol*, 35(4), 495-516.
- Feng S, Huang J, Wang J. (2011). Loss of the Polycomb group gene polyhomeotic induces non-autonomous cell overproliferation. *EMBO Rep*, 12(2), 157-163.

- Feng S, Thomas S, Wang J. (2012). Diverse tumor pathology due to distinctive patterns of JAK/STAT pathway activation caused by different *Drosophila* polyhomeotic alleles. *Genetics*, 190(1), 279-282.
- Ferrigno O, Lallemand F, Verrecchia F, L'Hoste S, Camonis J, Atfi A, Mauviel A. (2002). Yes-associated protein (YAP65) interacts with Smad7 and potentiates its inhibitory activity against TGF-beta/Smad signaling. *Oncogene*, 21(32), 4879-4884.
- Flaherty MS, Salis P, Evans CJ, Ekas LA, Marouf A, Zavadil J, Banerjee U, Bach EA. (2010). chinmo is a functional effector of the JAK/STAT pathway that regulates eye development, tumor formation, and stem cell self-renewal in *Drosophila*. *Dev Cell*, 18(4), 556-568.
- Frolov MV, Huen DS, Stevaux O, Dimova D, Balczarek-Strang K, Elsdon M, Dyson NJ. (2001). Functional antagonism between E2F family members. *Genes Dev*, 15(16), 2146-2160.
- Fu XY, Schindler C, Improta T, Aebersold R, Darnell JE, Jr. (1992). The proteins of ISGF-3, the interferon alpha-induced transcriptional activator, define a gene family involved in signal transduction. *Proc Natl Acad Sci U S A*, 89(16), 7840-7843.
- Geng Y, Eaton EN, Picon M, Roberts JM, Lundberg AS, Gifford A, Sardet C, Weinberg RA. (1996). Regulation of cyclin E transcription by E2Fs and retinoblastoma protein. *Oncogene*, 12(6), 1173-1180.
- Gharavi NM, Alva JA, Mouillesseaux KP, Lai C, Yeh M, Yeung W, Johnson J, Szeto WL, Hong L, Fishbein M, Wei L, Pfeffer LM, Berliner JA. (2007). Role of the Jak/STAT pathway in the regulation of interleukin-8 transcription by oxidized phospholipids in vitro and in atherosclerosis in vivo. *J Biol Chem*, 282(43), 31460-31468.
- Ghiglione C, Devergne O, Georgenthum E, Carballes F, Medioni C, Cerezo D, Noselli S. (2002). The *Drosophila* cytokine receptor Domeless controls border cell migration and epithelial polarization during oogenesis. *Development*, 129(23), 5437-5447.
- Gilbert MM, Weaver BK, Gergen JP, Reich NC. (2005). A novel functional activator of the *Drosophila* JAK/STAT pathway, unpaired2, is revealed by an in vivo reporter of pathway activation. *Mech Dev*, 122(7-8), 939-948.
- Girard F, Strausfeld U, Fernandez A, Lamb NJ. (1991). Cyclin A is required for the onset of DNA replication in mammalian fibroblasts. *Cell*, 67(6), 1169-1179.
- Golias CH, Charalabopoulos A, Charalabopoulos K. (2004). Cell proliferation and cell cycle control: a mini review. *Int J Clin Pract*, 58(12), 1134-1141.

- Goulev Y, Fauny JD, Gonzalez-Marti B, Flagiello D, Silber J, Zider A. (2008). SCALLOPED interacts with YORKIE, the nuclear effector of the hippo tumor-suppressor pathway in *Drosophila*. *Curr Biol*, 18(6), 435-441.
- Goyal L, McCall K, Agapite J, Hartwieg E, Steller H. (2000). Induction of apoptosis by *Drosophila* reaper, hid and grim through inhibition of IAP function. *Embo j*, 19(4), 589-597.
- Grether ME, Abrams JM, Agapite J, White K, Steller H. (1995). The head involution defective gene of *Drosophila melanogaster* functions in programmed cell death. *Genes Dev*, 9(14), 1694-1708.
- Gustafson KS, Ginder GD. (1996). Interferon-gamma induction of the human leukocyte antigen-E gene is mediated through binding of a complex containing STAT1alpha to a distinct interferon-gamma-responsive element. *J Biol Chem*, 271(33), 20035-20046.
- Halder G, Johnson RL. (2011). Hippo signaling: growth control and beyond. *Development*, 138(1), 9-22.
- Hamaratoglu F, Willecke M, Kango-Singh M, Nolo R, Hyun E, Tao C, Jafar-Nejad H, Halder G. (2006). The tumour-suppressor genes NF2/Merlin and Expanded act through Hippo signalling to regulate cell proliferation and apoptosis. *Nat Cell Biol*, 8(1), 27-36.
- Harrison DA, McCoon PE, Binari R, Gilman M, Perrimon N. (1998). *Drosophila* unpaired encodes a secreted protein that activates the JAK signaling pathway. *Genes Dev*, 12(20), 3252-3263.
- Hay BA, Wassarman DA, Rubin GM. (1995). *Drosophila* homologs of baculovirus inhibitor of apoptosis proteins function to block cell death. *Cell*, 83(7), 1253-1262.
- Heisenberg M. (1980). Mutants of brain structure and function: what is the significance of the mushroom bodies for behavior? *Basic Life Sci*, 16, 373-390.
- Heisenberg M. (1998). What do the mushroom bodies do for the insect brain? an introduction. *Learn Mem*, 5(1-2), 1-10.
- Heisenberg M, Borst A, Wagner S, Byers D. (1985). *Drosophila* mushroom body mutants are deficient in olfactory learning. *J Neurogenet*, 2(1), 1-30.
- Henriksen MA, Betz A, Fuccillo MV, Darnell JE, Jr. (2002). Negative regulation of STAT92E by an N-terminally truncated STAT protein derived from an alternative promoter site. *Genes Dev*, 16(18), 2379-2389.

- Hildebrand JG, Shepherd GM. (1997). Mechanisms of olfactory discrimination: converging evidence for common principles across phyla. *Annu Rev Neurosci*, 20, 595-631.
- Hinds PW, Mitnacht S, Dulic V, Arnold A, Reed SI, Weinberg RA. (1992). Regulation of retinoblastoma protein functions by ectopic expression of human cyclins. *Cell*, 70(6), 993-1006.
- Hombria JC, Brown S, Hader S, Zeidler MP. (2005). Characterisation of Upd2, a *Drosophila* JAK/STAT pathway ligand. *Dev Biol*, 288(2), 420-433.
- Hou SX, Zheng Z, Chen X, Perrimon N. (2002). The Jak/STAT pathway in model organisms: emerging roles in cell movement. *Dev Cell*, 3(6), 765-778.
- Hou XS, Melnick MB, Perrimon N. (1996). Marelle acts downstream of the *Drosophila* HOP/JAK kinase and encodes a protein similar to the mammalian STATs. *Cell*, 84(3), 411-419.
- Howard A, Pelc SR. (1951). Nuclear incorporation of P32 as demonstrated by autoradiographs. *Experimental Cell Research*, 2(2), 178-187.
- Hu X, Dutta P, Tsurumi A, Li J, Wang J, Land H, Li WX. (2013). Unphosphorylated STAT5A stabilizes heterochromatin and suppresses tumor growth. *Proc Natl Acad Sci U S A*, 110(25), 10213-10218.
- Huang J, Wu S, Barrera J, Matthews K, Pan D. (2005). The Hippo signaling pathway coordinately regulates cell proliferation and apoptosis by inactivating Yorkie, the *Drosophila* Homolog of YAP. *Cell*, 122(3), 421-434.
- Isomoto H, Kobayashi S, Werneburg NW, Bronk SF, Guicciardi ME, Frank DA, Gores GJ. (2005). Interleukin 6 upregulates myeloid cell leukemia-1 expression through a STAT3 pathway in cholangiocarcinoma cells. *Hepatology*, 42(6), 1329-1338.
- Ito K, Awano W, Suzuki K, Hiromi Y, Yamamoto D. (1997). The *Drosophila* mushroom body is a quadruple structure of clonal units each of which contains a virtually identical set of neurones and glial cells. *Development*, 124(4), 761-771.
- Ito K, Hotta Y. (1992). Proliferation pattern of postembryonic neuroblasts in the brain of *Drosophila melanogaster*. *Dev Biol*, 149(1), 134-148.
- Ivashkiv LB. (1995). Cytokines and STATs: how can signals achieve specificity? *Immunity*, 3(1), 1-4.

Jefferis GS, Marin EC, Watts RJ, Luo L. (2002). Development of neuronal connectivity in *Drosophila* antennal lobes and mushroom bodies. *Curr Opin Neurobiol*, 12(1), 80-86.

Johnson DG, Schneider-Broussard R. (1998). Role of E2F in cell cycle control and cancer. *Front Biosci*, 3, d447-448.

Johnson DG, Walker CL. (1999). Cyclins and cell cycle checkpoints. *Annu Rev Pharmacol Toxicol*, 39, 295-312.

Joiner WJ, Crocker A, White BH, Sehgal A. (2006). Sleep in *Drosophila* is regulated by adult mushroom bodies. *Nature*, 441(7094), 757-760.

Jones L, Richardson H, Saint R. (2000). Tissue-specific regulation of cyclin E transcription during *Drosophila melanogaster* embryogenesis. *Development*, 127(21), 4619-4630.

Justice RW, Zilian O, Woods DF, Noll M, Bryant PJ. (1995). The *Drosophila* tumor suppressor gene *warts* encodes a homolog of human myotonic dystrophy kinase and is required for the control of cell shape and proliferation. *Genes Dev*, 9(5), 534-546.

Kallio J, Myllymaki H, Gronholm J, Armstrong M, Vanha-aho LM, Makinen L, Silvennoinen O, Valanne S, Ramet M. (2010). Eye transformer is a negative regulator of *Drosophila* JAK/STAT signaling. *Faseb j*, 24(11), 4467-4479.

Kandel E, Abel T. (1995). Neuropeptides, adenylyl cyclase, and memory storage. *Science*, 268(5212), 825-826.

Karpowicz P, Perez J, Perrimon N. (2010). The Hippo tumor suppressor pathway regulates intestinal stem cell regeneration. *Development*, 137(24), 4135-4145.

Kisseleva T, Bhattacharya S, Braunstein J, Schindler CW. (2002). Signaling through the JAK/STAT pathway, recent advances and future challenges. *Gene*, 285(1-2), 1-24.

Krashes MJ, Keene AC, Leung B, Armstrong JD, Waddell S. (2007). Sequential use of mushroom body neuron subsets during *drosophila* odor memory processing. *Neuron*, 53(1), 103-115.

Krebs DL, Hilton DJ. (2003). A new role for SOCS in insulin action. Suppressor of cytokine signaling. *Sci STKE*, 2003(169), Pe6.

Kunz T, Kraft KF, Technau GM, Urbach R. (2012). Origin of *Drosophila* mushroom body neuroblasts and generation of divergent embryonic lineages. *Development*, 139(14), 2510-2522.

- Kwon EJ, Park HS, Kim YS, Oh EJ, Nishida Y, Matsukage A, Yoo MA, Yamaguchi M. (2000). Transcriptional regulation of the *Drosophila* raf proto-oncogene by *Drosophila* STAT during development and in immune response. *J Biol Chem*, 275(26), 19824-19830.
- Lai ZC, Wei X, Shimizu T, Ramos E, Rohrbaugh M, Nikolaidis N, Ho LL, Li Y. (2005). Control of cell proliferation and apoptosis by mob as tumor suppressor, mats. *Cell*, 120(5), 675-685.
- Leatherman JL, Dinardo S. (2008). Zfh-1 controls somatic stem cell self-renewal in the *Drosophila* testis and nonautonomously influences germline stem cell self-renewal. *Cell Stem Cell*, 3(1), 44-54.
- Lee LA, Orr-Weaver TL. (2003). Regulation of cell cycles in *Drosophila* development: intrinsic and extrinsic cues. *Annu Rev Genet*, 37, 545-578.
- Lee T, Lee A, Luo L. (1999). Development of the *Drosophila* mushroom bodies: sequential generation of three distinct types of neurons from a neuroblast. *Development*, 126(18), 4065-4076.
- Lee T, Luo L. (1999). Mosaic analysis with a repressible cell marker for studies of gene function in neuronal morphogenesis. *Neuron*, 22(3), 451-461.
- Lehner CF, O'Farrell PH. (1989). Expression and function of *Drosophila* cyclin A during embryonic cell cycle progression. *Cell*, 56(6), 957-968.
- Lei QY, Zhang H, Zhao B, Zha ZY, Bai F, Pei XH, Zhao S, Xiong Y, Guan KL. (2008). TAZ promotes cell proliferation and epithelial-mesenchymal transition and is inhibited by the hippo pathway. *Mol Cell Biol*, 28(7), 2426-2436.
- Levy DE. (1999). Physiological significance of STAT proteins: investigations through gene disruption in vivo. *Cell Mol Life Sci*, 55(12), 1559-1567.
- Li J, Li W, Calhoun HC, Xia F, Gao FB, Li WX. (2003). Patterns and functions of STAT activation during *Drosophila* embryogenesis. *Mech Dev*, 120(12), 1455-1468.
- Li L, Xie T. (2005). Stem cell niche: structure and function. *Annu Rev Cell Dev Biol*, 21, 605-631.
- Li R, Waga S, Hannon GJ, Beach D, Stillman B. (1994). Differential effects by the p21 CDK inhibitor on PCNA-dependent DNA replication and repair. *Nature*, 371(6497), 534-537.

Li WX. (2008). Canonical and non-canonical JAK-STAT signaling. *Trends Cell Biol*, 18(11), 545-551.

Lian I, Kim J, Okazawa H, Zhao J, Zhao B, Yu J, Chinnaiyan A, Israel MA, Goldstein LS, Abujarour R, Ding S, Guan KL. (2010). The role of YAP transcription coactivator in regulating stem cell self-renewal and differentiation. *Genes Dev*, 24(11), 1106-1118.

Lin G, Xu N, Xi R. (2010). Paracrine unpaired signaling through the JAK/STAT pathway controls self-renewal and lineage differentiation of drosophila intestinal stem cells. *J Mol Cell Biol*, 2(1), 37-49.

Liu L, Wolf R, Ernst R, Heisenberg M. (1999). Context generalization in Drosophila visual learning requires the mushroom bodies. *Nature*, 400(6746), 753-756.

Lukas J, Bartkova J, Rohde M, Strauss M, Bartek J. (1995). Cyclin D1 is dispensable for G1 control in retinoblastoma gene-deficient cells independently of cdk4 activity. *Mol Cell Biol*, 15(5), 2600-2611.

Luo H, Dearolf CR. (2001). The JAK/STAT pathway and Drosophila development. *Bioessays*, 23(12), 1138-1147.

Luo H, Rose P, Barber D, Hanratty WP, Lee S, Roberts TM, D'Andrea AD, Dearolf CR. (1997). Mutation in the Jak kinase JH2 domain hyperactivates Drosophila and mammalian Jak-Stat pathways. *Mol Cell Biol*, 17(3), 1562-1571.

Makki R, Meister M, Pennetier D, Ubeda JM, Braun A, Daburon V, Krzemien J, Bourbon HM, Zhou R, Vincent A, Crozatier M. (2010). A short receptor downregulates JAK/STAT signalling to control the Drosophila cellular immune response. *PLoS Biol*, 8(8), e1000441.

Malumbres M, Barbacid M. (2009). Cell cycle, CDKs and cancer: a changing paradigm. *Nat Rev Cancer*, 9(3), 153-166.

Matakatsu H, Blair SS. (2006). Separating the adhesive and signaling functions of the Fat and Dachsous protocadherins. *Development*, 133(12), 2315-2324.

Matsuda T, Nakamura T, Nakao K, Arai T, Katsuki M, Heike T, Yokota T. (1999). STAT3 activation is sufficient to maintain an undifferentiated state of mouse embryonic stem cells. *Embo j*, 18(15), 4261-4269.

McBride SM, Giuliani G, Choi C, Krause P, Correale D, Watson K, Baker G, Siwicki KK. (1999). Mushroom body ablation impairs short-term memory and long-term memory of courtship conditioning in Drosophila melanogaster. *Neuron*, 24(4), 967-977.

- Meyer CA, Jacobs HW, Datar SA, Du W, Edgar BA, Lehner CF. (2000). Drosophila Cdk4 is required for normal growth and is dispensable for cell cycle progression. *Embo j*, 19(17), 4533-4542.
- Moberg KH, Schelble S, Burdick SK, Hariharan IK. (2005). Mutations in erupted, the Drosophila ortholog of mammalian tumor susceptibility gene 101, elicit non-cell-autonomous overgrowth. *Dev Cell*, 9(5), 699-710.
- Montell DJ, Yoon WH, Starz-Gaiano M. (2012). Group choreography: mechanisms orchestrating the collective movement of border cells. *Nat Rev Mol Cell Biol*, 13(10), 631-645.
- Mui AL. (1999). The role of STATs in proliferation, differentiation, and apoptosis. *Cell Mol Life Sci*, 55(12), 1547-1558.
- Mukherjee T, Hombria JC, Zeidler MP. (2005). Opposing roles for Drosophila JAK/STAT signalling during cellular proliferation. *Oncogene*, 24(15), 2503-2511.
- Mukherjee T, Schafer U, Zeidler MP. (2006). Identification of Drosophila genes modulating Janus kinase/signal transducer and activator of transcription signal transduction. *Genetics*, 172(3), 1683-1697.
- Muller P, Kutenkeuler D, Gesellchen V, Zeidler MP, Boutros M. (2005). Identification of JAK/STAT signalling components by genome-wide RNA interference. *Nature*, 436(7052), 871-875.
- Muller R. (1996). A quarter of a century of place cells. *Neuron*, 17(5), 813-822.
- Musikacharoen T, Matsuguchi T, Kikuchi T, Yoshikai Y. (2001). NF-kappa B and STAT5 play important roles in the regulation of mouse Toll-like receptor 2 gene expression. *J Immunol*, 166(7), 4516-4524.
- Neufeld TP, de la Cruz AF, Johnston LA, Edgar BA. (1998). Coordination of growth and cell division in the Drosophila wing. *Cell*, 93(7), 1183-1193.
- Ngo KT, Wang J, Junker M, Kriz S, Vo G, Asem B, Olson JM, Banerjee U, Hartenstein V. (2010). Concomitant requirement for Notch and Jak/Stat signaling during neuro-epithelial differentiation in the Drosophila optic lobe. *Dev Biol*, 346(2), 284-295.
- Nicolas CS, Peineau S, Amici M, Csaba Z, Fafouri A, Javalet C, Collett VJ, Hildebrandt L, Seaton G, Choi SL, Sim SE, Bradley C, Lee K, Zhuo M, Kaang BK, Gressens P, Dournaud P, Fitzjohn SM, Bortolotto ZA, Cho K, Collingridge GL. (2012). The Jak/STAT pathway is involved in synaptic plasticity. *Neuron*, 73(2), 374-390.

- Niwa H, Burdon T, Chambers I, Smith A. (1998). Self-renewal of pluripotent embryonic stem cells is mediated via activation of STAT3. *Genes Dev*, 12(13), 2048-2060.
- Noveen A, Daniel A, Hartenstein V. (2000). Early development of the Drosophila mushroom body: the roles of eyeless and dachshund. *Development*, 127(16), 3475-3488.
- O'Shea JJ, Gadina M, Schreiber RD. (2002). Cytokine signaling in 2002: new surprises in the Jak/Stat pathway. *Cell*, 109 Suppl, S121-131.
- Ohtani K, DeGregori J, Nevins JR. (1995). Regulation of the cyclin E gene by transcription factor E2F1. *Proc Natl Acad Sci U S A*, 92(26), 12146-12150.
- Ohtsubo M, Theodoras AM, Schumacher J, Roberts JM, Pagano M. (1995). Human cyclin E, a nuclear protein essential for the G1-to-S phase transition. *Mol Cell Biol*, 15(5), 2612-2624.
- Ohtsubo T, Kamada S, Tsujimoto Y. (1996). [Inhibition of apoptosis by a baculovirus p35 gene]. *Nihon Rinsho*, 54(7), 1907-1911.
- Pan D. (2010). The hippo signaling pathway in development and cancer. *Dev Cell*, 19(4), 491-505.
- Pellegrini S, Dusanter-Fourt I. (1997). The structure, regulation and function of the Janus kinases (JAKs) and the signal transducers and activators of transcription (STATs). *Eur J Biochem*, 248(3), 615-633.
- Peng HW, Slattery M, Mann RS. (2009). Transcription factor choice in the Hippo signaling pathway: homothorax and yorkie regulation of the microRNA bantam in the progenitor domain of the Drosophila eye imaginal disc. *Genes Dev*, 23(19), 2307-2319.
- Perrimon N, Mahowald AP. (1986). l(1)hopscotch, A larval-pupal zygotic lethal with a specific maternal effect on segmentation in Drosophila. *Dev Biol*, 118(1), 28-41.
- Pitman JL, McGill JJ, Keegan KP, Allada R. (2006). A dynamic role for the mushroom bodies in promoting sleep in Drosophila. *Nature*, 441(7094), 753-756.
- Praskova M, Xia F, Avruch J. (2008). MOBKL1A/MOBKL1B phosphorylation by MST1 and MST2 inhibits cell proliferation. *Curr Biol*, 18(5), 311-321.
- Quinn WG, Harris WA, Benzer S. (1974). Conditioned behavior in Drosophila melanogaster. *Proc Natl Acad Sci U S A*, 71(3), 708-712.

- Ramos A, Camargo FD. (2012). The Hippo signaling pathway and stem cell biology. *Trends Cell Biol*, 22(7), 339-346.
- Rawlings JS, Rennebeck G, Harrison SM, Xi R, Harrison DA. (2004). Two Drosophila suppressors of cytokine signaling (SOCS) differentially regulate JAK and EGFR pathway activities. *BMC Cell Biol*, 5(1), 38.
- Ren F, Wang B, Yue T, Yun EY, Ip YT, Jiang J. (2010). Hippo signaling regulates Drosophila intestine stem cell proliferation through multiple pathways. *Proc Natl Acad Sci U S A*, 107(49), 21064-21069.
- Rieder CL. (2011). Mitosis in vertebrates: the G2/M and M/A transitions and their associated checkpoints. *Chromosome Res*, 19(3), 291-306.
- Rivas ML, Cobreros L, Zeidler MP, Hombria JC. (2008). Plasticity of Drosophila Stat DNA binding shows an evolutionary basis for Stat transcription factor preferences. *EMBO Rep*, 9(11), 1114-1120.
- Robinson BS, Huang J, Hong Y, Moberg KH. (2010). Crumbs regulates Salvador/Warts/Hippo signaling in Drosophila via the FERM-domain protein Expanded. *Curr Biol*, 20(7), 582-590.
- Rodrigues AB, Zoranovic T, Ayala-Camargo A, Grewal S, Reyes-Robles T, Krasny M, Wu DC, Johnston LA, Bach EA. (2012). Activated STAT regulates growth and induces competitive interactions independently of Myc, Yorkie, Wingless and ribosome biogenesis. *Development*, 139(21), 4051-4061.
- Schindler C, Fu XY, Improtta T, Aebersold R, Darnell JE, Jr. (1992). Proteins of transcription factor ISGF-3: one gene encodes the 91-and 84-kDa ISGF-3 proteins that are activated by interferon alpha. *Proc Natl Acad Sci U S A*, 89(16), 7836-7839.
- Schlegelmilch K, Mohseni M, Kirak O, Pruszk J, Rodriguez JR, Zhou D, Kreger BT, Vasioukhin V, Avruch J, Brummelkamp TR, Camargo FD. (2011). Yap1 acts downstream of alpha-catenin to control epidermal proliferation. *Cell*, 144(5), 782-795.
- Seidel HM, Milocco LH, Lamb P, Darnell JE, Jr., Stein RB, Rosen J. (1995). Spacing of palindromic half sites as a determinant of selective STAT (signal transducers and activators of transcription) DNA binding and transcriptional activity. *Proc Natl Acad Sci U S A*, 92(7), 3041-3045.
- Sherr CJ. (1994). G1 phase progression: cycling on cue. *Cell*, 79(4), 551-555.

Shi S, Calhoun HC, Xia F, Li J, Le L, Li WX. (2006). JAK signaling globally counteracts heterochromatic gene silencing. *Nat Genet*, 38(9), 1071-1076.

Shi S, Larson K, Guo D, Lim SJ, Dutta P, Yan SJ, Li WX. (2008). Drosophila STAT is required for directly maintaining HP1 localization and heterochromatin stability. *Nat Cell Biol*, 10(4), 489-496.

Shuai K. (2000). Modulation of STAT signaling by STAT-interacting proteins. *Oncogene*, 19(21), 2638-2644.

Singh SR, Liu W, Hou SX. (2007). The adult Drosophila malpighian tubules are maintained by multipotent stem cells. *Cell Stem Cell*, 1(2), 191-203.

Sopko R, Silva E, Clayton L, Gardano L, Barrios-Rodiles M, Wrana J, Varelas X, Arbouzova NI, Shaw S, Saburi S, Matakatsu H, Blair S, McNeill H. (2009). Phosphorylation of the tumor suppressor fat is regulated by its ligand Dachshaus and the kinase discs overgrown. *Curr Biol*, 19(13), 1112-1117.

Sousa-Nunes R, Cheng LY, Gould AP. (2010). Regulating neural proliferation in the Drosophila CNS. *Curr Opin Neurobiol*, 20(1), 50-57.

Staley BK, Irvine KD. (2010). Warts and Yorkie mediate intestinal regeneration by influencing stem cell proliferation. *Curr Biol*, 20(17), 1580-1587.

Starr R, Hilton DJ. (1999). Negative regulation of the JAK/STAT pathway. *Bioessays*, 21(1), 47-52.

Starr R, Willson TA, Viney EM, Murray LJ, Rayner JR, Jenkins BJ, Gonda TJ, Alexander WS, Metcalf D, Nicola NA, Hilton DJ. (1997). A family of cytokine-inducible inhibitors of signalling. *Nature*, 387(6636), 917-921.

Stec W, Vidal O, Zeidler MP. (2013). Drosophila SOCS36E negatively regulates JAK/STAT pathway signaling via two separable mechanisms. *Mol Biol Cell*, 24(18), 3000-3009.

Stec WJ, Zeidler MP. (2011). Drosophila SOCS Proteins. *J Signal Transduct*, 2011, 894510.

Strausfeld NJ, Hansen L, Li Y, Gomez RS, Ito K. (1998). Evolution, discovery, and interpretations of arthropod mushroom bodies. *Learn Mem*, 5(1-2), 11-37.

Tang S, Guo A. (2001). Choice behavior of Drosophila facing contradictory visual cues. *Science*, 294(5546), 1543-1547.

- Tapon N, Harvey KF, Bell DW, Wahrer DC, Schiripo TA, Haber D, Hariharan IK. (2002). salvador Promotes both cell cycle exit and apoptosis in Drosophila and is mutated in human cancer cell lines. *Cell*, 110(4), 467-478.
- Thompson BJ, Cohen SM. (2006). The Hippo pathway regulates the bantam microRNA to control cell proliferation and apoptosis in Drosophila. *Cell*, 126(4), 767-774.
- Tsai YC, Sun YH. (2004). Long-range effect of upd, a ligand for Jak/STAT pathway, on cell cycle in Drosophila eye development. *Genesis*, 39(2), 141-153.
- Tulina N, Matunis E. (2001). Control of stem cell self-renewal in Drosophila spermatogenesis by JAK-STAT signaling. *Science*, 294(5551), 2546-2549.
- Tups A. (2009). Physiological models of leptin resistance. *J Neuroendocrinol*, 21(11), 961-971.
- Uren AG, Pakusch M, Hawkins CJ, Puls KL, Vaux DL. (1996). Cloning and expression of apoptosis inhibitory protein homologs that function to inhibit apoptosis and/or bind tumor necrosis factor receptor-associated factors. *Proc Natl Acad Sci U S A*, 93(10), 4974-4978.
- Varelas X, Sakuma R, Samavarchi-Tehrani P, Peerani R, Rao BM, Dembowy J, Yaffe MB, Zandstra PW, Wrana JL. (2008). TAZ controls Smad nucleocytoplasmic shuttling and regulates human embryonic stem-cell self-renewal. *Nat Cell Biol*, 10(7), 837-848.
- Varelas X, Samavarchi-Tehrani P, Narimatsu M, Weiss A, Cockburn K, Larsen BG, Rossant J, Wrana JL. (2010). The Crumbs complex couples cell density sensing to Hippo-dependent control of the TGF-beta-SMAD pathway. *Dev Cell*, 19(6), 831-844.
- Vinkemeier U. (2004). Getting the message across, STAT! Design principles of a molecular signaling circuit. *J Cell Biol*, 167(2), 197-201.
- Walker DH, Maller JL. (1991). Role for cyclin A in the dependence of mitosis on completion of DNA replication. *Nature*, 354(6351), 314-317.
- Wang J, Ma X, Yang JS, Zheng X, Zugates CT, Lee CH, Lee T. (2004). Transmembrane/juxtamembrane domain-dependent Dscam distribution and function during mushroom body neuronal morphogenesis. *Neuron*, 43(5), 663-672.
- Wang J, Zugates CT, Liang IH, Lee CH, Lee T. (2002). Drosophila Dscam is required for divergent segregation of sister branches and suppresses ectopic bifurcation of axons. *Neuron*, 33(4), 559-571.

- Wang W, Li Y, Zhou L, Yue H, Luo H. (2011). Role of JAK/STAT signaling in neuroepithelial stem cell maintenance and proliferation in the *Drosophila* optic lobe. *Biochem Biophys Res Commun*, 410(4), 714-720.
- Wawersik M, Milutinovich A, Casper AL, Matunis E, Williams B, Van Doren M. (2005). Somatic control of germline sexual development is mediated by the JAK/STAT pathway. *Nature*, 436(7050), 563-567.
- White K, Grether ME, Abrams JM, Young L, Farrell K, Steller H. (1994). Genetic control of programmed cell death in *Drosophila*. *Science*, 264(5159), 677-683.
- Wolf R, Wittig T, Liu L, Wustmann G, Eyding D, Heisenberg M. (1998). *Drosophila* mushroom bodies are dispensable for visual, tactile, and motor learning. *Learn Mem*, 5(1-2), 166-178.
- Wong P, Severns CW, Guyer NB, Wright TM. (1994). A unique palindromic element mediates gamma interferon induction of mig gene expression. *Mol Cell Biol*, 14(2), 914-922.
- Wu J, Luo L. (2006). A protocol for mosaic analysis with a repressible cell marker (MARCM) in *Drosophila*. *Nat Protoc*, 1(6), 2583-2589.
- Wu S, Huang J, Dong J, Pan D. (2003). hippo encodes a Ste-20 family protein kinase that restricts cell proliferation and promotes apoptosis in conjunction with salvador and warts. *Cell*, 114(4), 445-456.
- Wu S, Liu Y, Zheng Y, Dong J, Pan D. (2008). The TEAD/TEF family protein Scalloped mediates transcriptional output of the Hippo growth-regulatory pathway. *Dev Cell*, 14(3), 388-398.
- Xu T, Wang W, Zhang S, Stewart RA, Yu W. (1995). Identifying tumor suppressors in genetic mosaics: the *Drosophila* lats gene encodes a putative protein kinase. *Development*, 121(4), 1053-1063.
- Yamamoto K, Miura O, Hirosawa S, Miyasaka N. (1997). Binding sequence of STAT4: STAT4 complex recognizes the IFN-gamma activation site (GAS)-like sequence (T/A)TTCC(C/G)GGAA(T/A). *Biochem Biophys Res Commun*, 233(1), 126-132.
- Yan R, Small S, Desplan C, Dearolf CR, Darnell JE, Jr. (1996). Identification of a Stat gene that functions in *Drosophila* development. *Cell*, 84(3), 421-430.

- Yasugi T, Umetsu D, Murakami S, Sato M, Tabata T. (2008). Drosophila optic lobe neuroblasts triggered by a wave of proneural gene expression that is negatively regulated by JAK/STAT. *Development*, 135(8), 1471-1480.
- Yeh TC, Pellegrini S. (1999). The Janus kinase family of protein tyrosine kinases and their role in signaling. *Cell Mol Life Sci*, 55(12), 1523-1534.
- Yu FX, Guan KL. (2013). The Hippo pathway: regulators and regulations. *Genes Dev*, 27(4), 355-371.
- Yu J, Zheng Y, Dong J, Klusza S, Deng WM, Pan D. (2010). Kibra functions as a tumor suppressor protein that regulates Hippo signaling in conjunction with Merlin and Expanded. *Dev Cell*, 18(2), 288-299.
- Zars T. (2000). Behavioral functions of the insect mushroom bodies. *Curr Opin Neurobiol*, 10(6), 790-795.
- Zhang J, Ji JY, Yu M, Overholtzer M, Smolen GA, Wang R, Brugge JS, Dyson NJ, Haber DA. (2009). YAP-dependent induction of amphiregulin identifies a non-cell-autonomous component of the Hippo pathway. *Nat Cell Biol*, 11(12), 1444-1450.
- Zhao B, Tumaneng K, Guan KL. (2011). The Hippo pathway in organ size control, tissue regeneration and stem cell self-renewal. *Nat Cell Biol*, 13(8), 877-883.
- Zhao B, Wei X, Li W, Udan RS, Yang Q, Kim J, Xie J, Ikenoue T, Yu J, Li L, Zheng P, Ye K, Chinnaiyan A, Halder G, Lai ZC, Guan KL. (2007). Inactivation of YAP oncoprotein by the Hippo pathway is involved in cell contact inhibition and tissue growth control. *Genes Dev*, 21(21), 2747-2761.
- Zhao B, Ye X, Yu J, Li L, Li W, Li S, Yu J, Lin JD, Wang CY, Chinnaiyan AM, Lai ZC, Guan KL. (2008). TEAD mediates YAP-dependent gene induction and growth control. *Genes Dev*, 22(14), 1962-1971.
- Zheng X, Wang J, Haerry TE, Wu AY, Martin J, O'Connor MB, Lee CH, Lee T. (2003). TGF-beta signaling activates steroid hormone receptor expression during neuronal remodeling in the Drosophila brain. *Cell*, 112(3), 303-315.
- Zoranovic T, Grmai L, Bach EA. (2013). Regulation of proliferation, cell competition, and cellular growth by the Drosophila JAK-STAT pathway. *Jakstat*, 2(3), e25408.